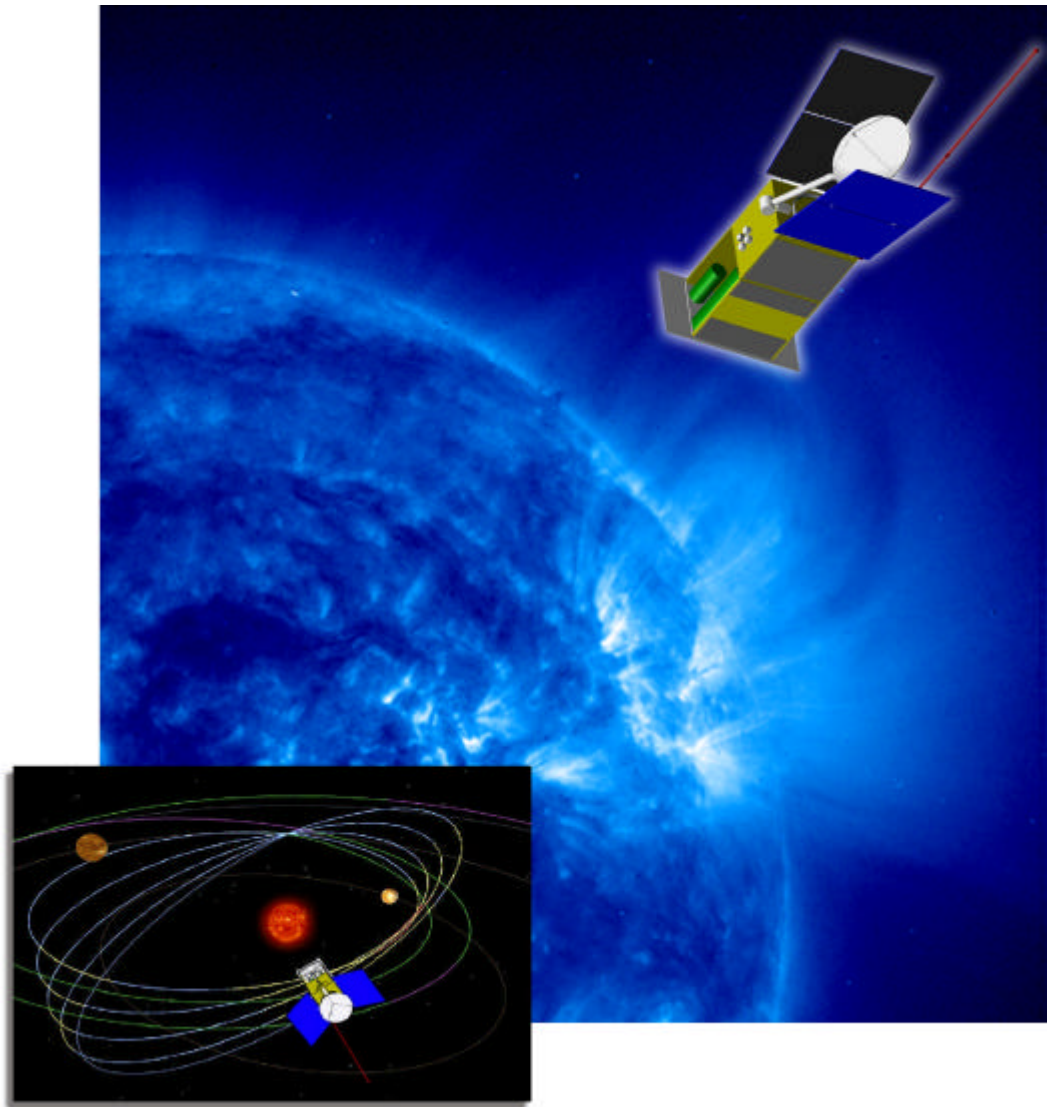


# Solar Orbiter

**A High-Resolution Mission to the Sun and Inner Heliosphere**



**Assessment Study Report  
July 2000**

SCI(2000)6



---

## FOREWORD

---

The Solar Orbiter Mission was proposed to ESA by an international team of scientists led by E. Marsch in response to the call for mission proposals for two flexible missions (F2 and F3) and submitted on January 27, 2000. In March 2000 ESA's Space Science Advisory Committee recommended the Solar Orbiter for further study based on a pre-assessment study performed in 1999 in the framework of ESA's Solar Physics Planning Group activities.

This document is the result of the “delta” assessment study, carried out by representatives of the European solar and heliospheric physics communities, in close co-operation with ESA staff.

### *STUDY TEAM MEMBERS:*

**E. Marsch**, Max-Planck-Institut für Aeronomie, Katlenburg-Lindau, Germany  
**E. Antonucci**, Osservatorio Astronomico di Torino, Pino Torinese, Italy  
**P. Bochler**, University of Bern, Switzerland  
**J.-L. Bougeret**, Observatoire de Paris, Meudon, France  
**R. Harrison**, Rutherford Appleton Laboratory, Chilton, UK  
**R. Schwenn**, Max-Planck-Institut für Aeronomie, Katlenburg-Lindau, Germany  
**J.-C. Vial**, Institut d'Astrophysique Spatiale, CNRS-Université de Paris-Sud, France

### *ESA STAFF MEMBERS:*

Study Scientists: **B. Fleck**, ESA/GSFC, Greenbelt, Maryland, USA  
**R. Marsden**, ESA/ESTEC, Noordwijk, The Netherlands  
Study Manager: **O. Pace**, ESA/ESTEC, Noordwijk, The Netherlands  
Solar System Mission Coordinator: **M. Coradini**, ESA HQ, Paris, France

**Y. Langevin**, Institut d'Astrophysique Spatiale, Orsay, France has provided important assistance on the Solar Orbiter mission design and analysis.

Valuable contributions and comments on the science objectives and instrumentation were provided by:

**T. Appourchaux**, ESA Space Science Department, ESTEC, Noordwijk, The Netherlands  
**R. Bruno**, Istituto Fisica Spazio Interplanetario del CNR, Roma, Italy  
**M. Decaudin**, Institut d'Astrophysique Spatiale, CNRS-Université de Paris-Sud, France  
**M. Collados**, Instituto de Astrofisica de Canarias, Spain  
**A. Fedorov**, Institute for Space Research, Moscow, Russia  
**S. Fineschi**, Osservatorio Astronomico di Torino, Pino Torinese, Italy  
**C. Fröhlich**, Physikalisch-Meteorologisches Observatorium, Davos, Switzerland  
**L. Gizon**, Stanford University, California, USA  
**K. Goetz**, University of Minnesota, USA  
**M. Hilchenbach**, Max-Planck-Institut für Aeronomie, Lindau, Germany  
**J.-F. Hochedez**, Observatoire Royal de Belgique, Brussels, Belgium  
**P. Lemaire**, Institut d'Astrophysique Spatiale, CNRS-Université de Paris-Sud, France  
**F. Lefevre**, LPCE, Orleans, France  
**B. Lites**, High Altitude Observatory, Boulder, USA  
**O. von der Lühse**, Kiepenheuer Institut für Sonnenphysik, Freiburg, Germany  
**V. Martinez Pillet**, Instituto de Astrofisica de Canarias, Spain  
**R.B. McKibben**, University of Chicago, USA  
**G. Naletto**, Università di Padova, Padova, Italy  
**E. Priest**, University of St. Andrews, UK  
**M. Romoli**, Università di Firenze, Firenze, Italy  
**H. Rucker**, Universität Graz, Austria  
**E. Sawyer**, Rutherford Appleton Laboratory, Chilton, UK  
**W. Schmidt**, Kiepenheuer Institut für Sonnenphysik, Freiburg, Germany  
**S. Solanki**, Max-Planck-Institut für Aeronomie, Lindau, Germany  
**P. Wurzel**, University of Bern, Switzerland



---

# TABLE OF CONTENTS

---

<b>FOREWORD .....</b>	<b>I</b>
<b>TABLE OF CONTENTS .....</b>	<b>III</b>
<b>1 EXECUTIVE SUMMARY.....</b>	<b>1</b>
<b>2 SCIENTIFIC RATIONALE .....</b>	<b>4</b>
2.1 INTRODUCTION.....	4
2.2 THE SUN'S MAGNETISED PLASMA: CLOSE-UP OBSERVATIONS OF THE SOLAR ATMOSPHERE.....	4
2.2.1 Photospheric magnetic flux elements.....	5
2.2.2 Basic processes and fundamental scales in the magnetised solar atmosphere.....	5
2.2.3 Waves in the corona.....	6
2.2.4 Coronal magnetic field .....	6
2.3 LINKING THE PHOTOSPHERE AND CORONA TO THE HELIOSPHERE: CO-ROTATION OBSERVATIONS .....	7
2.3.1 Global solar corona and solar wind.....	7
2.3.2 Global coronal sources of the solar wind.....	8
2.3.3 Magnetic network .....	9
2.3.4 Boundaries and fine structures in the corona and solar wind .....	9
2.3.5 Connections between the internal plasma states of the solar corona and the solar wind ..	10
2.3.6 Coronal and solar wind abundances and fractionation effects .....	10
2.3.7 Coronal transients .....	11
2.4 PARTICLES AND FIELDS: IN-SITU MEASUREMENTS IN THE INNER HELIOSPHERE.....	12
2.4.1 Microstate of the interplanetary solar wind .....	12
2.4.2 Solar wind ions as tracers of coronal structures .....	13
2.4.3 Magnetohydrodynamic turbulence .....	13
2.4.4 Acceleration and transport of solar energetic particles .....	14
2.4.5 Neutral particles from the Sun.....	15
2.4.6 Circumsolar and interplanetary dust.....	16
2.4.7 Solar neutrons.....	17
2.4.8 Solar radio emission.....	17
2.5 THE SUN'S POLAR REGIONS AND EQUATORIAL CORONA: EXCURSION OUT OF THE ECLIPTIC.....	17
2.5.1 The Sun's polar magnetic field and the dynamo .....	18
2.5.2 Polar rotation and internal flows .....	18
2.5.3 Polar observations of CMEs.....	19
2.5.4 Solar luminosity variations.....	20
2.5.5 Polar observation of the fast solar wind.....	20
2.5.6 Secular variation of the heliospheric magnetic flux .....	20
<b>3 SCIENTIFIC PAYLOAD.....</b>	<b>22</b>
3.1 MEASUREMENT REQUIREMENTS.....	22
3.2 IN-SITU HELIOSPHERIC INSTRUMENTS .....	22
3.2.1 Solar Wind Plasma Analyser (SWA).....	22
3.2.2 Radio and Plasma Waves Analyser (RPW).....	25
3.2.3 Coronal Radio Sounding (CRS).....	29
3.2.4 Magnetometer (MAG).....	30
3.2.5 Energetic Particle Detector (EPD).....	30
3.2.6 Dust Detector (DUD).....	32
3.2.7 Neutral Particle Detector (NPD).....	33
3.2.8 Neutron Detector (NED).....	34
3.2.9 Heliospheric instruments summary.....	36
3.3 REMOTE SENSING SOLAR INSTRUMENTS.....	36
3.3.1 General considerations.....	36

3.3.2	<i>Visible-Light Imager and Magnetograph (VIM)</i> .....	36
3.3.3	<i>EUV spectrometer (EUS)</i> .....	42
3.3.4	<i>EUV imager (EXI)</i> .....	47
3.3.5	<i>Ultraviolet and Visible-light Coronagraph (UVC)</i> .....	51
3.3.6	<i>Radiometer (RAD)</i> .....	54
3.3.7	<i>Other potential solar instruments</i> .....	55
3.3.8	<i>Solar remote-sensing instruments summary</i> .....	56
<b>4</b>	<b>MISSION PROFILE</b> .....	<b>57</b>
<b>5</b>	<b>SYSTEM DESIGN</b> .....	<b>60</b>
5.1	DESIGN REQUIREMENTS AND DRIVERS .....	60
5.2	MAIN SYSTEM DESIGN FEATURES .....	60
5.2.1	<i>Requirements and constraints</i> .....	61
5.2.2	<i>Spacecraft baseline design</i> .....	61
5.2.3	<i>Thermal Design</i> .....	64
5.2.4	<i>Power Supply</i> .....	65
5.3	DATA COLLECTION AND TRANSMISSION.....	66
5.4	RADIATION.....	68
5.5	MASS BUDGETS .....	68
	TOTAL LAUNCH MASS .....	68
<b>6</b>	<b>SUBSYSTEM DESIGN</b> .....	<b>69</b>
6.1	ATTITUDE AND ORBIT CONTROL.....	69
6.2	REACTION CONTROL SYSTEM .....	70
6.3	PROPULSION.....	70
6.4	STRUCTURE.....	71
6.5	THERMAL CONTROL.....	71
<b>7</b>	<b>GROUND SYSTEMS AND OPERATIONS</b> .....	<b>73</b>
7.1	GROUND SEGMENT FACILITIES AND SERVICES.....	73
7.2	GROUND STATIONS AND COMMUNICATIONS NETWORK .....	73
7.3	MISSION CONTROL CENTRE .....	74
7.4	COMPUTER FACILITIES AND NETWORK.....	74
7.5	FLIGHT CONTROL SOFTWARE SYSTEM .....	74
7.6	MISSION OPERATIONS CONCEPT .....	75
7.7	SCIENCE INSTRUMENT OPERATIONS AND TEAM STRUCTURE .....	75
<b>8</b>	<b>COMMUNICATION AND OUTREACH</b> .....	<b>77</b>
<b>9</b>	<b>MANAGEMENT</b> .....	<b>78</b>
9.1	F2/F3 PROCUREMENT APPROACH.....	78
9.2	PROCUREMENT PHILOSOPHY .....	78
9.3	SCIENTIFIC MANAGEMENT AND PAYLOAD SELECTION.....	78
9.4	INDUSTRIAL MANAGEMENT.....	79
9.5	DEVELOPMENT PHILOSOPHY AND SCHEDULE .....	79
9.5.1	<i>General</i> .....	79
9.5.2	<i>Payload model philosophy</i> .....	79
9.5.3	<i>Service module model philosophy</i> .....	79
9.5.4	<i>Schedule</i> .....	80
<b>10</b>	<b>LIST OF ACRONYMS</b> .....	<b>81</b>

---

# 1 EXECUTIVE SUMMARY

---

The Sun's atmosphere and the heliosphere represent uniquely accessible domains of space, where fundamental physical processes common to solar, astrophysical and laboratory plasmas can be studied in detail and under conditions impossible to reproduce on Earth or to study from astronomical distances.

The results from missions such as Helios, Ulysses, Yohkoh, SOHO, and TRACE have advanced enormously our understanding of the solar corona, the associated solar wind and the three-dimensional heliosphere. However, we have reached the point where further *in-situ* measurements, now much closer to the Sun, together with high-resolution imaging and spectroscopy from a near-Sun and out-of-ecliptic perspective, promise to bring about major breakthroughs in solar and heliospheric physics.

The Solar Orbiter will, through a novel orbital design and its state-of the-art instruments, provide exactly the required observations.

The Solar Orbiter will for the first time

- explore the uncharted innermost regions of our solar system,
- study the Sun from close-up (45 solar radii, or 0.21 AU),
- fly by the Sun, tuned to its rotation and examine the solar surface and the space above from a co-rotating vantage point,
- provide images of the Sun's polar regions from heliographic latitudes as high as 38°.

The scientific goals of the Solar Orbiter are

- to determine *in-situ* the properties and dynamics of plasma, fields and particles in the near-Sun heliosphere,
- to investigate the fine-scale structure and dynamics of the Sun's magnetised atmosphere, using close-up, high-resolution remote sensing,
- to identify the links between activity on the Sun's surface and the resulting evolution of the corona and inner heliosphere, using solar co-rotation passes,
- to observe and fully characterise the Sun's polar regions and equatorial corona from high latitudes.

The underlying basic questions which are relevant to astrophysics in general are

- Why does the Sun vary and how does the solar dynamo work?
- What are the fundamental physical processes at work in the solar atmosphere and in the heliosphere?
- What are the links between the magnetic field dominated regime in the solar corona and the particle dominated regime in the heliosphere?

In particular, we want

- to unravel the detailed working of the solar magnetic field as a key to understanding stellar magnetism and variability,
- to map and describe the rotation, meridional flows, and magnetic topology near the Sun's poles, in order to understand the solar dynamo,
- to investigate the variability of the solar radiation from the far side of the Sun and over the poles,
- to reveal the flow of energy through the coupled layers of the solar atmosphere, e.g. to identify the small-scale sources of coronal heating and solar wind acceleration,
- to analyse fluctuations and wave-particle interactions in the solar wind, in order to understand the fundamental processes related to turbulence at all relevant scales in a tenuous magnetofluid,
- to understand the Sun as a prolific and variable particle accelerator,
- to study the nature and the global dynamics of solar eruptive events (flares, coronal mass ejections, etc.) and their effects on the heliosphere ("space weather and space climate").

The near-Sun interplanetary measurements together with simultaneous remote sensing observations of the Sun will permit us to disentangle spatial and temporal variations during the co-rotational phases. They will allow us to understand the characteristics of the solar wind and energetic particles in close linkage with the plasma conditions in their source regions on the Sun. By approaching as close as 45 solar radii, the Solar Orbiter will view the solar atmosphere with unprecedented spatial resolution (35 km pixel size, equivalent to 0.05 arcsec from Earth). Over extended periods the Solar Orbiter will deliver images and data of the polar regions and the side of the Sun not visible from Earth.

The Solar Orbiter will achieve its wide-ranging aims with a suite of sophisticated instruments. Note that due to the Orbiter's proximity to the Sun the instruments can be fairly small, compared to instrumentation required at the Earth's orbit.

The payload includes two instrument packages, optimised to meet the solar and heliospheric science objectives:

- Heliospheric *in-situ* instruments: solar wind analyser, radio and plasma wave analyser, magnetometer, energetic particle detectors, interplanetary dust detector, neutral particle detector, solar neutron detector.
- Solar remote sensing instruments: Extreme ultraviolet (EUV) full-Sun and high resolution imager, high-resolution EUV spectrometer, high-resolution visible-light telescope and magnetograph, EUV and visible-light coronagraph, radiometer.

The Solar Orbiter spacecraft benefits from technology developed for the Mercury Cornerstone mission. This allows such an ambitious mission to be carried out within the frame of an F mission.

Using solar electric propulsion (SEP) in conjunction with multiple planetary swing-by manoeuvres, it will take the Solar Orbiter only two years to reach a perihelion of 45 solar radii at an orbital period of 149 days. Within the nominal 5 year mission phase, the Solar Orbiter will perform several swing-by manoeuvres at Venus, in order to increase the inclination of the orbital plane to  $30^\circ$  with respect to the solar equator. During an extended mission phase of about two years the inclination will be further increased to  $38^\circ$ .

The spacecraft will be 3-axis stabilised and always Sun-pointed. Given the extreme thermal conditions at 45 solar radii (25 solar constants), the thermal design of the spacecraft has been considered in detail during the assessment study and viable solutions have been identified. Telemetry will be handled via X-band low-gain antennae, and by a 2-axis steerable Ka-band high-gain antenna.

The total mass of the Solar Orbiter is compatible with a Soyuz-Fregat launch from Baikonur.

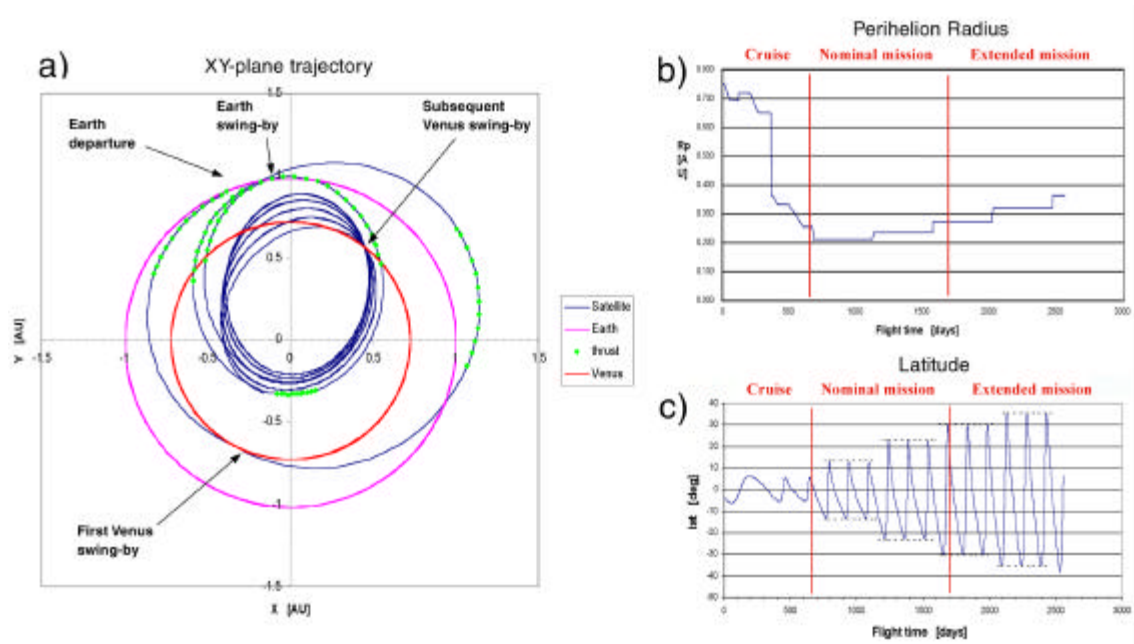


**Figure 1.1:** a) Ecliptic projection of the Solar Orbiter trajectory. Blue: Solar Orbiter. Pink: Earth Orbit. Red: Venus orbit. Green: SEP Thruster firings. b) Perihelion distance of the Solar Orbiter as a function of time. c) Spacecraft latitude with respect to the Sun's equator as a function of time.



<b>Mission Concept</b>	View the Sun from <b>near-Sun</b> and <b>out-of-ecliptic</b> perspectives and perform <ul style="list-style-type: none"> <li>• spectroscopy and imaging at <b>high resolution</b>,</li> <li>• <b>co-rotational</b> <i>in-situ</i> sampling of particles and fields,</li> <li>• remote-sensing of the <b>polar regions</b> of the Sun</li> </ul>
<b>Payload</b>	Mass: 130 kg Power: 125 W Telemetry: 75 kb/s  <b>Heliospheric instrumentation:</b> <ul style="list-style-type: none"> <li>• Solar Wind Plasma Analyser</li> <li>• Radio and Plasma Wave Analyser</li> <li>• Magnetometer</li> <li>• Energetic Particles Detector</li> <li>• Neutral Particle Detector</li> <li>• Dust Detector</li> <li>• Neutron Detector</li> <li>• Coronal Radio Sounding</li> </ul> <b>Solar remote sensing instrumentation:</b> <ul style="list-style-type: none"> <li>• Visible-light Imager and Magnetograph</li> <li>• EUV Spectrometer</li> <li>• EUV Imager</li> <li>• Ultraviolet and Visible Light Coronagraph</li> <li>• Radiometer</li> </ul>
<b>Spacecraft</b>	<ul style="list-style-type: none"> <li>• Design lifetime = 5 years</li> <li>• Consumables sized for 7 years</li> <li>• Total mass = 1308 kg</li> <li>• Dimensions: 3 m x 1.2 m x 1.6 m</li> <li>• 3-axis stabilised, Sun-pointing</li> <li>• Pointing stability better than 3 arcsec/15min</li> <li>• Solar electric propulsion system: 4 x 0.15 N plasma thrusters</li> <li>• Cruise solar arrays (28 m<sup>2</sup>) jettisoned after last SEP thrusting</li> <li>• Orbit solar arrays (10 m<sup>2</sup>): tiltable</li> <li>• X-band low-gain antennae, omni coverage</li> <li>• Ka-band high-gain antenna, 1.5m diameter</li> </ul>
<b>Launcher</b>	Dedicated launch with <b>Soyuz-LV Fregat</b> from Baikonur.

---

## 2 SCIENTIFIC RATIONALE

---

### 2.1 INTRODUCTION

The Sun's atmosphere and heliosphere represent uniquely accessible domains of space, where fundamental physical processes common to solar, astrophysical and laboratory plasmas can be studied under conditions impossible to duplicate on Earth and in detail not possible to achieve at astronomical distances.

Through a novel orbital design, the Solar Orbiter will explore *in-situ* the innermost heliosphere and will scrutinise, through high-resolution remote-sensing, the Sun and its atmosphere, while flying closer to the Sun than any other spacecraft and out of the ecliptic to higher latitudes. From there, the Solar Orbiter will provide the first observations of the polar regions of the Sun and the whole equatorial corona.

The results from missions such as Helios, Ulysses, Yohkoh, SOHO and TRACE have advanced enormously our understanding of the solar corona and the associated solar wind and three-dimensional heliosphere. However, we have reached the point where further *in-situ* measurements, now much closer to the Sun, together with high-resolution imaging and spectroscopy from a near-Sun and out-of-ecliptic perspective, promise to bring about major breakthroughs in solar and heliospheric physics.

There are four totally novel aspects to the Solar Orbiter mission, which allow unique science investigations to be performed. These are:

- Close-up remote sensing observations of the magnetised solar atmosphere providing unprecedented high-resolution;
- Unique heliosynchronous observations enabling us to understand the links between solar and heliospheric processes;
- *In-situ* measurements of the unexplored inner heliosphere;
- First out-of-ecliptic imaging and spectroscopic observations of the solar poles and equatorial corona from high latitudes.

The next four sections describe the new science and advances which will be made in these four areas.

### 2.2 THE SUN'S MAGNETISED PLASMA: CLOSE-UP OBSERVATIONS OF THE SOLAR ATMOSPHERE

The high-resolution imaging of the solar atmosphere will represent a major step forward by providing an order of magnitude improvement in spatial resolution over past missions. The Solar Orbiter instruments will, in concert, enable us to analyse thoroughly the time-variability, evolution and fine-scale structure of the dynamic chromosphere, transition region and corona, to study the Sun's magnetic activity on multiple scales, to investigate energetic particle acceleration, confinement and release, and to reveal plasma and radiation processes underlying the heating of the chromosphere and corona. The Sun is the only star that can be resolved at the level at which the physical processes responsible for magnetic activity take place.

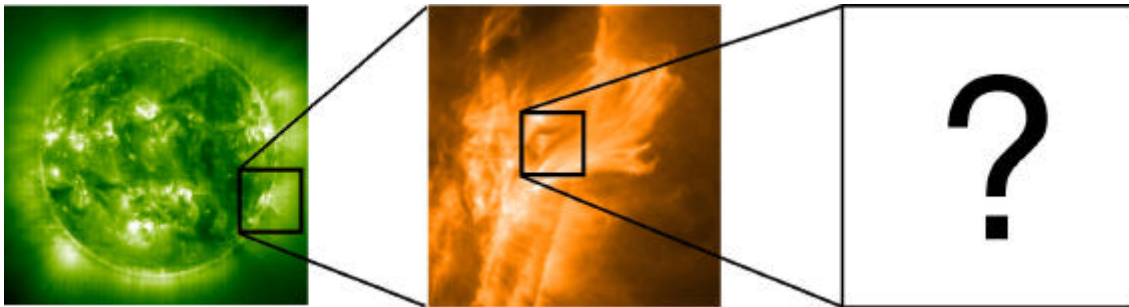


**Figure 2.1:** High-resolution field of view of the Solar Orbiter (right) as compared with EIT on SOHO (left) and TRACE (middle). Pixel size on the Sun of EIT and TRACE are 1850 and 350 km, respectively. The EUV imager on the Solar Orbiter will have a pixel size of 35 km on the Sun.

### 2.2.1 Photospheric magnetic flux elements

While our basic understanding of the equilibrium properties of the Sun has been validated by helioseismology, most notably by the impressive results from SOHO, our understanding of the non-equilibrium properties – primarily associated with magnetic fields – remains poor. Magnetic fields play a crucial role throughout astrophysics, ranging from the formation of stars to the extraction of energy from supermassive black holes in galactic nuclei. The Sun provides a natural laboratory for the study of cosmic magnetism under conditions not accessible on Earth and on scales not resolvable in distant astronomical objects.

A key goal of the Solar Orbiter is to advance our understanding of solar magnetism by measuring the structure and dynamics of the magnetic field at the solar surface down to its fundamental length scale. The major part of the magnetic flux permeating the solar photosphere outside sunspots is concentrated in small flux tubes of kilo-Gauss field strength. The scale of these magnetic flux tubes is believed to be determined by the pressure scale height, which is about 100 km. This is also near the typical photon mean free path at the photosphere whose dynamics is controlled largely by radiation processes at this scale.

The structure and dynamics of these fundamental elements of the near-surface magnetic field has profound implications for a number of basic questions:

- How do magnetic foot-point motion, wave excitation, flux cancellation and reconnection contribute to the flux of mechanical energy into the corona?
- In what way do the emergence, evolution and removal of magnetic flux elements determine the magnetic flux budget of the Sun? Is there a local dynamo operating on the scale of granulation?
- What is the origin of the facular contribution to the variability of the solar constant?
- What is the physics of the interaction between convection and magnetism?

Answers to these questions require the study of magnetic flux elements on their intrinsic spatial scale (<100 km). The Solar Orbiter will allow us to achieve this resolution, providing observations of magnetic field emergence, dynamics, twist, shearing, mutual interactions and possible coalescence and subduction in order to follow the evolution and understand the life cycles of magnetic flux elements.

### 2.2.2 Basic processes and fundamental scales in the magnetised solar atmosphere

We wish to understand the basic processes on all scales in the solar atmosphere, e.g. magnetic processes leading to particle acceleration or heating. It has been realised recently that very small-scale processes are at work in the solar atmosphere. For example, theoreticians have pointed out the difficulty of having both large-scale and rapid magnetic reconnection. This led to the concept of heating through numerous, globally distributed, small-scale “events” for which observers have candidates (e.g. SOHO observations of explosive events). Numerical simulations have been performed in the frame of Self-Organised Criticality or Cell Automation models whose outputs, in terms of temporal fluctuations and statistical properties, compare well with observations. Moreover, it seems that the observed distribution laws determined from SOHO data have self-similarity properties which point at sub-resolution processes. The nanoflare model of Parker is just an example of such models.

Whatever the scale, magnetic reconnection leads to particle dissipative heating and acceleration, and wave generation. Particle acceleration and wave dissipation have the net effect on the lower solar atmosphere of a local kinetic energy increase which can be revealed through high resolution extreme ultraviolet (EUV) imaging and spectroscopy. Wave propagation can be traced from the source site to the region of dissipation through observations of EUV-line broadening and Doppler shifts.

Between the very small scales implied by the above processes and the sizes of the smallest observed features, there are intermediate plasma scales. Indications of these intermediate scales are provided by the very small values of the filling factor derived from observations made of a large variety of solar structures. Thus, the transition region and inner corona are highly structured at scales even below those presently resolvable by SOHO and TRACE, and involve hot and cold plasmas at all temperatures between  $10^4$  K and  $10^7$  K. Widely differing temperature plasmas often co-exist side by side in hierarchies of filamentary structures, channelled by the magnetic field, which together form the solar atmosphere.

Given the high spatial resolution due to the spacecraft’s proximity to the Sun, combined with high temporal and spectral resolution, and multi-wavelength coverage, the Solar Orbiter will measure the signatures of the basic processes and the elementary structures of the solar atmosphere, providing plasma diagnostic information over the full temperature range existing in the solar atmosphere. This will enable

us to understand their nature and importance in the mass and energy budget of the solar atmosphere. For example, the Solar Orbiter will be used to measure

- the outflow and accelerated particles from magnetic reconnection sites on all scales,
- the proper motion, line broadening and Doppler shifts associated with wave propagation,
- the scale properties of MHD turbulence,
- the scales and evolution of the elementary structures.

### **2.2.3 Waves in the corona**

Magnetohydrodynamic waves generated in the photosphere by convective motion are primarily of low frequency. Small-scale magnetic activity is expected to continually produce waves. Their dissipation could involve cyclotron damping, which is observed to operate in the solar wind. The Solar Orbiter will make the first observations of such plasma processes from a near-Sun perspective and thus address the extended heating of the outer corona. In the small-scale magnetic structures of the strongly inhomogeneous network fields higher-frequency waves could be excited up to the kilo-Hertz range. Such waves would transfer their energy, e.g. into the transverse kinetic degrees of freedom of the protons, and particularly the heavy ions, and thereby heat the particles very effectively to high kinetic temperatures, a process for which the UVCS and SUMER instruments on SOHO have recently confirmed evidence in the strong Doppler broadening of emission lines.

Due to its proximity to the heating sites in the corona and the high sensitivity and spatial resolution of its instrumentation, the Solar Orbiter will for the first time be able to

- see very dim emissions, which are not visible from 1 AU due to the low density of the gas and the high contrast in emissivity, and long lines of sight; these difficulties are not encountered when observing plasma confined in small loops,
- resolve and diagnose dilute plasma on open fields and the outflow in coronal funnels,
- search for evidence of high-frequency waves in the corona (with reasonable chances of success due to the high temporal and spatial resolving capabilities of the dedicated instrumentation).

### **2.2.4 Coronal magnetic field**

A key scientific objective of the Solar Orbiter is to study the emergence and the cancellation of photospheric magnetic flux (the latter is the disappearance of opposite polarity regions in close contact), and to investigate the consequences of such processes for the overlying global coronal magnetic loops and for the chromospheric and transition region magnetic network. Flux cancellations are known to be the origin of various active phenomena, such as filament formation and eruption, evolution of small points of emission in radio, ultraviolet or X rays, or the occurrence of flares.

Magnetograms combined with EUV images as well as EUV spectra at high spatial resolution are the key data necessary to understand the influence that small-scale magnetic activity has on the corona. Such co-ordinated observations should reveal basic processes at work throughout the solar atmosphere which are drivers of the solar wind acceleration or coronal heating. Thus, the detailed understanding of the fine-scale processes in the magnetic fields at the base of the solar atmosphere is an essential goal of this mission.

On a larger scale, coronal loops are the very building blocks of the outer solar atmosphere, ranging from small loops in active regions, through loop arcades to active region interconnecting loops and helmet streamers. Observations from Yohkoh, SOHO and TRACE in extreme ultraviolet and X-ray wavelengths have revealed a truly complex, highly dynamic environment with loops confining plasmas at widely varying temperatures even in adjacent loops. It is within such loop systems that we witness the most dramatic of solar phenomena, the solar flares and mass ejections, as magnetic loop systems interact or become unstable. The study of the interaction and evolution of loop systems, through high-resolution EUV mapping combined with fine-scale diagnostic analysis using high-resolution spectroscopic observations, will be a major activity for Solar Orbiter scientists in particular in an effort to understand processes leading to mass ejection and flaring.

The TRACE extreme ultraviolet observations in particular illustrate the existence of fine-scale structures in the coronal loops, and reveal continuous dynamic activity in particular at the smallest scales. There is strong evidence that the size of the actual brightness structures lies well below the best current spatial resolution. This points to the need for still higher spatial resolution, which, as in the visible, can be obtained by modest means with the Solar Orbiter.

The wide coverage of coronal temperatures by the telescopes on the Solar Orbiter will enable complete images to be obtained in fast cadence. From these the density, temperature and flow distributions can be derived reliably for the full range of magnetic structures, allowing detailed studies such that coronal heating processes in current sheets, shock fronts, or acceleration in small explosive events and rapid plasma jets become clearly visible and can be resolved in time and space for the first time.

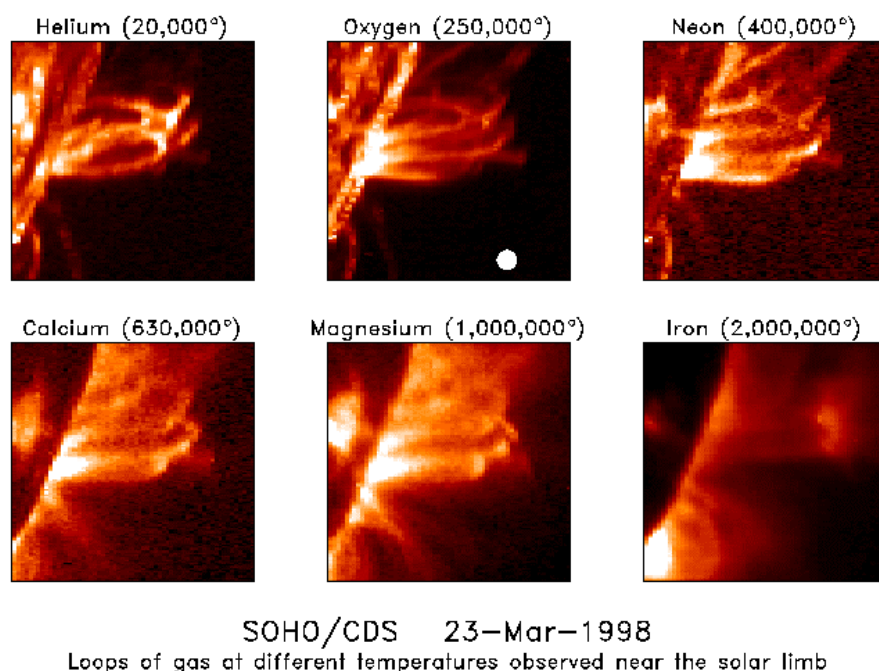


**Figure 2.2:** Images of plasma in magnetic loops observed on the Sun. In addition to hydrogen, the Sun's atmosphere contains ions of common elements like helium, oxygen and magnesium. The images are produced by detecting the emission lines from a number of ions, and their characteristic temperatures are given. One of the surprises that the SOHO/CDS data shows is that loops at widely differing temperatures can exist side-by-side in the same regions of the Sun's atmosphere. The disc plotted on the oxygen image shows the Earth to the same scale.

## 2.3 LINKING THE PHOTOSPHERE AND CORONA TO THE HELIOSPHERE: CO-ROTATION OBSERVATIONS

Studies of the evolution of solar features such as active regions, loops, prominences or sunspots are greatly complicated by the fact that their evolution time scales are comparable to the solar rotation period. Thus the evolution is entangled with other effects such as centre-to-limb variation, foreshortening and projection effects. In order to disentangle these effects it is necessary to co-rotate with the Sun. The Solar Orbiter will for the first time provide such an opportunity and will thus help resolve old and otherwise intractable problems related to the solar dynamo and the diffusion of the magnetic field across the solar surface. It will also allow for the first time to follow the evolution of sunspots and active regions as well as their influence on the corona above.

### 2.3.1 Global solar corona and solar wind

There are two characteristic types of solar corona and wind, prevailing at different heliographic latitude regions of the Sun and heliosphere. The high-speed flow is the basic equilibrium state of the solar wind. It is most conspicuous near solar minimum, when it emanates steadily from the magnetically open coronal holes around the poles, whereas the slow wind originates in a more gusty fashion from the equatorial streamers. These are for most of the time magnetically closed, but appear to open intermittently to release discrete mass ejections (CMEs) (see the subsequent Figure 2.4) and more continuously the slow wind embedding the heliospheric current sheet. The transient nature of the solar wind is also evident in the high variability of its abundances in helium and other heavier elements found in association with

large-scale magnetic activity on the Sun. The solar magnetic field in the equatorial regions reveals a rich morphology and many fine-scale structures, such as the low-latitude rays resembling the polar plumes, which are clearly evident in visible light coronagraph pictures and in the SOHO/EIT images. Remnants of these features are even found in the meso-scale stream variations of the solar wind, as observed *in-situ* by Helios and Ulysses and through interplanetary scintillations.

We can only resolve between the slow and transient solar wind, and understand them properly, by direct sampling close to the solar wind sources at a fixed heliographic longitude. It is a key advantage of the Solar Orbiter that from the co-rotational vantage point the temporal and spatial variations of the solar wind can be disentangled unambiguously. The observations to be made by the Solar Orbiter will concentrate on the slow streams and on solar disturbances associated with magnetic solar activity, flares, loops, erupting prominences, and CMEs, when the Solar Orbiter is close to the ecliptic, and on the fast streams, when the Solar Orbiter is close to maximum inclination. The temporal evolution and spatial structure of such phenomena at the coronal base will for the first time be measured at very high spatial ( $< 100$  km) and temporal resolution.

It is well known that the solar wind carries angular momentum from the Sun through kinetic and magnetic stresses. This will lead ultimately to a spin-down of the Sun's rotation within its remaining life time, a conclusion derived from the Helios measurements of the angular momentum as carried away by the wind near the ecliptic plane. The determination of the overall angular momentum loss associated with the solar wind outflow at higher latitudes is an important goal for the Solar Orbiter. Also, the analysis of the partial co-rotation of the outer corona and the detachment of the wind from solar rotation near the Alfvén surface may be possible by exploiting the co-rotational passes. Such measurements will produce novel results concerning the global angular momentum loss of the Sun as a star, which is an important issue in astrophysics.

The Solar Orbiter mission provides unique possibilities for complementary remote sensing and *in-situ* observations of the Sun from close distances (perihelion of 45 solar radii). Unprecedented spatial resolution at scales below 100 km will be achieved in the images obtained in various wavelength bands. Solar rotation will have a negligible influence on the observations during the heliosynchronous orbital phases of the mission. This will allow us to separate spatial from temporal variations. Therefore, time variability of the magnetic field and its optical and interplanetary-particles manifestations can be studied extensively for many days at a given heliographic longitude. The favourable vantage points of the Solar Orbiter along a heliosynchronous trajectory are unattainable by any other means.

The scientific success of the Solar Orbiter mission in this area is ensured by a comprehensive and well-focused suite of *in-situ* and remote-sensing instruments, which allow the local plasma and field environment to be connected with its plasma and magnetic sources on the Sun, and thus to establish spatial and temporal links with the location and evolution of these source regions in the highly structured and widely varying solar atmosphere. The Solar Orbiter will fly through field lines with foot points in the fields of view of its imagers, and therefore the characterisation of the properties of the plasma and its sources can be made, essentially by virtue of the co-rotation of the spacecraft with the Sun during the perihelion passes.

### **2.3.2 Global coronal sources of the solar wind**

Helios and Ulysses have clarified the global origin of the fast and slow solar wind in the large-scale corona. More recently, SUMER on SOHO has provided intriguing insight into the small-scale sources of the fast solar wind (see Figure 2.3). However, the detailed origin of the slow wind remains unclear. There are two main alternative ideas about the origin of the slow solar wind. One is that it arises from the outer edges of coronal holes, in magnetic field regions continuously open to interplanetary space. The other is that the slow wind arises in the middle and lower corona from the tops of helmet streamers, which are primarily closed magnetic field regions but do open intermittently to release the flow at heights beyond about two solar radii in the form of plasma blobs or plasmoids. Perhaps the slow wind consists of these two types of flow that intermingle at a few solar radii. The remote sensing observations of the corona combined with *in-situ* solar wind observations made by the Solar Orbiter during the co-rotational passes will allow us to distinguish between these two hypotheses, by providing accurate connections of *in-situ* solar wind structures with remotely-sensed coronal structures.

### 2.3.3 Magnetic network

The supergranulation network, which dominates the chromospheric plasma dynamics, is apparent in the EUV emission pattern as seen by the SUMER instrument on SOHO. Magnetograms from SOHO have revealed the ubiquitous appearance of small magnetic bipoles at the solar surface. After emergence, the polarities separate and are carried to the network boundaries by the supergranular flow, where they merge with the pre-existing network flux. This leads to flux cancellation, submergence and reconnection events. The magnetograms also show that the magnetic field exists in the network in two components side-by-side, i.e. in uncanceled unipolar fields together with a carpet of closed loops and flux tubes. The small loops will either emerge or contract downwards and collide, and thus constitute a permanent source of energy, which can be tapped by the particles through magnetic field dissipation. Numerical simulations suggest that many of the bipolar structures have scales smaller than 100 km.

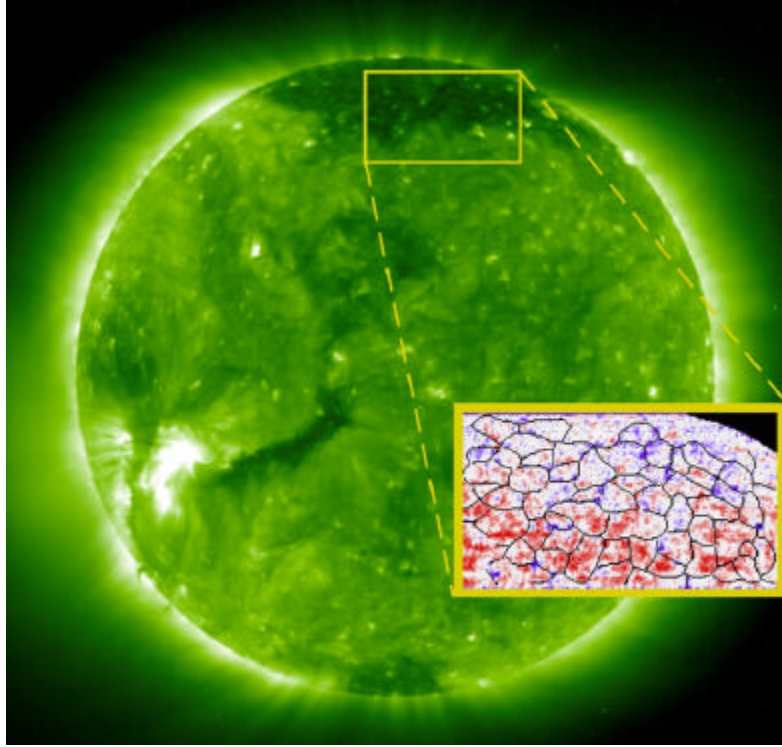


**Figure 2.3:** SOHO/SUMER observations of the solar-wind source regions and magnetic structure of the chromospheric network. The insert shows the measured Doppler shifts of Neon ions, indicating blue-shifts, i.e. outflow, at the network cell boundaries and lane junctions below the polar coronal hole, and red-shifts (downflow) in the network regions underlying the globally closed corona.

### 2.3.4 Boundaries and fine structures in the corona and solar wind

The boundaries and gradients between the fast and slow solar wind have been well characterised by the Helios and Ulysses spacecraft at 0.3 AU and beyond, but little is known about their microphysics and dynamics. For example, instabilities can be caused by velocity shear across a boundary and become a source of turbulence and friction, and thus alter the nature of the wind in the vicinity of stream boundaries and interaction regions. There are plenty of other fine-scale structures in the solar wind and corona, one example of which are the conspicuous plumes over the poles, which have been studied by SOHO in considerable detail. Plumes have been observed to extend beyond many solar radii, yet their *in-situ* signatures in the wind plasma are elusive. Material in plumes has been found to flow at much lower speeds than in the ambient darker lanes throughout the altitudes observed in coronal holes. By combining the Solar Orbiter data from the *in-situ* and remote-sensing instruments, we will be able to identify the genuine contributions of plumes to the fast wind.

Little is known currently about the projection of coronal substructures into the outer corona and near-Sun solar wind. There are many other meso-scale structures in the corona and particularly the slow solar wind, which is intrinsically variable in space and time and convects structures such as tangential discontinuities, the coronal origin of which remains a mystery. Many structures exist in the corona at a

wide variety of length scales. Structures very similar to the polar plumes have also been observed in interstreamer regions. At even smaller spatial scales, coronal spikes and EUV spicules with widths of order  $10^3$  km have been observed. Ground-based white light eclipse images show elongated and thin, thread-like structures that extend outward in the innermost corona and seem to be ubiquitous outside coronal holes. Further evidence of fine structure well below the spatial resolution of current optical instruments comes from interplanetary radio observations. The Solar Orbiter, by virtue of its proximity to the corona will be able to resolve such features with sufficient brightness contrast. It will trace their extensions from the solar atmosphere into space by measuring the remnant signatures in the more distant solar wind during the perihelion passes. Thus, the Solar Orbiter will examine fine-scale structures in the corona at much higher spatial resolution than ever employed before and associate them with their interplanetary manifestations.

### **2.3.5 Connections between the internal plasma states of the solar corona and the solar wind**

There are many closely-connected heliospheric and solar science objectives of the Solar Orbiter, which can be addressed in particular during the co-rotation passes enabling steady observational conditions from a fixed vantage point. The principal goals are:

- to determine the relationship between coronal and solar wind structure on all scales that can be resolved;
- to identify the coronal energy source for the solar wind and trace by remote-sensing the flow of energy through the different layers of the atmosphere.

Remnants of the processes that heat and accelerate the ions will still be detectable in the *in-situ* measured microscopic features of the solar wind particle velocity distributions (such as double ion beams, minor ion differential streaming, pronounced temperature anisotropies indicating cyclotron or Landau resonance between plasma waves and particles, or heat flux-carrying suprathermal tails, as already observed by Helios and Ulysses) and will allow clear inferences to be made on the coronal plasma processes. A related goal is to determine the role of turbulence and waves in heating the corona, accelerating the solar wind, and energising particles, and to determine how the particle populations, plasma waves, and magnetohydrodynamic turbulence evolve together with heliocentric distance in the inner-most heliosphere.

### **2.3.6 Coronal and solar wind abundances and fractionation effects**

Understanding the abundances of elements in the Sun and solar wind is an important issue in solar physics. The solar wind carries the material delivered from the outer convective zone of the Sun into the heliosphere. With the exception of the H and He isotopes, the elemental composition of the outer convective zone is close to the proto-solar nebula composition. The element helium, which is not visible in the photosphere, is highly variable and rather under-abundant in the solar wind and solar energetic particles. The two types of solar wind, fast and slow, differ considerably in their charge-state composition (a coronal signature) and elemental abundance (a chromospheric signature). Apparently, the elemental fractionation processes are fundamentally different in the fast and slow solar wind, although fractionation on the basis of the First Ionization Potential (FIP) is present to a different degree in both types of wind. The FIP effect seems to be active also in the chromosphere beneath the polar coronal holes, in the sources of the fast wind, but at a reduced strength. Charge-state spectra are also differing in the two types of streams: thermal equilibrium spectra prevail in fast streams, indicating a simple freezing-in process. The slow wind charge-state distribution, on the other hand, shows an excess of high charge states and indicates that different coronal temperature regimes may coexist in the source region.

The Solar Orbiter, while taking high-resolution images and making spectroscopic measurements of solar wind source regions that are magnetically linked to the spacecraft location and making simultaneous, *in-situ* measurements over the long co-rotation intervals, is ideally suited to address the critical issues of the chromospheric fractionation process. The coronagraph on the Solar Orbiter will determine for the first time the helium abundance (high FIP element) in those atmospheric layers where the acceleration of the slow and fast streams actually occurs, and where the charge states freeze in. The results expected will provide keys for the understanding of the processes at the origin of the solar wind and of the elemental composition in the heliosphere.

For the Solar Orbiter a new class of UV and visible-light coronagraph observations is envisioned, aiming at measuring directly and characterising in detail the properties of the two most abundant



elements, hydrogen and helium. In particular, this innovation will provide new and better views of the solar corona than possible with SOHO presently and STEREO in the future. In particular, the Solar Orbiter will be able to provide

- the first UV images of the full corona for the two most abundant elements,
- the first global maps of the solar wind outflow,
- the first images of the He II coronal emission.

The Solar Orbiter will allow us to do these new measurements of the corona also from out of the ecliptic, and will thus provide the first view of the entire equatorial corona and global observations of the coronal expansion near the equator.

### 2.3.7 Coronal transients

A subject that has recently attained much attention is forecasting of “space weather”. It is concerned with transient events such as flares, coronal mass ejections (CMEs), eruptive prominences, and shock waves and their impacts upon the Earth's magnetosphere and atmosphere. Fundamental questions in this area have not been answered, e.g.,

- What are the indicators for imminent violent eruptions? Can they be predicted?
- Why are there disparate types of solar transients?
- What determines their propagation properties?
- How far around the Sun do the resulting shock waves reach?

The Solar Orbiter will be ideally located, being closer to the sources of transients in the solar atmosphere, to measure the input into the heliosphere and to determine the boundary conditions near the Sun. These dramatic events can literally shatter the whole heliosphere, and their effects can be felt at all planets. The Solar Orbiter will be a key link in a chain of solar terrestrial observatories to be stationed in Earth's orbit and at the libration points in that it provides near-real-time event alerts from its unique orbit close to the Sun.

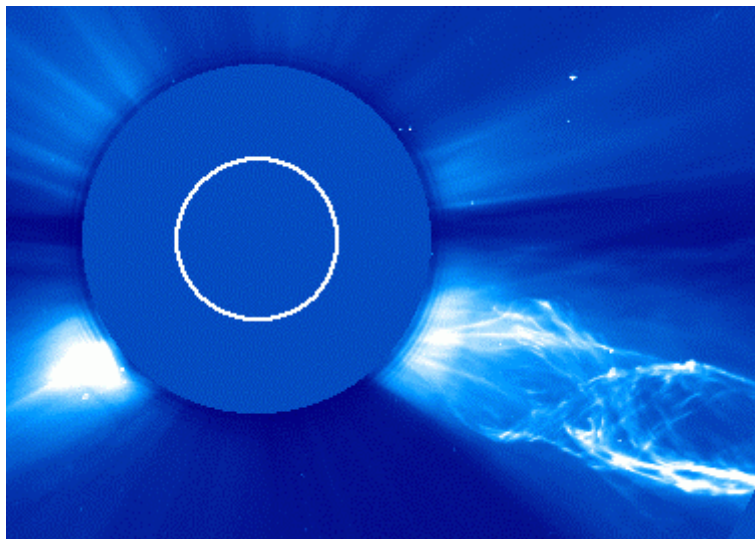


**Figure 2.4:** Giant coronal mass ejection as seen by LASCO on SOHO in 1998. The filament material of the ejected prominence exhibits twisted helix-shaped structures. The Solar Orbiter at its perihelion of  $45 R_s$  would be able to measure the ejecta *in-situ* and out of the ecliptic in much more detail than possible from the Earth's orbit.

The Solar Orbiter will provide high resolution images of the solar atmosphere as well as allow plasma diagnostics using spectroscopy. These, combined with a capability to determine the photospheric fields at the footpoints of coronal loops, provide the tools for a thorough, detailed analysis of the processes leading to eruptive events. The influence of the eruptions on the outer corona can be determined with coronagraph instrumentation, and the associated effects on the interplanetary medium can be studied with in-situ instrumentation without significant delays or transport-related changes of the particles and fields. The multi-wavelength, multi-disciplinary approach of the Solar Orbiter, combined with the novel location, produces a powerful tool for studies of the influence of eruptive events such as CMEs on interplanetary space.

## 2.4 PARTICLES AND FIELDS: *IN-SITU* MEASUREMENTS IN THE INNER HELIOSPHERE

According to recent SOHO findings, one must conclude that coronal expansion arises because of the high temperatures of the coronal ions, with the minor species reaching even  $10^8$  K at a few solar radii. In contrast, electrons are comparatively cool, in fact they are found to hardly reach the canonical coronal temperature of  $10^6$  K, and consequently the electric field (related to the electron partial pressure gradient) has a minor role in accelerating the ions. The high pressure of the coronal ions and the low pressure of the local interstellar medium lead to a supersonic solar wind extending to long distances from the Sun to some 100 AU. Yet, even after the SOHO mission the detailed physical mechanisms that heat the corona and accelerate the plasma to supersonic speed remain poorly understood, because the resolution of the SOHO imagers and spectrometers were still not sufficient, and because the solar wind plasma has never been directly sampled closer to the Sun than the Helios perihelion (0.3 AU).

The Solar Orbiter will provide the first opportunity of going closer to the Sun and into the inner heliosphere to 0.21 AU, but unlike Helios and Ulysses, the Solar Orbiter will also carry powerful, high-resolution optical instruments together with the *in-situ* instruments. In particular, the plasma and field instruments will have high temporal resolutions, ranging between 0.01 s and 1 s, and offer unique possibilities for resolving physical processes at their intrinsic scales. Therefore, this mission will reveal new insights in the plasma kinetic processes that structure the Sun's atmosphere, heat the extended corona and accelerate the solar wind as well as energetic particles.

### 2.4.1 Microstate of the interplanetary solar wind

The ultimate causes of interplanetary kinetic phenomena are to be found in the dynamic corona itself. The closer a spacecraft comes to the Sun the more likely it is to detect remnants of coronal heating and related plasma processes, occurring on a broad range of scales in space and time. The radial evolution of the internal state of the expanding wind resembles a complicated relaxation process, in which free energy stored in the form of stream structure and shear as well as in non-Maxwellian particle velocity distributions (see Figure 2.5) is converted into wave and turbulence energy.

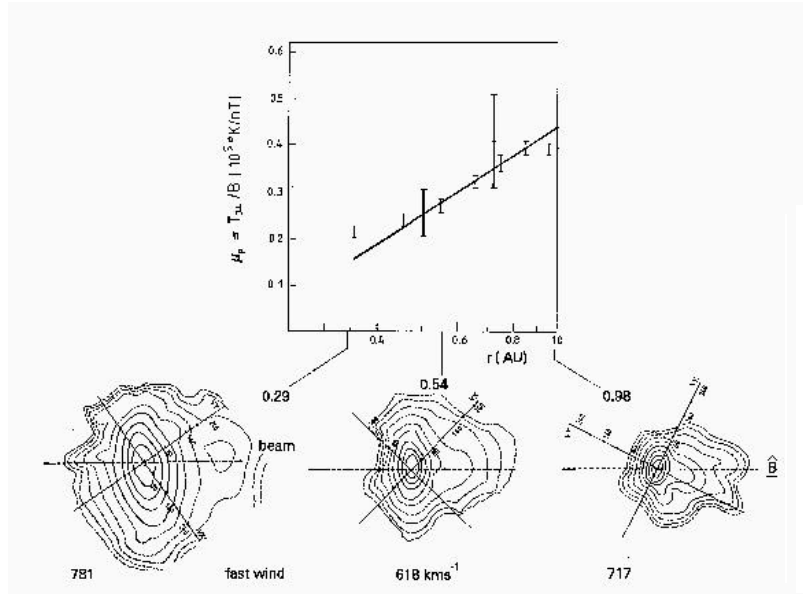


**Figure 2.5:** Bottom: Solar wind proton distribution functions illustrating non-thermal features such as temperature anisotropies and proton beams along the magnetic field. Top: Proton magnetic moment versus distance from the Sun. The radial increase indicates continuous heating in interplanetary space.

Plasma waves in the collisionless solar corona and wind play a role analogous to collisions in ordinary fluids. These wave modes can theoretically be excited by a variety of free energy sources, including drifts, currents, temperature anisotropies and beams, which must be resolved in detail. All the wave modes of primary importance together with the ions and electrons will be measured by the Solar Orbiter at high time resolution, in order to provide the comprehensive wave and particles diagnostics necessary to study the wave-particle interactions and kinetic processes.

The Solar Orbiter, while approaching the Sun to about 0.2 AU with its plasma and wave analysers, will enable high-resolution measurements of kinetic processes, and this has great potential for unexpected discoveries. It will address fundamental solar wind science and key plasma-physics questions such as

- How do particle distributions develop velocity-space gradients and deviations from Maxwellians?

- What processes drive plasma instabilities and cause wave growth and damping?
- How are new-born ions, e.g., sputtered from dust grains, incorporated into the solar wind flow in the inner heliosphere?
- What regulates transport and ensures the observed fluid behaviour in the collisionless solar wind?
- What are the radial, latitudinal and longitudinal gradients of plasma parameters in the inner heliosphere?
- What is the microstructure of, e.g. stream interfaces and boundary layers near the Sun?
- How does the chemical and charge-state composition of the plasma vary spatially?

#### 2.4.2 Solar wind ions as tracers of coronal structures

The solar wind carries information on its coronal source regions, e.g. through its elemental and isotope composition, and the ionisation states of the various atoms. At the coronal base, a compositional bias is introduced according to the first ionisation potential (FIP) of the elements. This FIP effect appears to be significantly different for slow and fast solar wind flows. Further, the ionisation state of various species indicates that the slow wind must have undergone substantially more heating than the fast wind. These signatures will be used for the first time to resolve fine structures and boundaries in the solar wind. This diagnostic technique works most reliably close to the Sun where the flow has not yet been processed (compressed, deflected, etc.) by interactions between streams of different speed. With Helios it was found that at least in the high-speed wind a basic flow-tube structure was still recognisable *in-situ* at 0.3 AU. The scale-size observed matches that of supergranules fairly well, if an appropriate flux-tube expansion is taken into account. The Solar Orbiter, using modern ion-composition instruments and being closer to the Sun, will

- reveal, through precise determination of compositional variations, the fine structures in all types of solar wind;
- link the flow tubes directly with the underlying chromospheric network observed remotely;
- identify pick-up ions stemming from dust and interplanetary sources.

#### 2.4.3 Magnetohydrodynamic turbulence

The solar wind plasma is in a highly turbulent state composed of various components. The energetically dominant component consists of largely incompressible Alfvénic fluctuations (see Figure 2.6 for the power spectrum). The minor component has a much lower amplitude than the Alfvénic fluctuations, is compressible and clearly enhanced in the mixed low-speed flows. The Solar Orbiter will scan a belt ranging roughly from  $-40^\circ$  to  $40^\circ$  in heliographic latitude, while being within 0.3 AU of the Sun. From these vantage points the Solar Orbiter will be able to answer important questions such as:

- How does MHD turbulence evolve spatially at higher latitudes near the Sun?
- What are the crucial conditions for *in-situ* turbulence generation?
- How does the turbulence pattern vary with stream structure closer to the Sun?

The overall radial trends as seen by Ulysses and Helios suggest strong variations of the local production rate of the Alfvénic fluctuations in the region just inside 0.3 AU. The reduction of the perihelion distance from 0.3 AU (Helios) to 0.2 AU (Solar Orbiter) will offer unique opportunities to study the local generation, non-linear coupling and spatial evolution of MHD waves near the Sun. Measuring Alfvénic fluctuations and MHD turbulence *in-situ* represents also a means of diagnosing their coronal sources. The Solar Orbiter will address these issues from its unique vantage point and help to answer basic questions such as:

- How and where are Alfvénic fluctuations generated in the solar corona?
- How does MHD turbulence evolve radially and dissipate in the inner heliosphere?
- Do the spectra contain indications or relics of high-frequency wave heating of the corona?

The solar wind is the only available plasma “laboratory” where detailed studies of MHD turbulence can be carried out free from interference with spatial boundaries, and in the important domain of very large magnetic Reynolds numbers. Detailed comparison between experimental *in-situ* data and theoretical concepts will allow us to put MHD turbulence theory on more solid physical ground, which will be of critical importance for understanding the solar (stellar) coronal heating mechanism and the role or turbulence in the solar (a stellar) wind.

#### 2.4.4 Acceleration and transport of solar energetic particles

A permanent source of difficulty has been our inability to predict the intensity of solar energetic particles at the Earth from observed transient activity on the Sun. An important part of the problem is that we do not know the suprathermal population that feeds the acceleration processes near the Sun. The efficiency for transferring energy from flares to energetic particles cannot be inferred from remote observations, because an unknown fraction of the accelerated ions remain trapped by strong magnetic fields near the Sun for a significant time after acceleration. Subsequent  $\gamma$ -ray and neutron emissions resulting from their eventual loss to the atmosphere are often too weak to be observable. Present observations indicate that small transients occur sufficiently often to allow a determination of the efficiency, e.g. by neutrons as proxies for the magnetically bound component. Our ability to solve this issue will be greatly enhanced by the Solar Orbiter, because during its multiple perihelion passages we will

- gain a better knowledge of the source spectrum;
- obtain new observations on particle motion in the hypothetical storage region;
- measure changes in the spectrum as the ions and electrons propagate from the Sun to the spacecraft after escape from the trapping region.

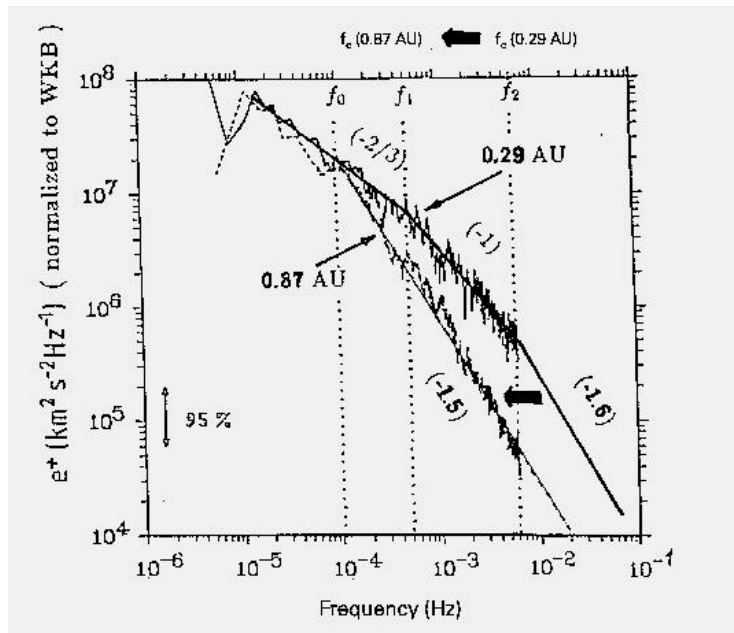


**Figure 2.6:** Normalised power spectra of Alfvénic fluctuations in the fast solar wind. The spectra steepen with radial distance from the Sun and indicate (see arrow) ongoing wave dissipation, leading to ion heating.

The Solar Orbiter will for the first time investigate the particle environment in close proximity to the different source regions on the Sun, such as coronal holes, streamers, coronal mass ejections (CMEs) and associated shocks, active regions, and flare locations. With regard to CMEs in particular, the Solar Orbiter will

- determine the solar source conditions for different particle species (e.g. e, p,  $^3\text{He}$ , heavy ions, p/He ratios) from composition measurements, energy spectra and time evolution;
- distinguish clearly between gradual (shock-associated) CME events and impulsive flare-type events related to magnetic reconnection;
- study the effects of particle acceleration and turbulence-moderated propagation at different locations with respect to the CME centre;
- find the differences between the particle signatures associated with parallel and perpendicular shocks at the east and west flanks of CMEs;
- probe the effects of magnetic reconfigurations in the aftermath of CME launches, at times when the acceleration processes still occur in the corona;
- detect perhaps for the first time energetic particle populations from microflares, a measurement which is not possible further away from Sun due to background problems.

In addition, we can study with the Solar Orbiter important global aspects of the Sun and heliosphere (see Figure 2.7) by

- utilising the energetic particles as probes for the coronal and heliospheric magnetic field;
- analysing the propagation of solar particles and modulation of galactic cosmic rays.

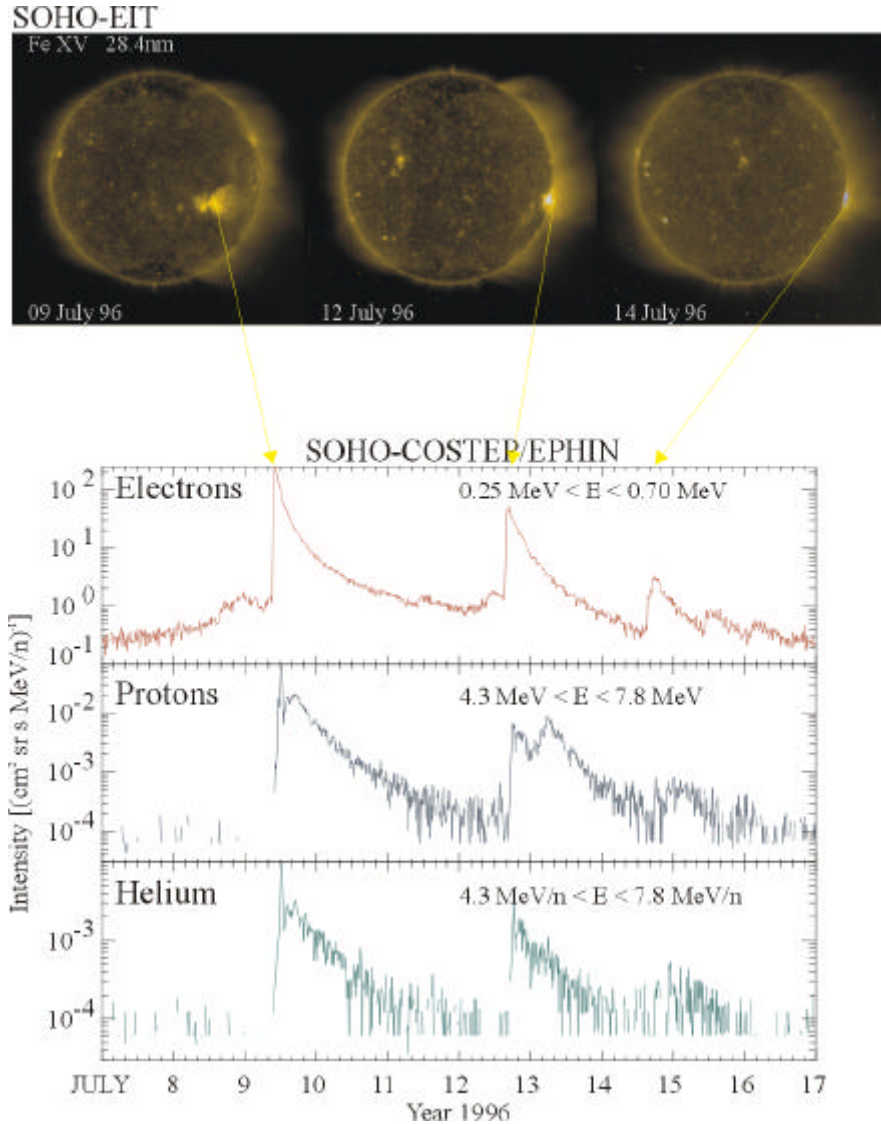


**Figure 2.7:** A series of solar energetic particle events observed in July 1996 with the COSTEP/EPHIN experiment onboard SOHO. The upper panel shows images of the Sun taken on July 9, 12, 14 with SOHO/EIT in Fe XV (28.4 nm). The bottom panel shows intensities of 0.25-0.7 MeV electron, 4.3-7.8 MeV proton and 4.3-7.8 MeV/n helium nuclei measured with the COSTEP/EPHIN. The intensity increases of energetic particles at SOHO were caused by flares and coronal mass ejections in an active region in the Sun's western hemisphere.

Generally, the processes which accelerate particles to very high energies are of great interest in astrophysics. Observations of energetic particles close to their sources on the Sun will allow us to study our nearest star, the Sun, as a particle accelerator.

#### 2.4.5 Neutral particles from the Sun

Neutral atoms are widespread in the heliosphere and their energies are in the range from a few eV to more than 100 keV. Contrary to charged particles, they can travel large distances through space, undisturbed by the interplanetary magnetic field. In the solar corona, the neutral hydrogen atoms are closely coupled to the emerging solar wind plasma and give rise to the prominent L $\alpha$  corona. The ratio of the densities of hydrogen and protons is very low,  $10^{-6}$  to  $10^{-7}$ , and the neutral particles therefore have a negligible impact on the plasma. The neutral atoms are a trace particle population originating from the solar wind plasma by charge exchange.

The in-situ observation of neutral hydrogen by a space-borne instrument in the vicinity of the Sun would be a "first" and an essential contribution to our knowledge of the solar corona. The Solar Orbiter provides the opportunity of observing neutral particles emitted from the Sun. By measuring the "neutral

solar wind”, we obtain an independent means of determining the solar wind velocity profile in the outer corona.

In addition, Energetic Neutral Atoms (ENAs) produced by charge-exchange processes in interplanetary space can be detected by the Solar Orbiter for the first time near the Sun. ENAs may be used for imaging the outer solar corona. The ENAs originating from a seed-ion population or background neutral gas will allow us to derive properties of the background gas as well as to remotely sense the energy distribution, spatial distribution and temporal evolution of the seed populations. The neutral gas could be either of interstellar origin or from a neutral component stemming from the solar wind itself, e.g. being produced by neutralisation of solar wind ions on interplanetary dust particles close to the Sun. Possible seed ion populations are the solar wind protons, energetic solar particles and anomalous cosmic rays. Measuring the neutrals means probing and inferring the physical properties of the circumsolar dust. Such measurements have great potential for unforeseen discoveries.

Direct observation of the neutral atoms will help to refine the physical models of the  $L\alpha$  corona, by providing information complementing the remote-sensing observations of the coronagraph on the Solar Orbiter, and thus will enhance our understanding of the coronal plasma processes and wave-particle interactions out to a few solar radii. Further out, within a few solar radii more and more of the neutral atoms become de-coupled from the plasma.

Coronal mass ejections (CMEs) are known to include a wide range of ion charge distributions, originating from very cold to very hot coronal plasma. Consequently, one expects to find also neutral particles in CME-related solar wind. However, up to now, no direct observations of such neutral particles exist. Since these particles are not magnetically trapped, they could give a clue to the understanding of the trigger process of the CMEs. This would be another "first" and important observation of the Solar Orbiter.

#### **2.4.6 Circumsolar and interplanetary dust**

The Solar Orbiter will also measure the size and flux distribution of dust particles surrounding the Sun. These particles are known to produce the zodiacal light and the F-corona and may stem from Sun-grazing comets. The large number of Sun-grazers discovered by the SOHO coronagraphs indicates that these comets must be a prolific dust source.

The observed distribution of interplanetary dust particles (IDPs), i.e. micrometeorites of submicron to millimetre size, forms a flat spheroid centred on the ecliptic plane. Its spatial density decreases with increasing heliocentric distance and increasing latitude. Different forces and effects are acting on IDPs: gravitational attraction, radiation pressure, corpuscular pressure, magnetic forces, planetary perturbations, erosion processes (sputtering, sublimation), and mutual catastrophic collisions. IDPs originate from comets and asteroids or even from interstellar space. They approach the Sun on time scales of 10000 to 100000 years due to the deceleration by the Poynting-Robertson effect. In the vicinity of the Sun, IDPs go through a complicated evolution process, which depends on the particle properties and chemical composition, caused by their progressive sublimation, as their temperature becomes higher.

On the other hand, these processes are the source of an additional ion population in the solar wind: outgassing, sublimation and sputtering produce neutrals which are then ionised and picked up by the solar wind. The study of these particles will contribute significantly to the understanding of the evolution of interplanetary dust in the vicinity of the Sun. The interaction between the plasma and the solar magnetic field with IDPs makes this picture even more complex: far-reaching, dense coronal structures as well as the changing pattern of the magnetic field can perturb the IDPs dynamics.

The present understanding of IDPs results from Zodiacal Light observations, *in-situ* impact detectors and laboratory analysis of collected particles. The processes taking place in the circumsolar region remain poorly understood. Their description is, to a large extent, based on theoretical studies. The possibilities of remote sensing experiments are limited due to instrumental problems. Especially the chemical composition and the dynamics of submicron grains can only be investigated by *in-situ* methods. The dust observations on the Solar Orbiter will

- render possible the first *in-situ* detection of grains which have suffered extreme radiation damage and corpuscular impacts, processes relevant in accretion discs and important for stellar winds from late-type stars and for star- and stellar-system formation,
- help in determining the extent of the dust-free zone near the Sun;
- provide the potential for discovery of a dust disc fed partly by Sun-grazing comets;
- deliver data relevant for understanding the physics of protoplanetary discs.

### 2.4.7 Solar neutrons

A large fraction of the particles accelerated by flares (and microflares) interact in closed magnetic field lines of the solar atmosphere (at heights much less than  $3 R_{\odot}$ ) and do not escape into interplanetary space. They are detected through X-ray,  $\gamma$ -ray, microwave and decimetric-metric radio emissions, and through secondary particles, such as neutrons produced in interactions with the dense layers of the solar atmosphere. The neutron flux varies dramatically with distance from the Sun because of beta decay. Note that the maximum distance neutrons can reach is given by the product of their speed and their mean lifetime (which is only eight minutes for non-relativistic neutrons!). In fact, at the Earth's orbit neutrons with energies less than 100 MeV can not be detected at all. Very few solar neutron events have been reported as compared with several hundreds of  $\gamma$ -ray events. During the perihelion passages of the Solar Orbiter, it will be possible to measure directly also the less energetic neutrons for the first time.

Neutrons (and  $\gamma$ -rays) are produced in interactions between the primarily accelerated ions and the constituents of the solar atmosphere. Information about the composition and charge states of energetic particles can provide important insights into the existence of distinct phases of proton acceleration. This process is either very prompt and occurs within seconds of the release of flare energy, or it is delayed and associated with the shock wave possibly generated by the flare ejecta. The Solar Orbiter will provide new information about the first phase of this process and about nuclear reactions in the solar atmosphere. Thus, the Solar Orbiter will open up a new window: solar neutron astronomy.

### 2.4.8 Solar radio emission

The Sun is an intense source of thermal as well as nonthermal radio emission. The nonthermal radiation is generated by suprathermal and/or highly energetic electrons produced by sudden releases of magnetic energy in the active corona. Nonthermal radiation at frequencies below 1 GHz is generally assumed to be plasma radiation emitted near the local electron plasma frequency which is a unique function of the local electron density. Consequently, the higher and lower frequencies correspond to the inner and outer corona, respectively, and remote sensing of the radial electron density profile is possible.

In the corona the non-thermal radio radiation is generated by energetic electrons. The measurement of this radiation will allow us to study the plasma processes associated with such electron populations and to address questions as:

- What is the elementary process of magnetic energy release?
- How are ions and electrons accelerated up to high energies within a few seconds?
- What are the relationships between flares, coronal mass ejections, radio bursts, interplanetary shocks, and energetic particle events?
- How does the quiet Sun produce suprathermal particles?

The radio spectrometer data are particularly valuable since they will be obtained in connection with complementary data from the optical telescopes imaging the activity site, and data of the particles and fields instruments onboard. Detailed correlative studies between the coronal/interplanetary electrons and the radio waves they generate will be possible for the first time from a near-Sun and out-of-ecliptic vantage point on the Solar Orbiter.

## 2.5 THE SUN'S POLAR REGIONS AND EQUATORIAL CORONA: EXCURSION OUT OF THE ECLIPTIC

Despite the great achievements of Ulysses and SOHO, significant scientific questions remain unanswered. They will be addressed by the Solar Orbiter with its combination of high latitude vantage points and remote-sensing instruments. For example, progress in understanding the solar dynamo will depend on how well we understand differential rotation and the circumpolar and meridional flows near the poles of the Sun. Torsional oscillations associated with the magnetically-active latitudes seem to originate close to the polar regions and then propagate toward the equator. Are the meridional flows observed at lower latitudes and these torsional oscillations associated? The poles appear to rotate comparatively slowly, but the polar vortex is still not well characterised due to the serious limitations of in-ecliptic observations. The Solar Orbiter will provide the first opportunity to measure directly the magnetic field at the poles, as well as the surface and subsurface flows there. We therefore anticipate that some of the outstanding problems related to the origin of solar magnetism will be solved.

The large-scale unipolar character of the magnetic field in coronal holes leads to the fast solar wind which super-radially expands into the heliosphere. The Solar Orbiter offers the opportunity of sampling the fast wind at distances where the plasma has retained some memory of the acceleration processes.

With regard to the sites of acceleration, SOHO spectroscopic measurements have identified the special role of the network, but only through very difficult Doppler measurements affected by a foreshortened line of sight. High latitude observations allow a normal line of sight which will provide a definite answer to the role of the network.

Even with new dedicated missions such as STEREO, it is impossible to determine the mass distribution of large-scale structures such as streamers and the true longitudinal extent of Coronal Mass Ejections (CMEs). The Solar Orbiter will provide the first observations of the complete equatorial corona and its expansion in the equatorial plane. Furthermore, it will provide the third dimension of CMEs.

### **2.5.1 The Sun's polar magnetic field and the dynamo**

The internal structure and dynamics of the near polar regions of the Sun is of paramount importance, and perhaps *the* key to our understanding of the solar activity cycle. There are strong empirical indications that the magnetic properties of the polar regions at solar minimum determine the strength of the forthcoming solar maximum. It has been found that the value of the geomagnetic aa index at its minimum is related to the sunspot number during the ensuing maximum. At solar minimum this geomagnetic index mostly depends on the solar wind from the polar regions. This means that a new sunspot cycle starts in the polar regions. This idea was used successfully to make a correct prediction of the current solar cycle from direct measurements of the polar magnetic field. This has been called the "Solar Dynamo Amplitude index method".

However, our understanding of how the solar dynamo actually operates is still very poor. Apparently, the polar field is directly related to the dynamo process, presumably as a source of a poloidal field to be wound up by the differential rotation at the shear layer at the base of the convection zone. Theoretical models indicate that the meridional circulation pattern found by SOHO could be crucial for the solar dynamo. Such a circulation pattern transports surface magnetic flux toward the poles and downward to the shear layer. The models predict a substantial magnetic flux concentration near the poles. The Solar Orbiter will allow us

- to measure reliably the strength of the polar field for the first time, and thus
- to provide a new and crucial observational constraint for dynamo models.

Studying the internal properties of the polar regions will help to solve the puzzle of the solar cycle, and it will provide a better understanding of how the solar dynamo works and how other stars generate magnetic fields.

### **2.5.2 Polar rotation and internal flows**

The polar regions are extremely dynamic. There is evidence that the differential rotation near the poles may vary on a short time scale. Evidence has been found for a significant variation of the subsurface high-latitude rotation with the solar cycle. While there are large uncertainties in these measurements because of our limited view of the polar regions, it is evident that mapping the internal flows near the poles will improve our understanding of the mechanism of the differential rotation and its role in the global circulation of the Sun. Various dynamic phenomena in the polar regions of the solar atmosphere and corona also show close connection to the solar cycle, e.g. the "rush" of H $\alpha$  filaments to the poles near the periods of magnetic polarity reversals and the sudden increase of the coronal temperature during these periods.

However, there is no basic understanding of how these variations are related to each other and to the internal dynamo processes. Therefore, studying the polar regions of the Sun is fundamental to one of the key open questions of solar physics and astrophysics:

- How and why does the Sun vary?

With the advent of helioseismology from space, our knowledge of the solar interior has made considerable progress. SOHO has provided helioseismic data of extreme precision. Large-scale differential rotation has been mapped in most of the convection zone, and temporal variations in the zonal flows beneath the Sun's surface have been detected as the present activity cycle unfolds. There have been



unexpected and still controversial discoveries, such as a buried jet-like flow and a surprisingly slow rotation rate at high latitudes (see Figure 2.8a).

To complement the techniques of global seismology, which has no resolution in longitude and cannot distinguish the northern from the southern hemisphere, new techniques of local helioseismology have recently been developed. In particular, time-distance helioseismology gives the opportunity to make 3-D tomographic maps of the sub-photospheric temperature inhomogeneities, magnetic field and flows. An important result concerns the observation at depth of the poleward meridional circulation (see Figure 2.8b).

The Solar Orbiter offers a unique opportunity to learn about the polar regions of the Sun, which remain largely unexplored. The main objective will be to map rotation and meridional flows near the poles using time-distance helioseismology. One week of data is sufficient to derive the rotation rate in the upper convection zone, and confirm or refute the existence of the high-speed jet at  $75^\circ$ . We will also be able to study the convergence of the meridional flow at the poles and observe how and where the solar plasma dives back into the Sun. Convective motions over the poles, in particular supergranulation, will also be studied.

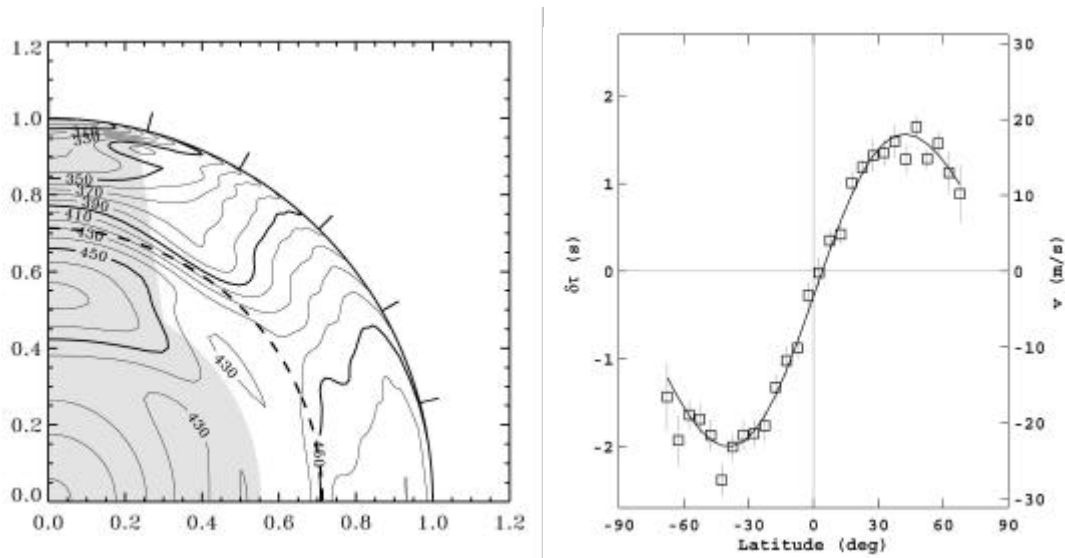


**Figure 2.8:** (a) Solar internal rotation. Lines are contours of constant angular velocity (in units of nHz). The uncertainty is large in the shaded region. Note the slow near-surface rotation at high latitudes, and the jet stream at latitude  $75^\circ$ . (b) Meridional circulation measured by time-distance helioseismology as a function of latitude. The scale on the left vertical axis gives the travel time difference in seconds between waves travelling in the southward and northward directions. On the right axis is the corresponding velocity, which is an average in the 34 Mm below the surface.

### 2.5.3 Polar observations of CMEs

The high inclinations to be reached by the Solar Orbiter will allow unique observations of CMEs and their distributions. This will allow us:

- to determine for the first time the longitudinal extent of CMEs,
- to provide in conjunction with a spacecraft in Earth orbit and ground-based observations a  $360^\circ$ -longitude observation of the entire Sun,
- to monitor global effects and to determine the extension of coronal waves associated with CMEs.

The high-latitude vantage point will allow us to determine for the first time the longitudinal extent of CMEs, a parameter which has never been measured yet is a basic measure of CME topology and is crucial for the identification of CME source regions. The high-latitude observations also allow a complete view of the equatorial corona and thus a global view of CME activity. This has never been done and is extremely important for the determination of CME longitudinal distribution, the occurrence of sympathetic CME activity and the identification of large, or even global ( $360^\circ$ ), CMEs. Global and large-area effects which may be related to CMEs can also be determined for the first time, such as the extent and timing of coronal waves and dimming in coronal emission lines.

#### **2.5.4 Solar luminosity variations**

The "solar constant", or total solar irradiance, is a measure of the total radiative output of the Sun from the X-rays over the visible to the infrared. As we have learned from satellite measurements, it is changing on two different time-scales. The solar output and activity exhibit variations that are anti-correlated over days, when large dark sunspots cross the disc, but they are correlated over the solar cycle. This apparent contradiction can be solved by understanding fully the role that the excess energy in faculae and the deficit energy in sunspots are playing on the different time scales. The variability of solar irradiance over a solar cycle, approximately 0.1 %, is too small to affect significantly the Earth's climate, however changes over longer periods might be responsible for larger global climatic variations.

The influence of faculae and sunspots on the value of the solar constant value can be eliminated only by observing the Sun above the poles, where these features are not expected to occur. Therefore, the Solar Orbiter, at its highest inclination with respect to the ecliptic, will allow a measurement of the "true solar irradiance" (TSI), as well as a quantification of the effects of solar activity through a comparison of these high-latitude measurements with the traditional irradiance measurements simultaneously made in the ecliptic.

By carrying out irradiance studies from out of the ecliptic and on the side away from the Earth, the Solar Orbiter will provide a unique opportunity to answer questions such as:

- How does the solar luminosity (i.e. the radiation escaping in all directions) vary? Does it change globally? Or is a brightening at the equator compensated for by a darkening over the poles?
- Why is the irradiance variability of the Sun a factor of three smaller than that of Sun-like stars?

One major difference between the Sun and Sun-like stars is that whereas we observe the Sun from almost directly above the equator, stars are on average seen from a latitude of approximately  $30^\circ$ . The Solar Orbiter will reach this latitude and test whether this inclination effect really is responsible for the Sun's apparently anomalous behaviour.

The TSI record is not only a highly sensitive diagnostic tool for the study of solar cycle related changes of the Sun, but also an important contribution to the issues of natural versus anthropogenic global change. For the latter, information over time scales of centuries is needed, which obviously cannot be assessed from measurements during a few 11-year solar activity cycles. Thus, an understanding of how the solar irradiance and luminosity are modulated is of paramount importance.

#### **2.5.5 Polar observation of the fast solar wind**

The Solar Orbiter will for the first time image directly the polar regions, where the fast solar wind is formed, from an out-of-ecliptic position. There, the expansion of the fast solar wind has not yet been determined directly, since the expansion is essentially perpendicular to the line of sight of spectroscopic instruments observing from the ecliptic, and therefore the Doppler effect is negligible. With increasing inclination angle of its orbit, the Solar Orbiter will perform out-of-ecliptic measurements and

- render possible velocity measurements due to a sizeable flow component along the line of sight,
- image the border of polar coronal holes and their deformation in response to the coronal waves that develop during CMEs,
- observe globally the entire streamer belt in the extended corona (beyond 2.6 solar radii at the end of the nominal mission and beyond 1.3 solar radii at the end of the extended mission),
- find the magnetic signal associated with coronal plumes and clarify their nature.

#### **2.5.6 Secular variation of the heliospheric magnetic flux**

The solar wind drags magnetic flux out of the Sun into the heliosphere in the form of the weak interplanetary magnetic field. Magnetic flux is also carried into the heliosphere by the sporadic and violent coronal mass ejections, that are frequently observed also during the minimum of solar activity. Some of the solar magnetic energy is then transferred to the near-Earth environment through magnetic reconnection of the interplanetary and the magnetospheric magnetic field. Recently, it has been shown that the total magnetic flux leaving the Sun has increased by a factor 1.4 since 1964. Indirect interplanetary magnetic field measurements seem to indicate that the increase has been a factor of 2.3 over a century. A doubling of the Sun's coronal magnetic field may thus have occurred during the past century. The change in magnetic flux may be related to a long-term change in the Sun's dynamo action.

The possible influence of this secular magnetic flux variation on the global climate on Earth has not yet been quantified.

The Solar Orbiter will determine with unprecedented accuracy the relative contributions of the solar wind and coronal mass ejections to the interplanetary magnetic field flux. From the out-of-ecliptic vantage point the Solar Orbiter will allow us for the first time to derive the longitudinal extent of coronal mass ejections and therefore give a much more accurate assessment of the magnetic flux dragged into the heliosphere during such huge events. Present space-borne and ground-based coronagraphs can only measure the latitudinal extent of coronal mass ejections. Furthermore, in the periods of co-rotation with the Sun, the ability of the Solar Orbiter to observe the long-term evolution of the magnetic configuration of a coronal streamer will allow us to study the processes that lead to magnetic reconnection. The contribution of ejected plasmoids to the heliospheric magnetic flux when detaching from the streamers as a consequence of reconnection events will also be determined.

---

## 3 SCIENTIFIC PAYLOAD

---

### 3.1 MEASUREMENT REQUIREMENTS

The Helios, Ulysses, Yohkoh, SOHO and TRACE missions may be used as a baseline for designing the payload of the Solar Orbiter. However, this mission will take a scientific space probe much closer to the Sun than has ever been reached before by a man-made object. In particular, the thermal load of almost 25 solar constants presents an unprecedented technical challenge. The instruments have to be designed accordingly. They may dwell on developments implemented in many space missions in the past, but the extreme thermal environment requires substantial redesign. In order to make sure that the ambitious mission goals of the Solar Orbiter can really be achieved, all individual instruments have been given extraordinary attention even at this stage. Indeed, some of the instruments have been designed to a level of detail not usually achieved at this phase of a mission. In addition, the study team has ensured that the technology required for these instruments is available within Europe.

The strawman payload discussed in this chapter contains sufficient design details to demonstrate feasibility. However, it is important to note that no pre-selection of instruments or instrument principles is implied.

The payload must be state-of-the-art, withstand the considerable thermal load at 45 solar radii, comply with the general requirements of a low-mass, compact and integrated design, make use of on-board data compression/storage and require a modest data transmission rate. The selected payload, which meets the solar and heliospheric science objectives of the mission, encompasses two instrument packages:

- *In-situ* heliospheric instruments (see Table 3.13 below): Solar wind plasma analyser measuring electrons and ions, magnetometer for DC and AC fields, particle detectors for solar energetic ions and electrons, interplanetary dust detector, neutral particle detector, solar neutron detector, radio instruments. The heritage for these instruments is from Helios, SOHO, Ulysses, Wind and ACE.
- Remote-sensing solar instruments (see Table 3.26 below): EUV full-Sun and high-resolution imager; high-resolution EUV spectrometer covering selected emission lines from the chromosphere to corona; high-resolution visible light telescope and magnetograph; EUV and visible-light coronagraph; and a radiometer. The heritage for these instruments is from Yohkoh, SOHO, TRACE.

### 3.2 IN-SITU HELIOSPHERIC INSTRUMENTS

#### 3.2.1 Solar Wind Plasma Analyser (SWA)

##### SCIENTIFIC DRIVERS

Three principal science goals require the inclusion of a solar wind plasma analyser in the payload:

- to provide observational constraints on kinetic plasma properties for a fundamental and detailed theoretical treatment of all aspects of coronal heating;
- to investigate charge- and mass-dependent fractionation processes of the solar wind acceleration process in the inner corona;
- to correlate comprehensive in-situ plasma analysis and compositional tracer diagnostics with space-based and ground-based optical observations of individual stream elements.

Furthermore, the SWA will

- investigate in detail  $^3\text{He}$  and “unusual” charge states in CME-related flows and to correlate the observations with other in-situ particle and field data and with optical observations;
- investigate the “recycling” of solar wind ions on dust grains in the distance range which has been located as the “inner source”. Freshly produced pick-up ions from this inner source are specially suited as test particles for studying the dynamics of incorporation of these particles into the solar wind.

The SWA will measure separately the three-dimensional distribution functions of the major solar wind constituents: protons,  $\alpha$ -particles and electrons. The basic moments of the distributions, such as density, velocity, temperature tensor, and heat flux vector will be obtained under all solar wind conditions and be sampled sufficiently rapidly to characterise fully the fluid and kinetic state of the wind. In this way we

will be able to determine possible non-gyrotropic features of the distributions, ion beams, temperature anisotropies, and particle signatures of wave excitation and dissipation.

In addition, measurements of representative high-FIP elements (the C, O, N group) and of low-FIP elements (such as Fe, Si or Mg) will be carried out in order

- to obtain their abundances, velocities, temperature anisotropies and charge states;
- to probe the wave-particle couplings (heavy-ion wave surfing);
- determine the freeze-in temperatures (as a proxy for the coronal electron temperature).

### INSTRUMENT CONCEPT

In view of the limited resources of mass, volume and telemetry allocated to the SWA, a compromise between sensitivity, mass/charge- and mass- and time resolution has to be found. The SWA has to cover a large dynamic range in ion fluxes. Since there is an enormous difference between the proton fluxes at perihelion (typically  $10^{14} \text{ m}^{-2} \text{ s}^{-1}$ ) and the fluxes of relevant minor ion tracers at 1 AU (e.g.  $\text{Fe}^{10+}$  at typically  $10^8 \text{ m}^{-2} \text{ s}^{-1}$  etc.) it is suggested to implement three different sensors:

1. A Proton/ $\alpha$ -particle Sensor (PAS) with the principal aim to investigate the velocity distribution of the major ionic species at a time resolution equivalent to the ambient proton cyclotron frequency.
2. An Electron Analysers System (EAS) consisting of two or three combined sensor heads covering a solid angle of almost  $4\pi$  and allowing the determination of the principal moments of the electron velocity distribution at high time resolution.
3. A Minor Ion Sensor (MIS) which allows the independent determination of the major charge states of oxygen and iron and a coarse mapping of the three-dimensional velocity distribution of some prominent minor species. Also, pick-up ions of various origins, such as weakly-ionised species ( $\text{C}^+$ ,  $\text{N}^+$ ,  $\text{Ne}^+$ ,  $\text{Mg}^+$ ,  $\text{Si}^+$ , etc.), will be measured.

The PAS is designed to resolve the relevant ion-kinetic scales. It will achieve a time resolution which is compatible with the characteristic ion cyclotron periods near perihelion. The characteristic time scale is about 10 ms. For the minor species (heavier than He) a time resolution of 1 s is needed.

To fulfil the requirements of compositional diagnostics, at least the charge state distributions of oxygen and iron should be measured routinely and with a time resolution of better than 10 s.

The instrument specifications are outlined in Table 3.1:

Sensor	Particles	Field of View	Energy resolution	Angular resolution	Time resolution
PAS	Protons and $\alpha$ -particles	Conical $\pm 45^\circ$	$E/\Delta E = 10$	Azimuth $30^\circ$ Zonal $\pm 5^\circ$	10 ms
EAS	Electrons	$4\pi$	$E/\Delta E = 10$	Azimuth $30^\circ$ Zonal $\pm 5^\circ$	10 ms
MIS	O, (3He, C, Ne, Mg, Si), Fe	Conical $\pm 45^\circ$			1 s

**Table 3.1:** Specifications of the SWA sensors.

The instrument package proposed for SWA is a further development of instruments successfully flown on several missions in the past, e.g., SWICS on Ulysses, CELIAS/CTOF on SOHO, TRIPLET on INTERBALL. A possible scheme for PAS based upon the design of TRIPLET is shown in Figure 3.1.

### RESOURCES AND REQUIREMENTS

#### Telemetry

The transmission of velocity distributions of the major species (protons, electrons and  $\alpha$ -particles) drives the telemetry requirements of SWA. In the normal mode of operation this information should be compressed to transmit the principal moments of the distributions. Periodically however, the transmission of the complete velocity distributions of protons and  $\alpha$ -particles with a (velocity) resolution of  $10 \times 10 \times 10$  pixels at a depth of 5 bits is needed. This requires 5 kb per spectrum. Correspondingly, at a time resolution of 10 ms, the required telemetry rate is 500 kb/s. This rate should be maintained during 1s, i.e. for some 100 ion cyclotron periods to cover a typical growth time of plasma instabilities. With an average telemetry rate of 5 kb/s a duty cycle of the order of 1% can be achieved.

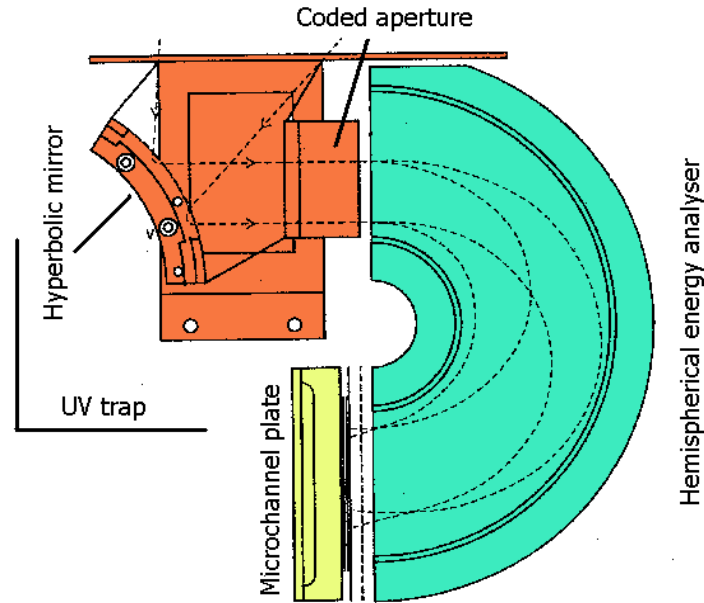


**Figure 3.1:** Schematics of PAS (following the design of TRIPLET on INTERBALL). A hyperbolic mirror maps the angular velocity distribution of solar wind ions onto a coded aperture. With this measure the information on the position at the entrance of the hemispherical energy analyser is transmitted (at the cost of  $\sim 50\%$  reduction in beam intensity) to the exit aperture of the analyser. The additional information on energy per charge is contained in the exit location and convoluted with the entrance location. Deconvolution of the entrance angle and the energy per charge by the onboard DPU allows the reconstruction of the complete three-dimensional velocity distribution of solar wind protons and  $\alpha$  particles with a time resolution of 10 ms.

#### *Allocations of mass, volume, and power.*

- A mass allocation for MIS of 4 kg, 1 kg for PAS and 1 kg for EAS (excluding the electronics) is foreseen.
- The volume allocation for MIS is  $20 \times 20 \times 20 \text{ cm}^3$ , and  $10 \times 10 \times 10 \text{ cm}^3$  for PAS and for each of the two EAS sensors.
- The total power allocated to SWA is 5 W.

#### *Thermal and radiation requirements*

The instrument should be able to operate under the specified spacecraft conditions. Special attention has to be devoted to the extreme solar UV radiation flux. The design of the particle instruments should reject this radiation to a sufficiently low level in order not to compromise the detection of rare particles.

#### *Electrostatic cleanliness*

Special care has to be taken to ensure near-equipotential conditions in the vicinity of the EAS entrance apertures.

#### *Instrument summary*

Instrument	Mass (kg)	Power (W)	Volume ( $\text{cm}^3$ )	Data rate (b/s)
PAS	1	1.2	1000	2000
EAS	1	0.8	2000	2000
MIS	4	3	7000	1000
Total SWA	6	5	10000	5000

**Table 3.2:** SWA resource requirements.

### 3.2.2 Radio and Plasma Waves Analyser (RPW)

#### SCIENTIFIC DRIVERS

*In-situ* wave investigations on many spacecraft (e.g., Ulysses, Wind) have amply demonstrated the crucial role of wave observations in the study of a broad range of solar terrestrial phenomena. Wave observations have been particularly useful in correlation with SOHO optical and EUV observations. Typical waves instrumentation provides measurements of both the electric field and magnetic field in a broad frequency band, usually from a fraction of a Hertz up to several tens of MHz, covering characteristic frequencies in the solar corona and interplanetary medium. Both electrostatic waves and electromagnetic waves can be measured, leading to different diagnostics: electrostatic waves mostly provide *in-situ* information in the vicinity of the spacecraft, while electromagnetic waves can provide an extensive remote sensing of energetic phenomena in the solar corona and interplanetary medium.

Solar radio astronomy in a broad range of frequencies provides a unique means to monitor, track and analyse energetic phenomena taking place in the solar corona and interplanetary medium, in association with solar activity. Radio emission is essentially generated through the interaction of energetic electrons (produced in solar flares and shock waves) with the ambient solar wind plasma. Most radiation mechanisms produce radiation at a frequency close to the local plasma frequency which is directly proportional to the square root of the electron density  $N_e$ , leading to the strong frequency-distance dependence shown in Table 3.3.

	electron density $N_e$ ( $\text{cm}^{-3}$ )	radio frequency
Low corona	$\sim 10^8 - 10^{10}$	100 MHz – 1 GHz
Medium corona	$\sim 10^6 - 10^8$	10 MHz – 100 MHz
$\sim 10$ Rs	$\sim 10^4$	$\sim 1$ MHz
$\sim 40$ Rs	$\sim 10^3$	$\sim 300$ kHz
$\sim 1$ AU	$\sim 10$	$\sim 30$ kHz

**Table 3.3:** Radio frequency as function of electron density.

Using proven techniques, the Solar Orbiter mission profile will allow a radio and plasma wave package to face quite different and new situations: access to waves and turbulence that occur much closer to the Sun; access to viewing angles from well out of the ecliptic plane, permitting for the first time studies of the north-south symmetry of the radio radiation in the solar corona.

#### INSTRUMENT CONCEPT

The Radio and Plasma Waves Analyser (RPW) comprises two main sub-systems: the Plasma Waves Analyser (PWA) covering *in-situ* measurements and the Radio Spectrometer (RAS) for remote sensing. The two sub-systems share some of the sensors (essentially the low frequency boom antenna) and have a common digital signal processing unit and interface with the spacecraft.

The same receivers can be used to analyse the different types of waves detected by different sensors, for instance electric antennae and magnetic coils. There is a lot of experience in the design of the sensors and receivers, as well as in the analysis techniques. Also all aspects of electromagnetic cleanliness, are well understood and are no longer a problem for modern spacecraft designs (e.g. Ulysses, Wind/Polar, Cassini, IMAGE, Cluster).

#### Concept of the PWA

The PWA will identify the various plasma waves and kinetic modes comprising the high-frequency part of the fluctuation and turbulence spectra. We provide below a brief description of the characteristics of the plasma waves expected to be present at 0.2 AU.

The expected field strength may range between a few  $\mu\text{V/m}$  and  $\text{mV/m}$ , and up to about  $1 \text{ V/m}$  for the convection electric field. The magnetic field strength is expected to vary between a few nT and  $\mu\text{T}$ , with large differences between the longitudinal and transverse components with respect to the mean magnetic field and the solar wind flow direction (substantial Doppler shifts are to be expected).

From Helios observations one can estimate that a sensitivity equal to  $10^{-6} \text{ nT}/(\text{Hz})^{1/2}$  will be required at 0.2 AU to identify without ambiguity whether the observed waves are electromagnetic or electrostatic.

At and above the electron plasma frequency intense electron plasma oscillations and solar radio waves are expected. Helios observations show that wave intensities associated with type III bursts increase very rapidly with decreasing radial distance from the Sun. Intense emission could extend up to  $10^{-4}$  nT/Hz<sup>1/2</sup>.

The measurement requirements necessary for the identification and analysis of the various electromagnetic phenomena expected to be measured at 0.2 AU are given in Table 3.4.

Phenomenon	Frequency band	Minimum amplitude (nT/Hz <sup>1/2</sup> )	Maximum amplitude (nT/Hz <sup>1/2</sup> )
Doppler-shifted ELF/VLF waves and turbulence	1 Hz – 10 kHz	$10^{-5}$ at 10 Hz	$10^{-1}$ at 10 Hz
Ion acoustic waves and Radio waves	10 kHz – 10 MHz	A few $10^{-7}$ at 1 MHz	$10^{-4}$ at 1 MHz

**Table 3.4:** Measurement requirements for the fluctuating magnetic field.

The PWA will cover a broad band in frequencies, extending from about 1 Hz into the MHz range. Resolving the vector components of the electric and magnetic fields is scientifically highly desirable to determine wave modes unambiguously. However, due to different constraints of the mission, we propose to measure one electric field component only, with a boom antenna mounted in the anti-Sun direction, i.e. in the shadow of the spacecraft. The three components of the fluctuating magnetic field can be easily measured with a 3-axial search coil magnetometer arranged in a compact configuration and mounted on a short boom which should also point into the anti-Sun direction. This boom is required for magnetic cleanliness reasons and could be shared with the MAG (see 3.2.4) as long as a minimum distance between the two sensors is respected. There is a strong heritage for those sensors mounted on three-axis stabilised spacecraft, e.g. on Galileo, Cassini, STEREO. The PWA will also benefit from studies and developments under progress for the Solar Probe.

The PWA will perform on-board processing of the data and deliver selectable wave forms (Time Domain Sampler, TDS), to identify non-linear coherent fluctuations and correlate them with measurements from the EPD.

### Concept of the RAS

The RAS will measure the solar and interplanetary radio waves in the frequency range from 100 kHz to 1 GHz, with a sweep period between 0.1 s and 10 s and a high spectral resolution ( $\Delta f/f \approx 0.07$ ). The RAS will observe plasma processes associated with energetic electrons from the low corona up to about 0.5 AU. It will probe the plasma at distances ranging from the solar surface to the spacecraft location, thereby connecting the low-altitude coronal regions observed by the optical instruments with the near-Sun heliospheric conditions specified by the in-situ measurements. Since radio radiation is generally beamed (beam widths sometimes down to a few tens of degrees) more or less along a radial direction from the Sun, this technique is particularly relevant for different vantage points, for instance when the Solar Orbiter observes the far side of the Sun. The time history provided by the regular acquisition of the radio dynamic spectrum will help to trace the development of an active region in a synthetic manner. Activity indices could thus be produced.

The time resolution required to detect the rapidly varying solar bursts varies with the radio frequency. Typically, the duration of a type III burst (stream of energetic electrons) is  $\Delta t(s) = 220 / f(\text{MHz})$ . This points to time resolutions of the order of 0.1 s or better for the high frequencies and of 10 s for the low frequencies.

A single boom antenna can be used for the low frequency part of the band (below, e.g. 20 MHz), where the sensitivity is essentially determined by the sky background radiation. Above 20 MHz and particularly above 200 MHz, the background is determined by the receiver temperature and gain is needed in order to detect solar radio bursts: a simple boom cannot be used anymore. A broad-band antenna with significant gain is thus required. Each one of the receivers will be fed by different antenna or search coil systems.

The RAS instrument could be divided into three sub-spectrometers, for instance:

- RAD1: 100 kHz - 16 MHz
- RAD2: 16 MHz - 200 MHz
- RAD3: 200 MHz - 1 GHz



Different designs are used on many space missions and the heritage goes right back to the birth of space radio astronomy at long wavelengths.

### RPW instrument description

An overall block diagram of the Solar Orbiter RPW instrument is shown on Figure 3.2.

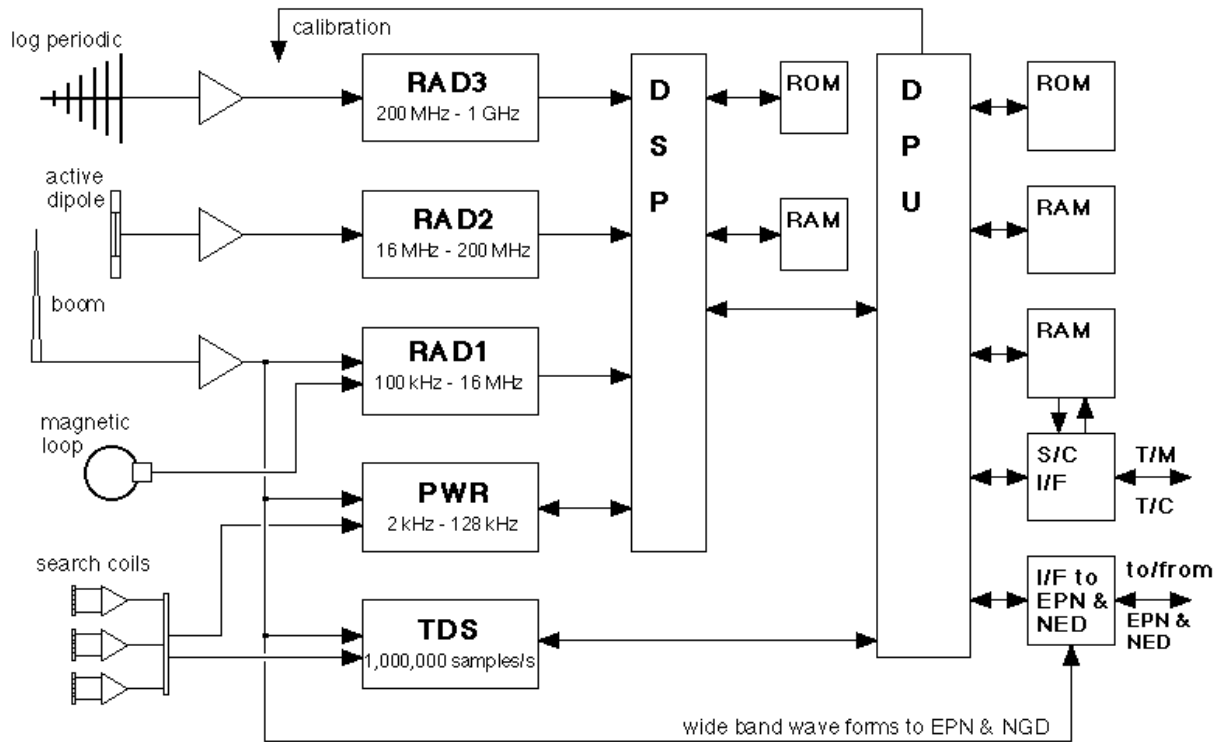


**Figure 3.2:** Block diagram of the Solar Orbiter RPW instrument.

Plasma waves and low frequency activity will be monitored by a receiver covering the band from about 1 kHz up to 100 kHz. In order to allow for a high time resolution, whilst minimising resources, it can be of the type flown on Wind and planned for STEREO, using a digital filtering technique.

The wave form analyser or Time Domain Sampler (TDS) is a broad band waveform sampler with 4 channels (1 electric field component and 3 magnetic field components). The signal from the boom antenna and search coil are sampled at a rate up to  $10^6$  samples per second. Events are detected on board and transmitted according to the available bit-rate. This is done using “intelligent” algorithms which can return a quality value for the events. A number of random events can be sent to the ground without regard of their quality in order to provide unbiased statistics. Real time triggers can be sent to the EPD for special studies of wave-particle phenomena.

The radio receivers can be of the classical super-heterodyne type. Frequency synthesisers will allow for a maximum flexibility in the choice of the observing frequencies (for instance to avoid “polluted” frequencies on the spacecraft). Each sub-receiver can consist of up to 256 selectable channels. Only a selection of these channels could be transmitted to the telemetry stream.

The DPU will command the different subsystems and interface with the spacecraft. The variety of instruments call for a packetised telemetry system, that can be managed by the DPU itself, as is done for similar packages on the Wind spacecraft (fixed format telemetry system) and STEREO. The DPU will interface with other instruments on board the spacecraft, particularly the EPD. The DPU could be shared with some other instruments from the payload, e.g. with MAG.

Tables 3.5a, 3.5b, 3.5c provide the main characteristics of the sensors and analysers comprised in the RPW investigation. Numbers are indicative and can vary according to design options

	Magnetic sensors	frequency band	Sensitivity (nT/Hz <sup>1/2</sup> )	Size	mass (g)	power
B1	Search coils	1 Hz – 10 kHz	10 <sup>-5</sup> at 10 Hz	3 rods, 18 cm each	500	200 mW
B2	Magnetic loop (optional)	10 kHz – 10 MHz	10 <sup>-6</sup> at 1 MHz	20 cm diameter	600	200 mW
<i>Total</i>					1100	

**Table 3.5a:** Main characteristics of the RPW magnetic sensors.

	Electric sensors	frequency band	Size	mass (g)	power
E1	Radio boom	1 Hz – 20 MHz	5 m boom	1300	N/A
E2	Active dipole	20 MHz – 200 MHz	~ 1m x 2cm x 2 cm	800 (TBC)	300 mW
E3	Log-periodic antenna	200 MHz – 1 GHz	~ 1m x 1m x 1cm	1500 (TBC)	N/A
<i>Total</i>				2600	

**Table 3.5b:** Main characteristics of the RPW electric sensors.

Analyser	frequency band	Sensor(s)	Sensitivity	mass (g)	Bitrate (b/s)	Power (W)
TDS	wave form 1,000,000 samples/s	E1, B1	30mV/m, 0.2 pT	800	1700	1.0
PWR	2 kHz – 128 kHz	E1, B1	10 nV/Hz <sup>1/2</sup> , 10 <sup>-5</sup> nT/Hz	800	1250	0.7
RAD1	100 kHz – 16 MHz	E1, (B2)	10 nV/Hz <sup>1/2</sup> , 10 <sup>-6</sup> nT/Hz <sup>1/2</sup>	800	800	0.8
RAD2	16 MHz – 200 MHz	E2	~ 10 <sup>-20</sup> W m <sup>2</sup> Hz <sup>-1</sup>	700	600	0.7
RAD3	200 MHz – 1 GHz	E3	~ 10 <sup>-20</sup> W m <sup>2</sup> Hz <sup>-1</sup>	700	600	0.7
DSP/DPU				1200		1.5
Converter				800		1.2
Harness etc.				500	50 (H/K)	
<i>Total</i>				6300	5000	6.8

**Table 3.5c:** Main characteristics of the RPW analysers and subsystems.

## RESOURCES AND REQUIREMENTS

### Antenna systems

Antenna systems for the range from 20 MHz to 1 GHz are readily available off the shelf for ground based systems, including “portable” ones. Different types and techniques are available, and the theory of the measurement is well known. They would have to be developed specifically for the Solar Orbiter mission. The RAD2 band (16 MHz - 200 MHz) could be covered by an active dipole antenna and the RAD3 band (200 MHz - 1 GHz) by a log-periodic antenna. These two antenna systems can be grouped together and mounted on the same boom in order to have a common mechanical (deployment mechanism) and electrical interface with the spacecraft. They would have to be pointed to the Sun (accuracy of a few degrees) and thus protected from the direct sunlight by a shield not affecting the radio wave propagation. The whole system can be kept to a reasonable size (longest element of the order of 1 m) and provide the required gain. The beam shape of the antennae mounted on the spacecraft will have to be modelled and measured using existing techniques.

### Electro-Magnetic Cleanliness (EMC)

Many of the RPW scientific objectives are based on the measurement of low-level signals for which maximum sensitivity is required. Several inexpensive measures can be taken at the spacecraft and project level to ensure that the Solar Orbiter spacecraft is clean from the point of view of both conducted and radiated electromagnetic interference. The sensitivity of the RPW instrument will be approximately  $10^{-8}$  V/m/Hz<sup>1/2</sup> in the frequency range of 1 kHz to 20 MHz and  $3 \times 10^{-7}$  V/m/Hz<sup>1/2</sup> below 100 Hz. In addition, the wave form analyser is sensitive to impulsive interference of duration as short as a fraction of a microsecond. Although these sensitivities may appear to require an excessively "clean" spacecraft, they are not difficult to achieve if good EMC practices are incorporated in the spacecraft design.

### INSTRUMENT SUMMARY

#### RPW Sensors:

- triaxial search coil mounted on the magnetometer boom,
- magnetic loop antenna,
- boom antenna (5 to 6 m on side opposed to Sun),
- VHF/UHF system comprising an active dipole and a log-periodic antenna.

#### Role of main subsystems:

- RPW/PWA: identify plasma waves and kinetic modes (high frequency part of the fluctuation and turbulence spectra)
- RPW/RAS: measure and track solar and interplanetary radio bursts; connect low-altitude coronal regions observed by the optical instruments with the *in-situ*, local solar wind conditions at the spacecraft, study directivity of radio emissions

Instrument	Mass (kg)	Power (W)	Volume (cm <sup>3</sup> )	Data rate (b/s)
<b>Total RPW</b>	10	7.5	7500	5000

**Table 3.6:** RPW resource requirements.

### 3.2.3 Coronal Radio Sounding (CRS)

A passive radio science experiment can be carried out using the available radio links. The spacecraft will pass behind the Sun (superior solar conjunction) on many occasions, making it possible to investigate the solar corona by radio sounding at solar distances much less than the perihelion distance and down to at least 2 solar radii. Integrated line-of-sight parameters such as electron content (densities), Faraday rotation, scintillations and angular broadening can be recorded. The Solar Orbiter orbit and the proximity of the spacecraft to the Sun will create unique situations for this kind of analysis. The CRS investigation with a two-way radio link via the spacecraft high-gain antenna (ranging capability) would require a radio subsystem with dual-frequency phase coherent downlinks at X-band and Ka-band. Linear polarisation of the downlink signals would enable Faraday rotation measurements as an option. The RF power for both radio links (X and Ka) planned for this mission is sufficient for this investigation. A two-way dual-frequency coherent radio link (X-band uplink; X-band and Ka-band simultaneous coherent downlinks) is considered as the optimal configuration for a sufficiently stable link and for detecting signatures of CME events traversing the radio ray path.

It is presently unclear whether or not an ultra-stable oscillator would be necessary to guarantee the frequency stability of the downlinks. If only a one-way radio link (spacecraft to ground) is feasible due to operational constraints during solar conjunction, the transmitted radio signal must be stabilised by an onboard ultra-stable oscillator (frequency stability  $10^{-11}$  to  $10^{-12}$  at 3 s integration time, 200g, 3 W). The practicality of using linear polarised signals for Faraday rotation measurements is another trade-off to be explored. The final decision depends critically on the geometry and mission operation plan. Considerable interaction between the radio scientists and the spacecraft's radio subsystem contractor is a prerequisite for conducting a successful coronal sounding experiment. The occultation geometry during the solar conjunctions is another aspect that needs to be studied in detail.

### 3.2.4 Magnetometer (MAG)

#### SCIENTIFIC DRIVERS

Knowledge of the magnetic field is of crucial importance for characterising the state of the local interplanetary medium and is indispensable for the interpretation of measurements of energetic particles and thermal plasma particles.

The magnetometer will measure the three orthogonal components of the interplanetary magnetic field vector over a broad dynamic range from a few nT up to the  $\mu$ T range, and for frequencies well below the local heavy-ion or proton gyrofrequencies.

#### INSTRUMENT CONCEPT

The magnetometer may consist of a triaxial identical sensor system. A compromise has to be found between the requirements of the spacecraft and payload systems and the demand of the magnetometer for magnetically clean conditions.

The heritage of MAG includes dozens of similar instruments flown on various magnetospheric, planetary and deep space missions. The MAG proposed for the STEREO mission might serve as a guideline. It is in turn based on the design used for the NEAR and ACE missions. The MAG sensor and electronics for the Solar Orbiter require no new development. State of the art instruments can be built for less than 1 kg. Further mass savings may be possible.

MAG might consist of a 3-axis fluxgate magnetometer with the sensor mounted at the end of an extendable boom (length <1m) which is positioned in the shadow of the Orbiter. Other mounting locations such as on the high-gain antenna structure appear possible, provided MAG stays in permanent shadow. It measures fields in 8 ranges (automatically selected) from 4 nT to 65536 nT with a resolution of 30 ppm, from DC up to AC frequencies of 500 Hz. The parameters can be adjusted according to the particular needs of the Solar Orbiter mission. The DPU of MAG could be shared with either the plasma instruments or the wave instruments.

#### RESOURCES AND REQUIREMENTS

The mass of the sensor package will be less than 1 kg, the average power consumption is about 1 W, and the required telemetry is of the order of 200 b/s.

Magnetic cleanliness of a spacecraft as required by a magnetometer on board has been a cost driver for some missions in the past. However, more recent experience has shown that there are in fact acceptable low-cost engineering solutions possible. A reasonable magnetic cleanliness program can be performed, if the MAG experimenters work in close contact with the all other teams in order to ensure proper engineering at an early phase and to make other precautions without impacting the mission schedule. Similar schemes were applied in the past for several successful missions.

#### INSTRUMENT SUMMARY:

Instrument	triaxial fluxgate magnetometer
Telemetry	< 200 b/s
Mass	< 1 kg
Power	< 1 W
Special requirements	mounting on short boom (<1 m), in shadow of spacecraft, basic magnetic cleanliness of spacecraft.

**Table 3.7:** MAG resource requirements.

### 3.2.5 Energetic Particle Detector (EPD)

#### SCIENTIFIC DRIVERS

The Solar Orbiter will allow us to study the sources, acceleration and propagation of solar energetic particles in association with coronal and interplanetary shocks. Energetic pick-up particles originating from outgassing or sputtering of near-Sun dust should be measured as well in conjunction with the plasma

---

measurements. It is essential that all measurements are done fast, typically at 1 s, with complete angular coverage to resolve the pitch-angle distributions. The EPD will

- determine *in-situ* the generation, storage, release and propagation of different species of solar energetic particles in the inner heliosphere;
- identify the links between magnetic activity and acceleration on the Sun of energetic particles, by virtue of combined remote-sensing of their source regions and *in-situ* measurements of their properties, while staying magnetically connected with the acceleration sites during solar co-rotation passes;
- characterise gradual (CMEs) and impulsive (flares) particle events and trace their spatial and temporal evolution near the Sun.

### INSTRUMENT CONCEPT

The EPD will determine chemical and charge composition and energy spectra of ions in a wide energy range, from about the typical solar wind energies of a few keV to several 100 MeV/nucleon for protons and heavy ions. Electrons should be measured from 10 keV to 10 MeV. The combination of electrostatic E/Q-analysis with time-of-flight E/M-determination and subsequent direct energy measurement in a solid state detector has been employed in many EPDs in the past and is also a possible design option for the Solar Orbiter.

The specific design suggested here resembles closely the one recently selected for the IMPACT instrument on the STEREO mission. It is a multi-head sensor system using solid state technology. Ongoing research in this field is promising and will certainly lead to further improvements concerning energy thresholds and noise level as well as to size reduction.

### RESOURCES AND REQUIREMENTS

The measurement requirements can be met readily by a low-mass and compact sensor assembly with different lines of sight and modest aperture sizes. We propose to place several detectors at different positions onboard the spacecraft, in order to obtain a sufficient field of view and angle-of-incidence coverage without using a scanning platform. The whole EPD package will have a total mass not exceeding 4 kg and consume an average power of 3 W. The required telemetry rate is 1.8 kb/s.

The characteristics of the EPD could, e.g. resemble the 4 sensors of the IMPACT instrument on STEREO, as given in Table 3.8.

Sensor	Energy (MeV/nucleon)	GF (cm <sup>2</sup> sr)	FOV (° x °)	Name
EPT	e: 0.02 - 0.40 p: 0.02 - 7.00	4 x 0.30, 4 x 0.24, 4 view cones		Electron Proton Telescope
SIT	0.03 - 2	0.3, 1 view cone	17 x 44	Supra-thermal Ion Telescope (He – Fe)
LET	1.5 - 40	4.5, 10 view cones	130 x 30	Low Energy Telescope (He – Ni)
HET	13 - 100	2.4, 2 view cones	48 x 48	High Energy Telescope (He – Fe)

**Table 3.8:** EPD instrument characteristics.

### INSTRUMENT SUMMARY

Instrument	Mass (kg)	Power (W)	Volume (cm <sup>3</sup> )	Data rate (b/s)
<b>EPT</b>	0.94	0.60	300	300
<b>SIT</b>	0.78	0.55	620	500
<b>LET</b>	0.44	0.12	430	700
<b>HET</b>	0.27	0.04	210	300
<b>DPU/H-L-VPS</b>	1.37	1.17	3000	
<b>Total EPD</b>	3.80	2.48	4560	1800

**Table 3.9:** EPD resource requirements.

### 3.2.6 Dust Detector (DUD)

#### SCIENCE DRIVERS

The DUD will analyse interplanetary dust particles with respect to their composition and orbital characteristics and determine *in-situ* the distribution, composition and dynamics of dust particles in the near-Sun heliosphere in and out of the ecliptic. The spatial distribution of particles with masses ranging between  $10^{-16}$  g and  $10^{-6}$  g will be determined. DUD will

- help outlining the extent of the dust-free zone around the Sun;
- discover the sources of dust, e.g. from Sun-grazing comets;
- unravel the role played by near-Sun dust for pick-up ions;
- deliver data relevant for an understanding of proto-planetary discs.

#### INSTRUMENT CONCEPT

The science objectives can be met with an instrument of, e.g. Giotto heritage. The dust experiment may consist of a multiple sensor assembly, with each sensor looking in a different direction to resolve incidence angles. A low-mass dust-detecting element could look as sketched in Figure 3.3. The dust particles enter the detector through a thin aluminium foil and evaporate during impact on a gold target. A set of wires in front of the target plate collects the ions produced. The signal is analysed to deduce the mass and possibly speed of the dust particle.

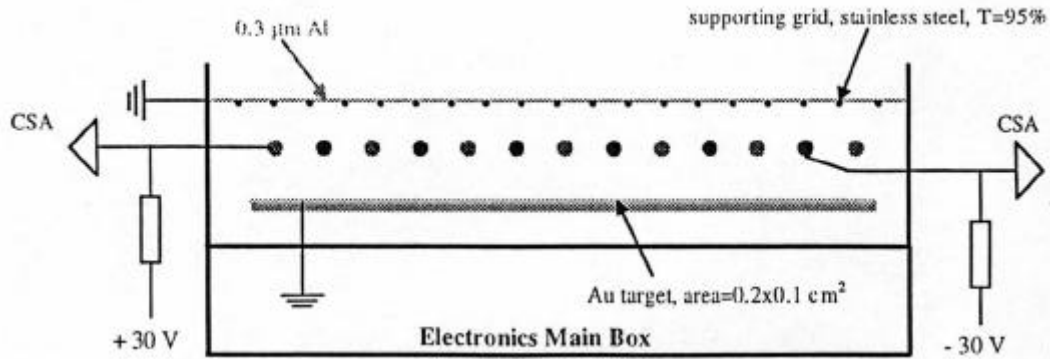


**Figure 3.3:** Instrument design of DUD.

Full chemical analysis and mass resolution of the important elements H, C, N, O of carbonaceous material and the metals like Na, Mg, Al, Si, Ca and Fe contained in chondritic silicates is desirable but may require a more sophisticated design.

#### RESOURCES AND REQUIREMENTS

Two identical detector units should be located on the sides of the spacecraft body, one looking  $90^\circ$  off the spacecraft-Sun line in the orbital plane to measure the near-ecliptic dust particles, the other one in the direction perpendicular to the orbital plane in order to measure dust particles in orbits highly inclined to the ecliptic. The field of view of each sensor is  $\pm 80^\circ$ .

The mass of each sensor is 0.5 kg. Each one consumes a power of 0.3 W and has a volume of  $1200 \text{ cm}^3$ . The average bit-rate will not exceed 50 b/s. The DPU should be shared with other particle instruments.

#### INSTRUMENT SUMMARY

Instrument	Mass (kg)	Power (W)	Volume ( $\text{cm}^3$ )	Data rate (b/s)
DUD	1	0.6	2400	50

**Table 3.10:** DUD resource requirements.

### 3.2.7 Neutral Particle Detector (NPD)

#### SCIENTIFIC DRIVERS

The  $L\alpha$  line of neutral hydrogen is used in spectroscopic observations on SOHO to determine the solar wind velocity profile in the corona up to several solar radii. The NPD on the Solar Orbiter will measure primarily neutral hydrogen atoms and thus render possible the detection of the interplanetary "neutral solar wind". The instrument should detect neutral atoms in the typical solar-wind and supra-thermal velocity range between about 350 and 5000 km/s.

The neutral atom flux is expected to be about  $100\text{--}1000\text{ atoms cm}^{-2}\text{ s}^{-1}$  at 0.21 AU, but it could be up to  $10^6\text{ atoms cm}^{-2}\text{ s}^{-1}$  in a CME. The NPD will also measure energetic neutral atoms emitted from various coronal sources, and thus enable images of these coronal emission regions to be constructed from rays of neutral atoms with different velocities.

#### INSTRUMENT CONCEPT

Neutral atom detectors have been flown on SOHO, Cassini and IMAGE. Time-of-flight instruments are for example flown on Ulysses, SOHO and ACE.

As a baseline, the instrument parameters of the NPD on the Solar Orbiter could be: Energy/mass range: 0.6 to 100 keV/nucleon, moderate velocity resolution; mass resolution is a secondary objective. The field of view (for the imaging capability) of the NPD should be centred at about  $17^\circ$  off the spacecraft-Sun-centre line.

The instrument entrance system must block radiation emerging from the solar disc. The UV scattered in the solar corona, i.e.  $L\alpha$ , must be suppressed by a factor of more than  $10^{-10}$ . The entrance system must reduce ions and electrons of the solar wind plasma by a factor of about  $10^{-8}$  whilst transmitting neutral atoms.

A feasible neutral atom detector (see Figure 3.4) may consist of two sections: the first compartment accommodates the baffle plates keeping out solar UV and the deflection unit for keeping off unwanted charged particles. The second section contains a time-of-flight (TOF) double-coincidence detector. Between the two sections is the pin-hole/slit that defines the optical properties of the neutral atom detector.

The direct solar radiation is blocked by a collimator. For the suppression of scattered light within the collimator, the plates are covered with sawtooth-like structures. The collimator consists of, alternatively positive and negative, high-voltage biased plates and therefore acts as a charged-particle deflector. The collimator plate length, distance and potential determine the cut-off of the charged-particle transmission (about 100 keV/q).  $L\alpha$  light is transmitted through the collimator. The grid in front of the pin-hole reflects the UV. The grid consists of 2 gratings with a grating constant matching the  $L\alpha$  peak. The grids are more transparent for particles than for UV photons (ratio up to 105 per grating, in dependence on the UV wavelength).

The neutral atoms pass through the pin-hole (or slit) and a  $0.5\text{ to }1.1\text{ }\mu\text{g/cm}^2$  carbon foil. As they pass the carbon foil, they release secondary electrons which are accelerated towards a START MCP (multi-channel plate). The atoms travel through a 3-cm-wide TOF drift region and hit the rear STOP MCP. The time of flight for 1 keV/n-100 keV/n atoms is about 8 to 80 ns. The position resolution is 1-D for the START MCP and 2-D for the STOP MCP. The flight pass of the neutral atom can be calculated from these measurements by an inversion of the instrument function. The detector determines the velocity (energy/nucleon) and the flight pass (imaging) of the neutral atoms.

#### RESOURCES AND REQUIREMENTS

The NPD can be built for a mass of 1 kg. The power consumption is 2 W. The required telemetry rate is less than 0.3 kb/s. It is envisaged to use a common DPU and to share the mechanical structure with the SWA. The FOV has to be  $17^\circ$  off the spacecraft-Sun line because of the typical  $10^\circ$  aberration of a 1 keV hydrogen atom travelling at solar wind speed.

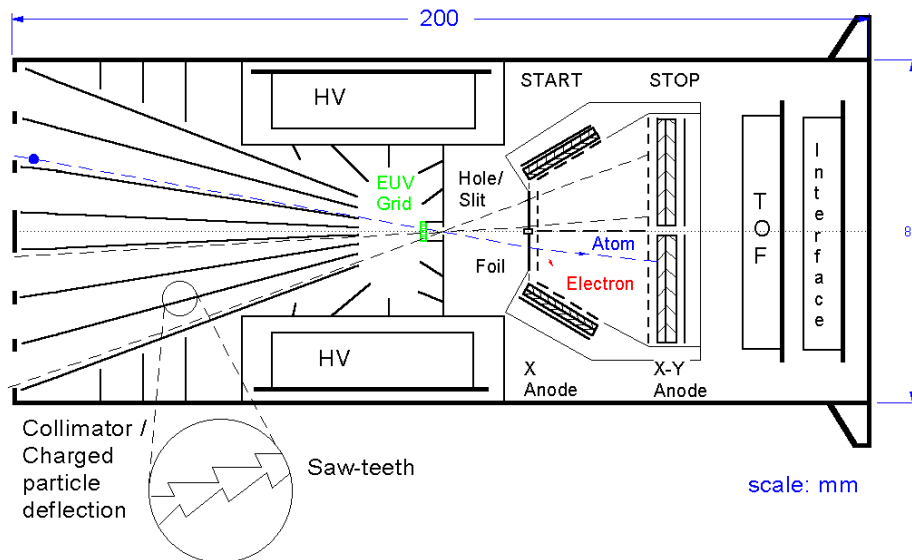


**Figure 3.4:** Instrument schematics of the Neutral Particle Detector.

### INSTRUMENT SUMMARY

Instrument	Mass (kg)	Power (W)	Volume (cm <sup>3</sup> )	Data rate (b/s)
NPD	1.00	2.00	2000	300

**Table 3.11:** NPD resource requirements.

### 3.2.8 Neutron Detector (NED)

#### SCIENTIFIC DRIVERS

Solar neutrons (and  $\gamma$  rays) are a by-product of solar flares due to spallation reactions between energetic protons and  $\alpha$ -particles. The overwhelming majority of these neutrons are thermalised within minutes and later absorbed by hydrogen to form deuterium and the well known 2.2 MeV  $\gamma$ -line. Some neutrons, however, escape into space and can eventually be detected (before they decay with a half-life of 619.9 s) by a sensor located in close proximity to the Sun. The temporal correlation of neutron fluxes with solar energetic particle fluxes and with optical observations in the EUV provides valuable information on the solar particle acceleration process, which is inaccessible by other means.

The advantage of neutrons over charged particles not being delayed by travel along complicated paths through magnetic fields will allow an unambiguous temporal correlation with optical observations of features of flares in different energy ranges.

Including the NED on the Solar Orbiter offers routine monitoring of neutron fluxes and, optionally,  $\gamma$ -rays and will be a “first” in solar science. A major contribution to the solar  $\gamma$ -ray flux stems from the 2.2 MeV line, which is due to the reaction of thermal neutrons with protons to form deuterium. Hence, the  $\gamma$ -ray detector registering “extinct” solar neutrons would ideally complement the neutron detector, which is to record “live” neutrons in-situ.

#### INSTRUMENT CONCEPT

Following the design of the instrument proposed for the Solar Probe the heart of the suggested NED instrument consists of a cell containing thin ( $<10\ \mu\text{m}$ ) thorium foils. With a cross section of typically 100 mbarn (at energies above 1 MeV) an efficiency of  $10^{-5}$  for producing fission fragments - to be detected in a pulse ionisation chamber - can be achieved. The anti-coincidence chamber surrounding the sensitive volume contains a counting gas, e.g. methane or argon, and energetic particles which might produce false counts in the ionisation chamber will be detected with an efficiency of close to 100%. The angular resolution of the NED will not be sufficient to map individual features on the solar surface.



Optionally, incorporation of a facility to monitor solar  $\gamma$ -rays into the experiment would greatly enhance the scientific return.

Planetary flybys could be used to block the solar neutron flux and to determine the intrinsic background rate of the spacecraft. Further information, also on the average energy of solar neutrons will be gained by comparison of long time averages of the neutron flux at different solar distances.

### RESOURCES AND REQUIREMENTS

The main concern with NED will be to minimise the energetic particle background in the sensor cell. On one hand the anti-coincidence cell should be as efficient as possible to prevent false coincidences, on the other hand, the location of the sensor within the payload has to be chosen such that as to keep the particle radiation level to a minimum.

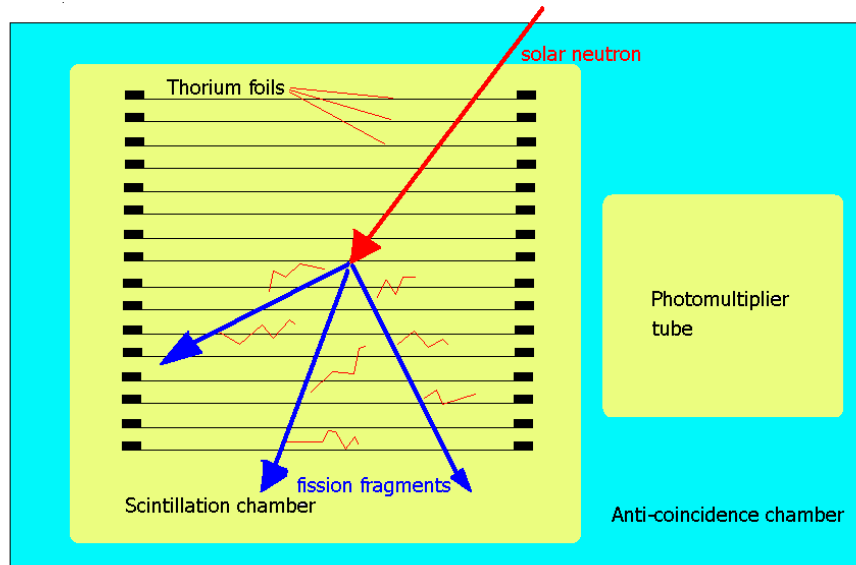


**Figure 3.5:** Schematics of the NED sensor.

### INSTRUMENT SUMMARY

Instrument	Mass [kg]	Power [W]	Volume [cm <sup>3</sup> ]	Data rate [b/s]
NED	1	1	1000	100
NED+ *)	2	1.5	2000	150

\*) Version including  $\gamma$ -ray detection facility

**Table 3.12:** NED resource requirements.

### 3.2.9 Heliospheric instruments summary

Name	Acronym	Measurement	Specifications	Mass (kg)	Size (cm x cm x cm)	Power (W)	Telemetry (kb/s)
Solar Wind Plasma Analyser	SWA	Thermal ions and electrons	0-30 keV/Q; 0-10 keV	6	20 x 20 x 20	5	5
Radio and Plasma Wave Analyser	RPW	AC electric and magnetic fields	$\mu\text{V/m}$ - $\text{V/m}$ $0.1\text{nT}$ - $\mu\text{T}$	10	15 x 20 x 30 (electronics box)	7.5	5
Radio Sounding	CRS	Wind density and velocity	X-band Ka-band	(USO 200g)	5 x 5 x 5	3	0
Magnetometer	MAG	DC magnetic field	to 500 Hz	1	10 x 10 x 10	1	0.2
Energetic Particle Detector	EPD	Solar and cosmic-ray particles	Ions and Electrons .01-10 MeV	4	10 x 20 x 20	3	1.8
Dust Detector	DUD	Interplanetary dust particles	Mass (g): $10^{-16}$ - $10^{-6}$	1	10 x 10 x 10	1	0.05
Neutral Particle Detector	NPD	Neutral hydrogen and atoms	0.6 – 100 keV	1	10 x 10 x 20	2	0.3
Neutron detector	NED	Solar neutrons	$e>1\text{MeV}$	2	10 x 10 x 10	1	0.15

**Table 3.13:** *In-situ* heliospheric instrumentation.

## 3.3 REMOTE SENSING SOLAR INSTRUMENTS

### 3.3.1 General considerations

An integrated ensemble of high resolution remote sensing instruments is proposed for the Solar Orbiter. The instruments are described in this section with emphasis on the scientific requirements and the feasibility of the instrument concepts. All the disc-observing instruments will resolve the small-scale dynamical processes in the solar atmosphere. The combination of instruments proposed here will provide a complete set of multi-wavelength measurements required to understand the Sun's magnetised atmosphere – from below the photosphere up into the extended corona.

Critical issues like heat input, mechanical structure, mass and power requirements have been investigated for each instrument.

### 3.3.2 Visible-Light Imager and Magnetograph (VIM)

#### SCIENTIFIC DRIVERS

The purpose of the VIM is to determine the magnetic field boundary conditions for the MHD processes observed by other remote sensing instruments. It will observe the morphology, dynamics, and strength of the magnetic elements and flux tubes at the photospheric level with a resolution that is consistent with the resolution of the EUV telescopes. It will also provide images, Dopplergrams and magnetograms from the side of the Sun, which is invisible from Earth.

VIM will be a vector magnetograph. Having vector capabilities is of fundamental importance to understand the nature of photospheric fields. Are they vertical unipolar fields? Do they harbour complex neutral lines with horizontal sheared fields? Having vector capabilities is the only way in which quantitative inferences of the magnetic field in the transition region and corona can be made (from force-free or full 3D MHD extrapolations). The importance of such data for the understanding of coronal processes (like, e.g., the initiation of CMEs) has been amply demonstrated by SOHO.

VIM will also produce line-of-sight velocity maps by observing two points on either side of a spectral line. These maps can be used, through local helioseismology techniques, to investigate subsurface flows.

The internal structure and dynamics of the near-polar regions of the Sun is of paramount importance and perhaps *the* key to our understanding of the solar cycle.

The key scientific goals of the VIM are

- to resolve solar magnetism down to its fundamental length scale (<100 km).
- to provide measurements of the “magnetic carpet” which drives chromospheric and coronal activity.
- to observe and accurately quantify for the first time the surface polar magnetic field of the Sun.
- to unveil the small-scale photospheric dynamo,
- to provide the first magnetograms and Dopplergrams of the far side of the Sun.
- to measure rotation and flows near the Sun’s poles using techniques of local area helio-seismology and thereby provide crucial constraints on solar dynamo theories.

### *INSTRUMENT CONCEPT*

The optics of the VIM include

- 25 cm diameter High Resolution Telescope (HRT),
- 5 cm diameter Full Disc Telescope (FDT), and
- Filtergraph Optics (FO).

The two telescopes, HRT and FDT, deliver an image of the Sun at a common telescope focal plane. The FO produces a magnified image of the telescope focus on the instrument's only detector. While the HRT provides an image with a high resolution at its diffraction limit, the FDT adjusts its focal length such as to fill the detector with the solar disc. The filtergraph optics include a double Fabry-Perot interferometer equipped with a narrow-band interference filter as a prefilter, tuned to the Fe I 630.2 nm line. This filtergraph is easily adjusted to the lineshifts which occur due to Sun-spacecraft relative velocities up to 40 km s<sup>-1</sup>. The three components are described in the following sections.

#### *High Resolution Telescope (HRT)*

##### *- General description*

The HRT is a 250 mm diameter Gregorian reflector. It provides an image with a spatial resolution as high as 75 km on the solar surface during the near-Sun orbital phase. A polarisation modulator is foreseen in the optical path behind the main mirror in the f/17 beam and before the first oblique reflection.

The secondary mirror is actively mounted with three translation degrees of freedom for telescope alignment control and pointing.

Figure 3.6 shows an annotated perspective view of the HRT and FO.

##### *- Thermal control*

The HRT will have to withstand the heat load during the near-Sun orbital phases. The primary mirror will be made from SiC and passively cooled to dispose off the approximately 170W of radiation which is absorbed in its reflective layer. SiC enjoys better static and dynamic thermal stability than other mirror blank materials.

The Gregorian design permits rejecting 96% of the incident radiation at its primary focus with a field stop. The field stop is an inclined mirror with a 2 mm central hole which transmits the observed field. The reflected light is directed out of the spacecraft. The field stop will also absorb about 170 W which will require passive cooling.

A broadband interference filter will be included after M2 to reduce the amount of light in the filtergraph optics.

#### *Full Disc Telescope (FDT)*

It is impractical to combine the functions of full-disc and high resolution viewing of the Sun into a single telescope. Therefore, a separate telescope will provide a full disc image at the same position as the secondary image of the HRT. The filtergraph is therefore shared by both telescopes. A folding mirror which delivers the FDT image is movable and can be inserted into the optical path of the HRT. The mechanism will be such that the mirror will be removed from the optical beam in the case of a mechanism failure, the high resolution function will therefore have precedence.

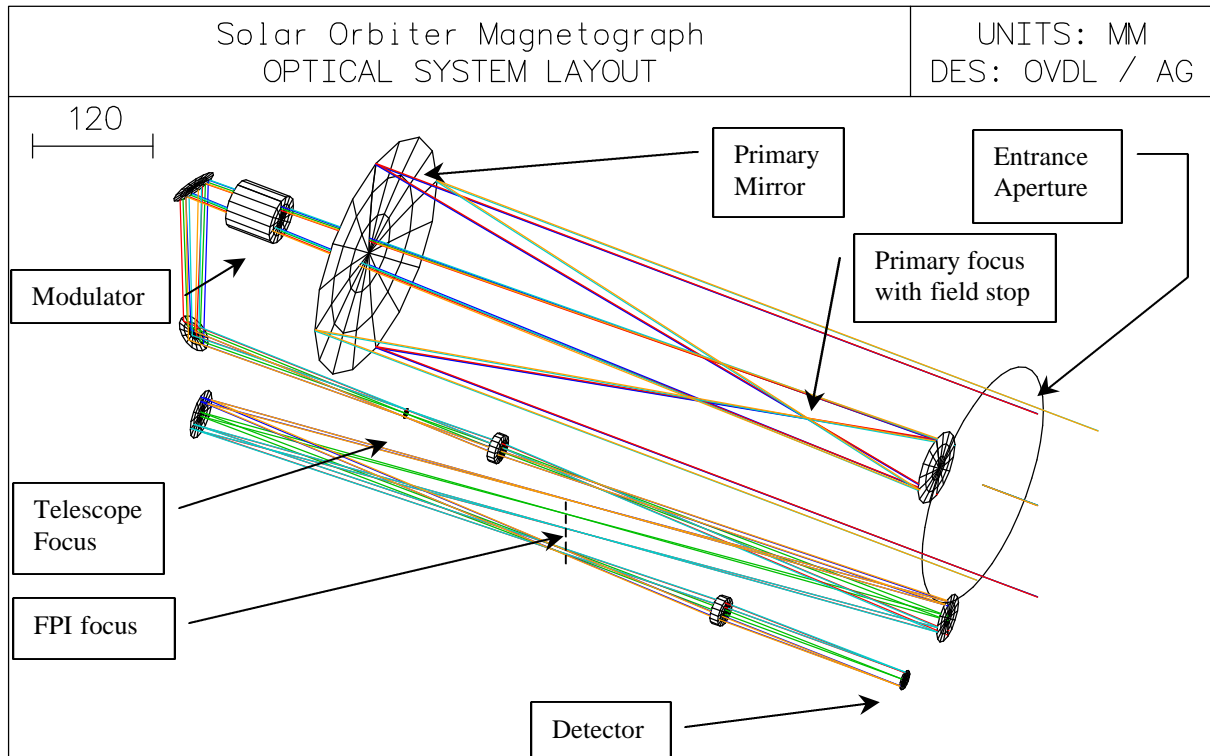


**Figure 3.6:** Perspective view of the optical layout of the high resolution telescope and filtergraph.

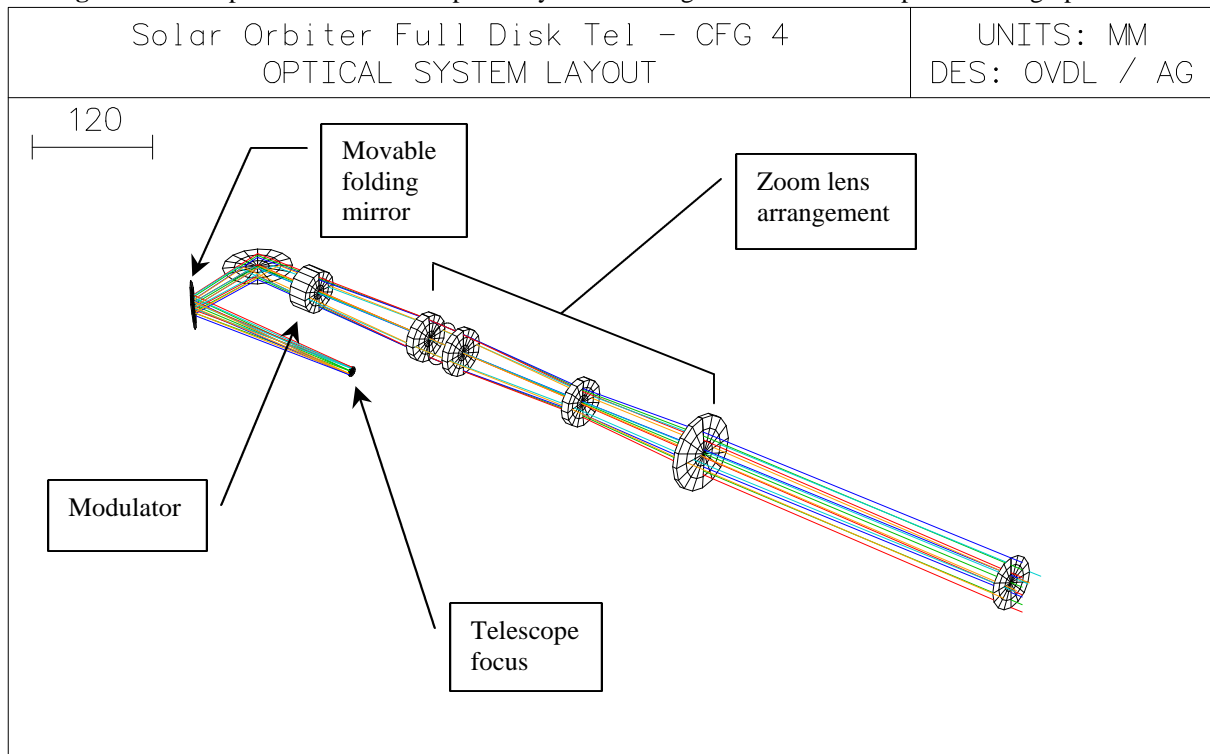


**Figure 3.7:** Perspective view of the optical layout of the full disc telescope.

The FDT has its own pointing alignment control system, which consists of a simple limb sensor and the same combination of tip-tilt mirror and dichroic as the HRT. It shares the control electronics with the HRT.

The FDT consists of a refractor with a focal length which varies between 233 mm and 888 mm. The telescope provides a full-disc image of the Sun of constant diameter on the detector during all orbital phases between 0.22 and 0.9 AU. The zoom lens consists of a classical afocal PNP triplet followed by a fixed aperture stop and a camera lens which provides a focus at a fixed position. All lenses will be singlets as chromatic aberration is not a concern with the narrow-band filtergraph. A mechanism which drives the middle lens of the triplet and the camera lens provides the zoom function. The diameter of the entrance pupil varies between 20 mm and 50 mm as the focal length increases, resulting in a diffraction

limited sampling of the detector at all distances from the Sun. The optical design is diffraction limited for all settings of the focal length.

An interference filter at the entrance aperture reflects most of the incident sunlight so that the radiation load is not a problem for the FDT.

Figure 3.7 shows the annotated optical layout of the FDT from a similar point of view as the HRT in Figure. 3.6. Note that the layout is "horizontal" (in the XZ plane) compared to the vertical (YZ plane) layout of the HRT proper. A separate modulator is necessary for the FDT in order to perform polarisation modulation within the centred optical path before the first oblique reflection.

### Filtergraph Optics (FO)

The FO consists of two singlet lenses which combine the functions of collimator and camera with a 1:2 magnification. A system of two off-axis ellipsoid and paraboloid mirrors provide a 1:1 pupil relay function and produce an f/66 telecentric intermediate image plane.

Two 50 mm diameter Fabry-Perot etalons at the telecentric image plane provide the required spectral resolution of typically 5 pm. One etalon will provide the spectral resolution while the other blocks the secondary transmission maxima of the first. A separate interference filter with a 1 nm band blocks the secondary transmission maxima of the combined etalons.

We consider using two solid state etalons with fixed resonator widths which are mounted on a common rotating stage for fine tuning. About  $\pm 1^\circ$  of rotation angle is required for a shift of the passband of  $\pm 100$  pm, which is sufficient to cover both line width and Sun-spacecraft velocity shifts.

The FO is mounted together with the FDT on a common optical bench.

Figure 3.8 shows a plane view of the filtergraph optics. The etalons are not included but their position indicated.

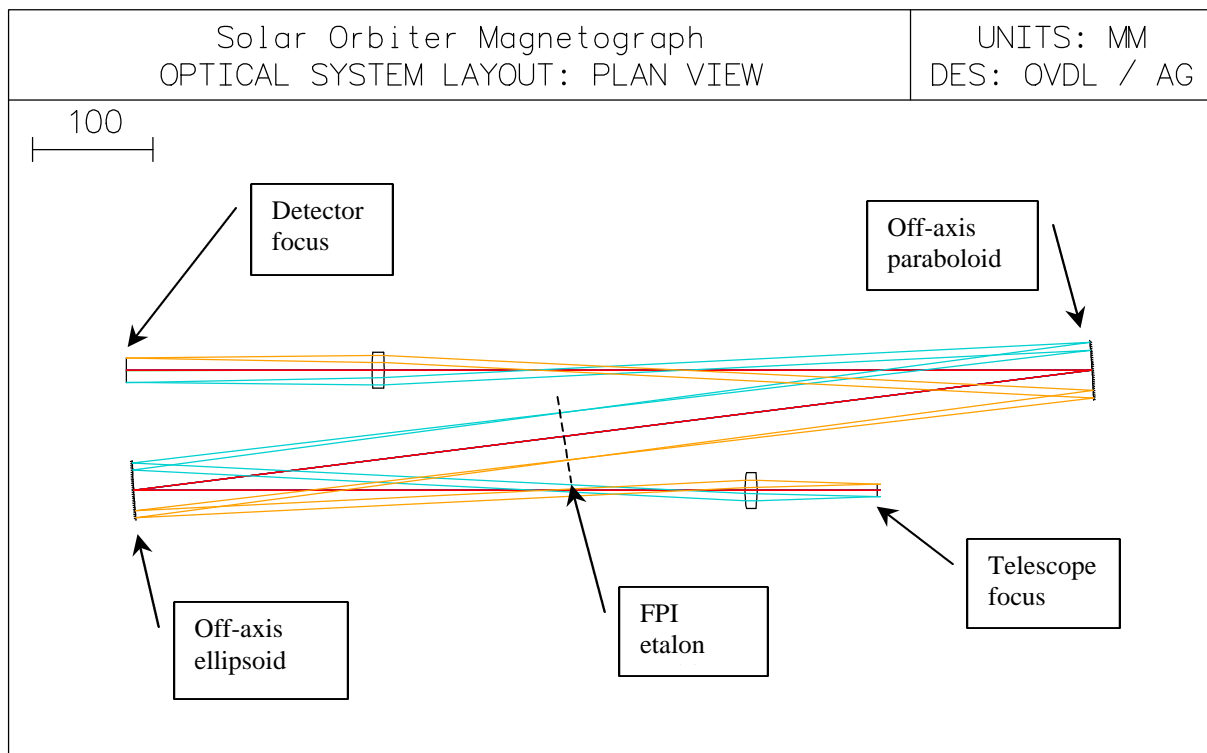


**Figure 3.8:** Arrangement of filtergraph optics.

### Overall configuration

The combination of all optical subsystems is shown in Figure 3.9. The HRT is the large cylinder on top of the Y and Z views. The FDT is to the lower left of the Z view and near the bottom of the X view. The FO are to the lower left of the Z view and near the top of the X view.

### Polarisation Modulation Package (PMP)

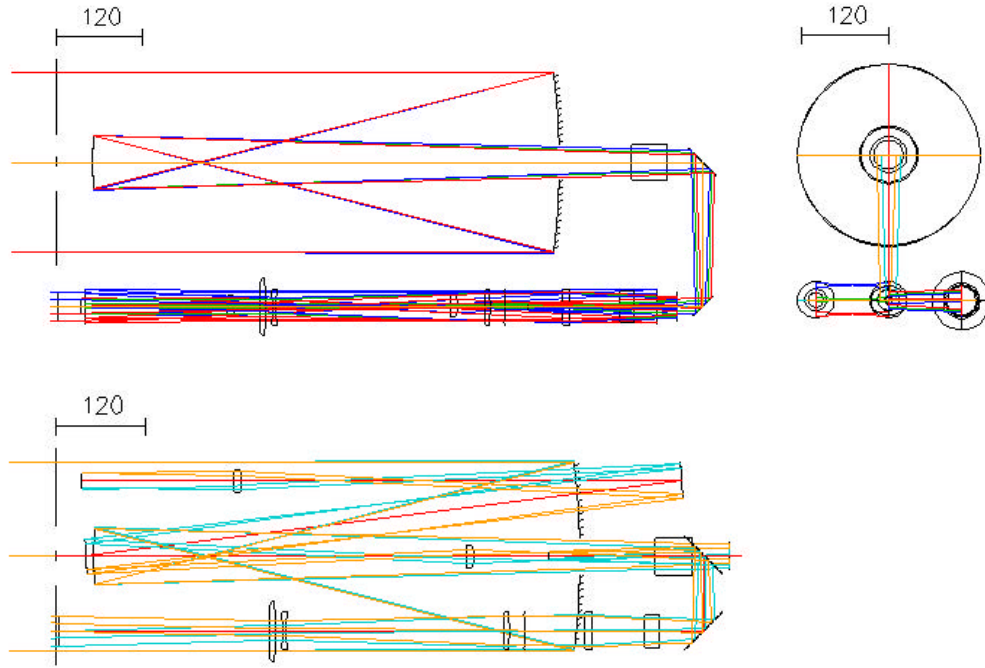


**Figure 3.9:** Plain views (top left: Y, top right: Z, bottom: X) of the combined VIM. The HRT is arranged above the FDT and the FO, both of which are mounted on a common optical bench. The optics fit a 300 mm x 400 mm x 1100 mm envelope.

The PMP will allow VIM to provide vector magnetograms of the region being observed. The PMP will produce the modulation of the intensity at the CCD as a function of the input polarisation state. These intensity changes of the CCD measurements will be used to recover the Stokes vector of the solar light.

VIM will use two PMPs, one for the HRT and one for the FDT. Each PMP will be composed of a rotating retarder and followed by a fixed linear polariser. The retarder follows the design of the Solar-B instrument, which is based on the Advanced Stokes Polarimeter (ASP) used at Sacramento Peak observatory. The retarder will be positioned at 8 different positions per half rotation, each separated by  $22.5^\circ$ . At each of these positions the CCD will be read and the 8 readouts combined in different ways to determine the final Stokes parameters (I,Q,U,V).

#### *Optical alignment and image stabilisation*

The optical alignment of the VIM is an important and critical issue. Due to large temperature gradients during the mission, it is important to have reliable and accurate in-flight alignment capabilities. To this end, we propose a wavefront control system which is capable to detect low order modes of wavefront deformations in the telescope. A wavefront sensor measures the actual state of the optical alignment and generates an appropriate error signal. A control system converts this error signal into actuation signals which are used to drive the position of the secondary mirror M2 and the tip-tilt mirror (M3).

Figure 3.10 shows a sketch of the wavefront sensor which is located in the vicinity of the secondary focus. The sensor consists of a collimating lens, a hexagonal lenslet array with seven - one central and six peripheral - elements which cover the pupil of the telescope, and lenses which reimage the lenslet array focal plane onto a matrix array detector (CCD camera). The image scale of the pupil on the array is chosen such that the illuminated areas of the lenslets are equal, taking also into account the central obstruction. All lenslets are partially illuminated.

#### *CCD cameras*

A variety of CCD detectors exist on the market that are fully adequate for the VIM. The HRT and FDT telescopes have been designed for a 2k x 2k CCD with  $10\ \mu\text{m}$  pixels. Such CCDs are already common on the market today.

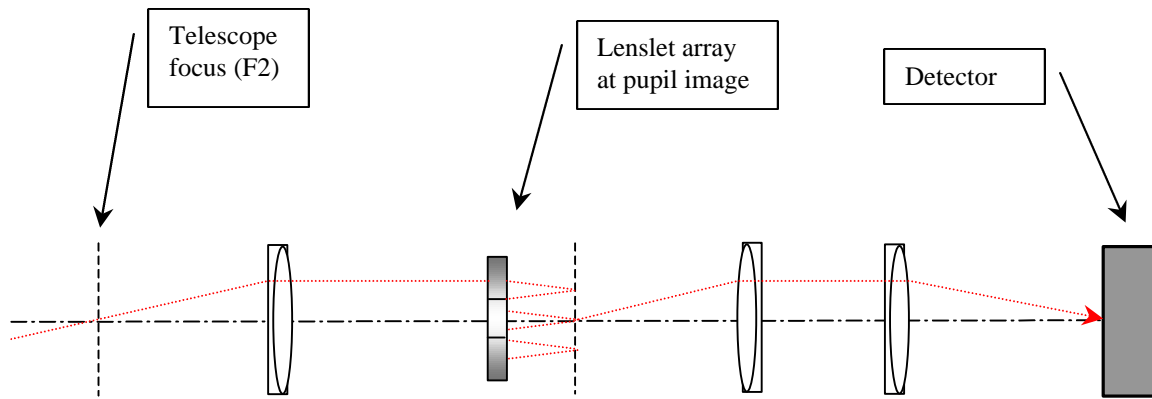


**Figure 3.10:** Optical configuration of wavefront sensor.

## RESOURCES AND REQUIREMENTS

### *Telemetry needs – data compression.*

VIM will have various high cadence data acquisition modes, each optimised for the specific scientific requirements of local-area helioseismology measurements and magnetic field dynamics observations. For example, one can read only 1024 x 1024 pixels (smaller FOV, but still large enough for magnetic field studies) or readout the CCD with 2 x 2 on-chip summing (preserving FOV with reduced spatial resolution, but still adequate for local helioseismology). In this case, 1 full frame (1024 x 1024, 12 b/pixel) at a cadence of 1 per minute produces a data rate of 200 kb/s. By using efficient lossy compression algorithms with a reduction factor of 10, the average data rate will be around 20 kb/s. In this mode only one physical quantity would be stored (e.g. the LOS magnetic field or the LOS velocity). Another option will be to read all 2048 x 2048 pixels, and send 4 physical magnitudes (for example all 4 Stokes parameters) at a cadence of 1 frame each 15 minutes using a similar data rate. In the low rate observing mode (3 kb/s), one can send 2 physical magnitudes at full resolution at a cadence of 1 per hour.

### *Mass breakdown and power requirements*

	Mass (g)
<b>1. High Res. Telescope (incl. ISS, re-imaging, filter, CCD)</b>	<b>18000</b>
- 25 cm telescope (mirrors + structure)	3000
- prefilter (@ primary hole)	400
- rotating quarter wave plate	800
- linear polariser	200
- folding mirror	400
- tip-tilt mirror + PZT (incl. electronics)	1700
- cube beam-splitter	200
- ISS lens	200
- ISS detector	800
- re-imaging system (4x200)	800
- Fabry-Perot and Oven	3000
- shutter	300
- CCD camera + electronics	2700
- harness (25% of total above)	3500
<b>2. Full Disc Telescope</b>	<b>3000</b>
- prefilter	200
- focal lenses (4x200)	800
- rotating quarter wave plate	800
- linear polariser	200
- folding mirror	400
- harness (25% of total above)	600
<b>3. VIM enclosure</b>	<b>5000</b>
<b>4. VIM TOTAL</b>	<b>26000</b>

**Table 3.14:** VIM mass break-down.

	Power (W)
CCD	5
Image Stabilisation System	5
Fabry Perot & Oven	10
PMP (x2)	5
<b>TOTAL</b>	<b>25</b>

Table 3.15: VIM power requirements.

## INSTRUMENT SUMMARY

<b>Telescope</b>	HRT: Gregorian reflector - 250 mm diameter - effective focal length 8500 mm FDT: zoom lens - aperture: 20 – 50 mm - effective focal length: 233 – 888 mm
<b>Spatial resolving element</b>	0.28 arcsec pixel size (40 km on Sun at 0.2 AU)
<b>Spectrometer</b>	- Fabry-Perot double etalon - tuning by rotation
<b>Spectral resolution</b>	FWHM: <50 mÅ
<b>Field of View/Pointing</b>	80 x 80 Mm <sup>2</sup> ; pointing to anywhere on Sun by tilting and decentering secondary mirror.
<b>Detector</b>	CCD: - 10 µm pixels - 2048 x 2048 array - back thinned
<b>Stability</b>	Active image stabilisation system and low order wavefront correction.
<b>Telemetry</b>	20 kb/s
<b>Mass</b>	26 kg
<b>Power</b>	25 W
<b>Size</b>	Optics box: 110 cm x 40 cm x 30 cm

Table 3.16: VIM instrument summary.

## 3.3.3 EUV spectrometer (EUS)

## SCIENTIFIC DRIVERS

Observations of the UV/EUV spectral range are critical for the determination of plasma diagnostics in the solar atmosphere across the broad temperature range from tens of thousands to several million K. Analysis of the emission lines, mainly from trace elements in the Sun's atmosphere, provides information on plasma density, temperature, element/ion abundances, flow speeds and the structure and evolution of atmospheric phenomena. Such information provides a foundation for understanding the physics behind a large range of solar phenomena.

Current spacecraft instrumentation (SOHO) provides EUV spatial and spectral resolving elements of order 2-3 arcsec and 0.01 nm, respectively, and UV resolutions of 1 arcsec and 0.002 nm. There are no plans for EUV or UV spectroscopic measurements from the NASA STEREO mission (2004 launch), the NASA Solar Dynamics Observatory (~2005 launch) and the Solar Probe (~2007 launch). The only planned EUV spectrometer for a future mission is the EIS instrument on Solar-B with 1 arcsec (750 km on the Sun) and 0.001 nm resolving elements. However, this instrument is tuned to active region observations with almost no transition region capability.

The European solar physics community has a well established expertise in solar EUV/UV spectroscopy as illustrated by the successful CDS and SUMER instruments on SOHO.



## INSTRUMENT CONCEPT

Whilst recognising that an EUV spectrometer is an essential component of the Solar Orbiter, we must be aware that it must be compact and light-weight, must not be too telemetry ‘thirsty’ and must be able to cope with the thermal and particle environment of such an orbit.

A Ritchey-Chretien telescope design, feeding a spectrometer, has been chosen to minimise the size of the EUS instrument. It has the disadvantage of one extra reflection over, for example, a single-mirror off axis paraboloid system, but the wavelength range selected is geared to bright solar EUV lines.

The instrument structure would be made of carbon fibre, with silicon carbide (SiC) optical components. Multilayers will be considered if the final wavelength selection requires it.

### Basic optical layout

In the current design, the primary and secondary mirrors are separated by 900 mm, with the focal plane 200 mm beyond the primary, making a total telescope length of 1.1 m. The telescope diameter is 120 mm, making an overall diameter of the telescope “tube” of about 150 mm. The telescope effective focal length is 3.7 m.

The slit assembly lies at the focal plane and beyond this is the spectrometer, with a toroidal grating forming a focus at a 2-D detector. The grating ruling spacing is yet to be decided but we take 4800 l/mm as a guide for the current calculations. For the wavelength bands selected (see Table), and assuming a spectrometer magnification of 1.5, the spectrometer will project 1.2 m beyond the focal plane with a 1.76 m distance to the detector. The detector will lie 0.55 m off-axis, adjacent to the primary mirror. Thus, without a spectrometer, the instrument cross-section would be of order  $15 \times 15 \text{ cm}^2$  but the off-axis path of the spectrometer will ensure that the back-end of the instrument is wider, making an overall boot-shaped instrument of maximum dimensions of order 230 cm x 15 cm x 55 cm. The 55 cm dimension is dependent on the choice of grating and the wavelength selection.

The secondary mirror presents a portion of the Sun at the slit and can be rotated to allow rastered images (i.e. exposures interlaced with mechanism movements to build up images simultaneously in selected wavelengths). Only some 20% of the Sun will be visible to the secondary. The instrument can be re-pointed to acquire particular targets.

Calculations of the spot-size at the focus from ray-tracing codes have been performed for various angles of the secondary. This confirms that the concept of rastering with the secondary is workable for the scientific requirements over the planned range. We plan a  $9 \mu$  detector pixel size and a field of view of  $34 \times 34$  arcmin.

The heritage of this instrument comes from the SOHO/CDS, SOHO/SUMER and Solar-B/EIS projects.

### Resolution/detector

We size the instrument to an observing distance of 0.2 AU (perihelion). A spatial resolving element of 0.1 arcsec represents 75 km on the Sun from the Earth; the same resolution can be achieved at 0.5 arcsec from 0.2 AU. With regard to spectral resolution, our basic aim is to return sufficient numbers of well separated spectral lines to allow thorough spectroscopic studies.

A detector array of  $4k \times 4k \times 9 \mu$  pixels is baselined. Thus, the EUS has a spectral range of 4 nm at 0.001 nm/pixel. The same array will give a spatial extent (vertical distance on the detector = slit length) of  $0.5 \text{ arcsec} \times 4096 = 2048 \text{ arcsec} = 34 \text{ arcmin}$ . The solar diameter at 0.2 AU is 170 arcmin, i.e. we have a slit length of 0.2 of the solar diameter. Thus, a pointing mechanism is required. For a given pointing location, rastered imaging will be made up from movement of the secondary mirror in only one direction.

We baseline an APS (Active Pixel Sensor) detector system. The SOHO CCD detectors receive many “cosmic ray” particle hits, occasionally have “bleeding” of charge for the brightest intensities (e.g. EIT flares and LASCO planets) and there must be some degradation due to protons causing damage to the silicon lattice (this creates “traps” that can steal charge which can be transferred to other parts of the image).

In an APS device, the signal charge is sensed by an amplifier within the pixel (each pixel has its own). Therefore, it avoids the charge transfer problem. Pixels will still be hit, but the damage will not propagate because of the transfer process used for CCDs.

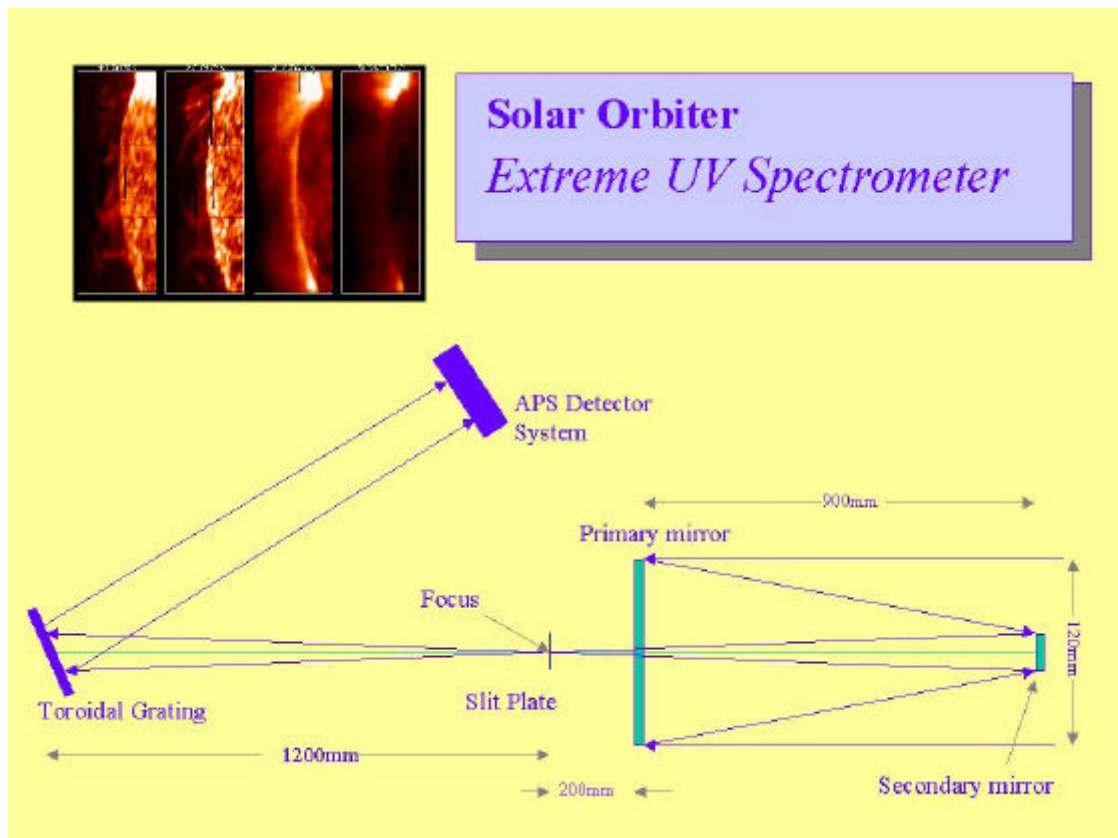


**Figure 3.11:** Optical scheme of the EUS.

This charge “trap” problem has been experienced by Chandra, mainly because the CCDs have a direct line of sight to space for protons and the damage was done mainly by relatively low energy protons (~100 keV) of which there are many. In SOHO, there is a lot more shielding. However, this effectively means that the degradation will be at a slower rate, not that there will be no degradation. For a long duration mission (7 years) heading into a more intense particle environment, we have to consider this seriously. We expect a more intense particle environment because the Solar Orbiter is more likely to encounter accelerated protons from solar events.

Intense sources display bleeding on CCD devices. This is not the case for the APS detector system. This alone could be a tremendous advantage.

The APS detectors are still silicon chip devices, it is just that they incorporate individual pixel amplification and charge extraction. The EUV sensitivity will be provided in the same way as with CCDs, in this case with back-thinned devices. There is no mass overhead in using such a system, relative to the CCD approach.

## RESOURCES AND REQUIREMENTS

### Telemetry

For EUS we baseline 17 kb/s telemetry. The instrument detector has 4096 x 4096 pixels. It is clear that data from individual exposures will have to be selected carefully, as given by pre-defined observing sequences – i.e. only selected fractions of the full range would be returned in any exposure. In addition, a number of compression schemes should be available with a common (“lossless”) compression of order 3-5 but other schemes up to a factor of 10 would be available.

In order to cope with the limited telemetry resources, a combination of novel compression schemes, large dedicated instrument memory and careful emission line selection will be applied. In the light of the successful operation of the CDS instrument on SOHO – where a similar selection and compression consideration was applied - and the new opportunities given by the Orbiter’s location, it is anticipated that this instrument can make significant advances with a telemetry rate of order 17 kb/s.

### *Stability/pointing*

Given our plan to achieve 0.5 arcsec resolution elements, we must choose one of the following options:

- do not include an image stabilisation system, assuming that the variations of the spacecraft stability occur on timescales much less than the exposure time of the spectrometer and thus any corrections could be done on the ground;
- include an image stabilisation system, possibly making use of VIM limb sensor error signals to drive adjustments to the secondary mirror.

The EUS instrument would require an independent pointing system to enable independent observation of any solar location. This would be done using actuators at the legs of the instrument.

### *Thermal environment*

At 1 AU the average solar intensity is  $1.371 \text{ W/m}^2$ . During the nominal phase, in each 149 day period, the spacecraft will encounter a range from  $2142 \text{ W/m}^2$  (0.8 AU) to  $34275 \text{ W/m}^2$  (0.2 AU – 25 times the value at 1 AU). This presents a severe thermal challenge which we tackle in a number of ways.

The SiC primary mirror “sees” the full Sun. SiC optical components can run hotter than traditional components, but the primary receives  $310.6 \text{ W}$  at 0.2 AU. Gold-coating is used to reduce the absorption (to 0.2). We run the primary mirror at  $70^\circ\text{C}$ , and require a dedicated radiator of  $0.11 \text{ m}^2$  ( $33 \text{ cm} \times 33 \text{ cm}$ ).

Some  $248.5 \text{ W}$  are reflected from the primary. The secondary is sized such that it catches only 20% of this, i.e. it only sees 20% of the solar image, and much of the image is reflected back out of the aperture. Thus,  $49.7 \text{ W}$  is received by the secondary mirror which will also be gold coated. Thus it absorbs  $9.9 \text{ W}$  which will require dissipation via a small radiator of area about  $11 \text{ cm} \times 11 \text{ cm}$ . We run the secondary at  $83^\circ\text{C}$ .

The reflected component, now  $39.8 \text{ W}$  continues toward the spectrometer aperture in the primary. This beam can be reduced considerably by stops; only about 1/100 of this incoming beam is required for each exposure.

Finally, the APS detector system should run cold and this would require a cold finger to a further radiator. For the current design we assume passive radiators to space. With regard to the remaining structure, the design would include thermal blankets and the front panel could include a solar shield. Heaters will be required to maintain the correct temperature gradients throughout the orbit.

### *Instrument pointing and the spacecraft shield*

The EUS can view a  $34 \times 34$  arcmin area of the Sun, which has an apparent diameter of about 170 arcmin at 0.2 AU. Thus an independent pointing mechanism is required which needs to cover the range of about  $\pm 3^\circ$ . The instrument has an aperture of 120 mm. This must match a viewing port in the spacecraft +X-plate shield. To minimise the viewing port size, the instrument will be mounted on six legs (like the SOHO/CDS instrument) with the actuators at the back and the pivot near the front of the instrument. Thus, we envisage a port size of approximately 130 mm. The front shield of the EUS instrument will act as a secondary to the spacecraft shield when the aperture edge and viewing port edge are not aligned.

### *Mass breakdown*

A rough breakdown of the estimated mass is given in Table 3.17. We take the view that this is a new generation instrument made of light-weight materials which really ought to be significantly lighter than, for example, the equivalent (100 kg) instruments on SOHO.

Component	Mass (kg)
Primary mirror	0.5
Mirror support	0.3
Secondary mirror	0.1
Mirror scan mechanism	0.6
Slit assembly	0.3
Grating assembly	0.6
OPS	1.5
Detector	1
Detector electronics.	1.5
Baffles	0.5
Structure	5.4
Thermal subsystem	3.5
Harness	1.2
Main electronics incl. PSU	5
GRAND TOTAL	22

**Table 3.17:** Mass breakdown of the EUS.*INSTRUMENT SUMMARY*

<b>Telescope</b>	<ul style="list-style-type: none"> <li>- Ritchey-Chretien type:</li> <li>- 120 mm diameter</li> <li>- 900 mm primary to secondary</li> <li>- 1100 mm secondary to focus</li> <li>- effective focal length 3.7 m</li> <li>- gold-coated SiC mirrors</li> </ul>
<b>Spectrometer</b>	Normal Incidence: <ul style="list-style-type: none"> <li>- 4800 l/mm toroidal grating</li> <li>- slit/grating distance 1200 mm</li> <li>- grating/detector distance 1760mm</li> </ul>
<b>Spatial resolving element</b>	0.5 arcsec (75 km on Sun at 0.2 AU)
<b>Spectral resolving element</b>	0.001 nm/pixel (5 km/s)
<b>Raster Mechanism</b>	Through motion of the secondary
<b>Detector</b>	Active Pixel Sensor (APS): <ul style="list-style-type: none"> <li>- 9 <math>\mu</math> pixels</li> <li>- 4096 x 4096 array</li> <li>- back thinned</li> </ul>
<b>Preliminary Wavelength Selection</b>	<ul style="list-style-type: none"> <li>- First Order: 58 –62 nm</li> <li>- Second Order: 29 –31 nm</li> </ul> (e.g. Fe XII 291, Si X 293, He I 584, Si IX 296, O III 599, He II 304, Mg X 610, Fe XIX 592).
<b>Slit Length/Width</b>	34 arcmin length; width <9 $\mu$
<b>Field of View/Pointing</b>	Raster over 34 arcmin; pointing to anywhere on Sun with independent pointing mechanism.
<b>Telemetry</b>	17 kb/s
<b>Mass</b>	22 kg
<b>Power</b>	25 W
<b>Size</b>	Instrument : 230 cm x 15 cm x 55 cm Electronics box: 20 cm x 20 cm x 20 cm
<b>Thermal</b>	Mirror operating temperatures 70 and 83°C, both with radiators. APS detector cooled with cold finger and radiator. Possible shield at front. Standard thermal blankets with heaters for thermal control.
<b>Operation</b>	On board deferred command store in which can be loaded time-tagged observation sequences designed on the ground.
<b>Stability</b>	Active image stabilisation system at secondary may be considered if jitter is significant over common exposure times.

**Table 3.18:** EUS instrument summary.

### 3.3.4 EUV imager (EXI)

#### SCIENTIFIC DRIVERS

Observations from Yohkoh, SOHO and TRACE in extreme ultraviolet and X-ray wavelengths have revealed a truly complex, highly dynamic solar atmosphere with magnetic loops confining plasmas at widely varying temperatures. The TRACE EUV observations in particular illustrate the existence of fine-scale structures in coronal loops, and reveal continuous dynamic activity in particular at the smallest scales. In the quiet Sun, various "events" of different sizes (e.g., bright points, explosive events, jets, blinkers) all provide evidence for small-scale heating, probably related to magnetic reconnection. The observed distribution functions have self-similarity properties which point at sub-resolution processes. The results from Yohkoh, SOHO, and TRACE led to new questions concerning the real basic dimensions of coronal structures, the role played by nanoflares in the heating of the quiet solar corona, and the structuring of the corona above the poles.

Dramatic new results can be obtained by increasing the spatial resolution by one order of magnitude on one hand and from connecting chromospheric/coronal phenomena with close *in-situ* measurements on the other hand.

This is where an EUV Imager (EUI) on the Solar Orbiter can fully exploit the unique capabilities of the mission. EUI will provide EUV images with an angular resolution increased by one order of magnitude in order to reveal the fine-scale structure of coronal features. The closeness of the Sun makes this task easier. EUI will also provide full disc EUV images of the Sun in order to reveal the global structure of inaccessible regions such as the "far side" of the Sun and the polar regions.

The European solar physics community has a well established expertise in solar EUV/UV imaging as illustrated by the successful EIT instrument on SOHO. Some studies concerning the thermal (radiative) load on the optics have been shared with European teams involved in the remote sensing package of the Solar Probe mission.

#### INSTRUMENT CONCEPT

A single telescope, providing both high spatial resolution and a full disc field-of-view, faces two difficulties:

1. limited number of pixels on current detectors and telemetry constraints;
2. thermal (radiative) load at perihelion (25 solar constants on the first optical element if the field-of-view is not reduced).

These considerations led to a separation of the EUI into two instruments: a High Resolution Imager (HRI) and a Full Sun Imager (FSI). In this way, one can find specific solutions for the thermal load and have realistic detectors.

#### High Resolution Imager (HRI)

The design driver is the need to get rid of the unwanted solar radiation which goes along the direct light path. A first step consists in reducing the entrance aperture of the instrument to about 2 cm and to fully use the available length of the payload module. In doing so, one can cluster a few telescopes together, each one dedicated to one wavelength, which eliminates any moving part, takes full use of the aperture and allows for *simultaneous* observations in different wavelengths.

Essentially one reduces the FOV through the use of an entrance baffle and one sets the FOV to 70 000 km (or 500 arcsec when at perihelion) for a 2 x 2 K detector. This sets the equivalent pixel size to 35 km on the Sun (or 0.25 arcsec, equivalent to 0.05 arcsec from Earth). The pixel size of the detector is baselined at 9  $\mu$ m, so the equivalent focal length is 7.2 m.

We baseline a set of three telescopes working at 13.3, 17.4, and 30.4 nm. These three wavelengths cover a very wide range of temperatures (from  $5 \times 10^4$  K up to  $1.6 \times 10^7$  K) and targets (from quiet Sun to flares). Note that the 13.3 nm band includes a very hot line (Fe XXIII), visible only during flares and that the 17.4 nm band only selects the 17.4 nm Fe X line, excluding the cooler Fe IX line at 17.1 nm.

The basic feature of each telescope relies upon the use of a long baffle to reduce the FOV and the stray light, an entrance metallic filter and an off-axis Gregory telescope with multilayers fitted to each wavelength. The Gregory concept allows to put stops at the focal plane and at the image of the entrance aperture, which leads to a significant reduction of straylight. Figure 3.12 shows the optical scheme of the HRI.

A carbon-carbon composite structure is planned.

We baseline 2k x 2k pixel APS detectors (see EUS section in 3.3.3). Diamond or GaN/AlGaIn new generation detectors are interesting alternatives. They are robust, solar-blind (allowing a better instrumental sensitivity) and hard-rad.

For the 17.4 nm and 30.4 nm channels, the small aperture will give a few counts per pixel per second. One can cope with this low number by increasing the exposure time and/or on-board binning. The count number for the 13.3 nm channel can be much higher but only on very active regions and flares.

The electronics (including the DPU) is common to the three detectors and to the FSI telescope. Its volume should fit within the overall volume given in the Table 3.22.

### Full Sun Imager (FSI)

The Full Sun Imager needs a wide field (about  $5^\circ$ ) when at perihelion in order to cover the full lower solar corona with about 50 % margin in each direction. In order to solve the issue of thermal (radiative) load on the entrance filter of the FSI, different schemes have been investigated. One possibility is to move the entrance filter as far back as possible (1800 mm) and as close as possible to the M1 mirror. Then the mirror combination (all off-axis) allows for an image quality of the order of the pixel size ( $9 \mu$ ). The entrance filter is crossed twice by the light. This system can work e.g. in the 17.4 nm line with an appropriate multilayer (Mo/Si) coating. Another solution exists if one works above 120 nm (e.g. in the  $L\alpha$  line at 121.6 nm). The dimensions of such an instrument are of the order 2000 mm x 250 mm x 400 mm, i.e. shorter but wider than the HRI.

Figure 3.13 shows the optical scheme of the FSI.

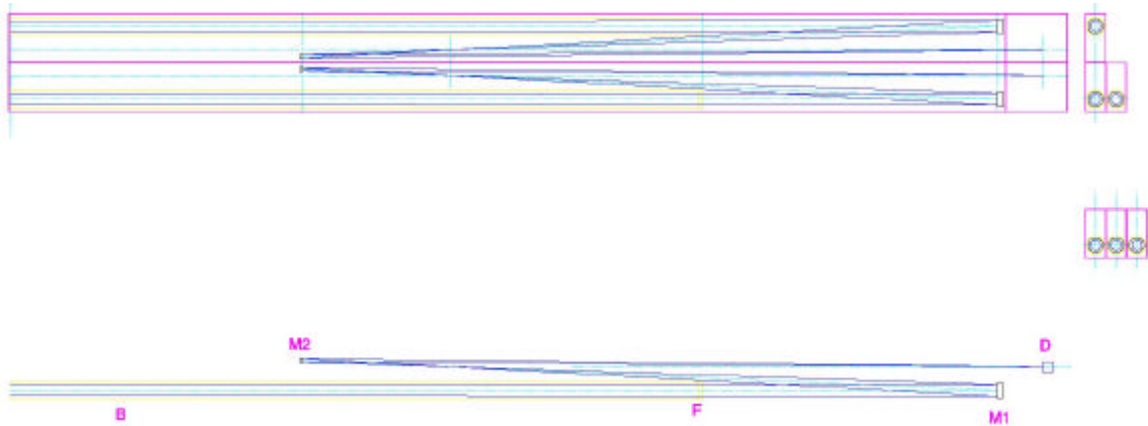


**Figure 3.12:** HRI optical scheme with its basic components (bottom) : B: baffle, M1: primary mirror, M2: secondary mirror, F: entrance filter, D: detector. The figure also shows two possible implementations of the three telescopes (top and bottom; boxes on the right-hand side).

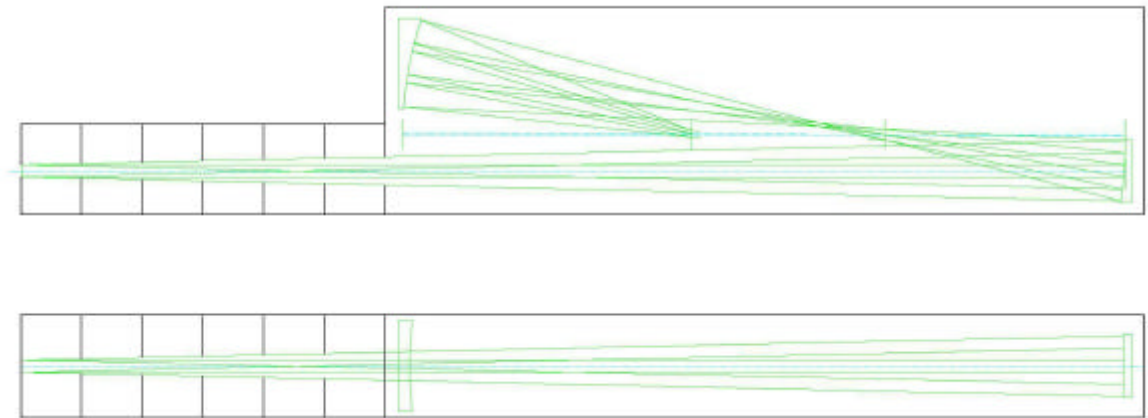


**Figure 3.13:** FSI optical scheme with the same components as in Fig. 3.12.

## RESOURCES AND REQUIREMENTS

### HRI telemetry

With all three telescopes working together at a 10 seconds cadence, we arrive at a *peak* telemetry rate of 720 kb/s after data compression. An average rate of less than 20 kb/s can be obtained by a combination of further compression/selection schemes (e.g. on-board 2x2 binning, or cascade time differentiation) and by adopting appropriate observing strategies (e.g. interleaved high/low time resolution sequences, observations in only one channel, etc.). We assume that we can compress the data by a factor 20. Actually, with a Rosetta-type compression scheme, tests performed on solar images indicate that compression factors as high as 50 can be achieved.

### HRI mass budget

The overall HRI mass budget is given in the Table 3.19.

Component	Mass (kg)
Structure (including the baffle) :	6.0
Optics (including mounts) :	0.2
Detector (including electronics and shielding) :	0.5
Miscellaneous (harness, ..)	0.1
Margin	0.7
 Total per telescope	 7.5
Total for 3 telescopes	22.5
Pointing mechanism	2.0
Electronics shared between the 4 telescopes	1.0
 Grand total for the HRI	 25.5

**Table 3.19:** Mass breakdown of the HRI of EUI

### HRI power

The power requirements have been considered for the detector, electronics and the pointing actuator (common to the three telescopes). For a given telescope, we anticipate a constant power requirement of about 4 W for the cycling (power on, integration, dump to memory). With reasonable margins and the required power for pointing, the total is 5 W. If the three telescopes are working simultaneously, they will consume about 15 W for basic functions (above) to which one has to add about 2 W for data compression and dumping by the common DPU. Non-simultaneous (sequential) observations of course lead to a smaller power consumption.

### HRI stability/pointing

Given our plan to achieve 0.25 arcsec resolution elements and the fact that exposure times are of the order of 10 seconds, an image stabilisation system should be included, possibly making use of the VIM limb sensor error signals to drive adjustments to the secondary mirror.

The three telescope cluster has its own pointing mechanism since the limitation of the FOV prevents any independent internal pointing. The pointing is performed by a joint displacement of the three telescopes. The spacecraft has an offset capability of about 10°, much larger than that required (2.5° at perihelion), and thus in principle it would be possible to point to a solar target using the whole spacecraft.

### FSI requirements

An average rate of 0.5 kb/s is sufficient to transmit one compressed full Sun image every 4800 s (about every hour and 20 minutes).

The FSI mass is about 10.5 kg (structure: 6.5 kg; optics and mountings: 3 kg; detector and associated electronics: 1 kg).

Power is only required for the detector (3 W) since the electronics is common with HRI.

The FSI also relies on the pointing stability of the payload module but with constraints much less stringent than for the HRI.

The HRI and FSI characteristics are summarised in the Tables 3.20 and 3.21, respectively..

3 Telescopes	Off-axis Gregory; 20 mm diam.
Spatial resolving element	0.25 arcsec pixel size (35 km on Sun at perihelion)
Pointing	Common pointing mechanism for the three components
Detector	Baseline 9 $\mu$ , 2000 x 2000 pixels
Field of View	70x70 Mm <sup>2</sup> at perihelion
Peak Telemetry	720 kb/s (with compression 20)
Average Telemetry	19.5 kb/s
Mass	25.5 kg
Power	17 W (essentially detectors; shared electronics and DPU)
Size	Instrument = 2500 mm x 150 mm x 240 mm
Thermal	Operating temperature 20°C with passive cooling; 140 cm long baffle at the entrance of each telescope
Stability	Active image stabilisation at secondary.

**Table 3.20:** Characteristics of the HRI of EUI

Telescope	Off-axis Gregory; 20 mm diam.
Spatial resolving element	9 arcsec (1300 km on Sun at perihelion)
Pointing	Pointed at Sun centre
Detector	Baseline - 9 $\mu$ , 2000 x 2000 detector
Field of View	4 x 4 solar radii at perihelion
Peak Telemetry	240 kb/s (with compression 20)
Average Telemetry	0.5 kb/s
Mass	10.5 kg
Power	3 W
Size	Instrument = 2000 mm x 250 mm x 400 mm
Thermal	Operating temperature 20°C with passive cooling; 600 cm long baffle at the entrance of each telescope

**Table 3.21:** Characteristics of the FSI of EUI

## INSTRUMENT SUMMARY

HRI and FSI	Off-axis Gregory Telescopes; 20 mm diam.
Spatial resolving element	HRI : 0.25 arcsec pixel size (35 km on Sun at perihelion) FSI : 9 arcsec (1300 km on Sun at perihelion)
Pointing	HRI : pointing mechanism to point anywhere on the Sun FSI : pointed at Sun centre
Detector	Baseline - 9 $\mu$ , 2000 x 2000 pixels
Field of View	HRI : 70x70 Mm <sup>2</sup> at perihelion FSI : 4 x 4 solar radii at perihelion
Average Telemetry	20 kb/s
Mass	36 kg
Power	20 W
Size	Instrument = within 2500 mm x 400 mm x 400 mm
Thermal	Operating temperature 20°C with passive cooling

**Table 3.22:** EUI instrument summary.



### 3.3.5 Ultraviolet and Visible-light Coronagraph (UVC)

#### SCIENTIFIC DRIVERS

Co-rotation, during the helio-synchronous phases of the orbit, will freeze for many days coronal structures in the plane of the sky. This condition will be most favourable to investigate the evolution of the magnetic configuration of streamers in order to test the hypothesis of magnetic reconnection as one of the main processes leading to the formation of the slow solar wind.

The out-of-ecliptic vantage point will allow for the first time a unique view of the plasma distribution and solar wind expansion in the coronal low-latitude/equatorial belt. Therefore it will be possible to measure the longitudinal extent of coronal streamers and coronal mass ejections. These parameters, that at present are unknown, are essential to determining the magnetic flux carried by plasmoids and coronal mass ejections in the heliosphere.

UVC will allow the first determination of the absolute abundance (i.e. relative to hydrogen) of helium in corona. Helium, the second largest contributor to the density of coronal plasma, is important for the dynamics of solar wind, and it may act as a regulator to maintain a nearly constant solar wind mass flux.

UVC will also determine the differential outflow speed of the major components (H, He) of the solar wind and discriminate the mechanisms of solar wind acceleration.

The European solar community has a well established expertise in visible light and UV coronagraphy as illustrated by the successful LASCO and UVCS instruments on SOHO.

#### INSTRUMENT CONCEPT

UVC is an externally occulted telescope designed for narrow-band imaging of the EUV corona in the He II 30.4 nm and H I 121.6 nm lines, and for broad-band polarisation imaging of the visible K-corona, in an annular field of view between 1.2 and 3.5 solar radii, when the Solar Orbiter perihelion is 0.21 AU. When it moves to 0.3 AU, at the end of the nominal mission, the UVC field-of-view is within 1.8 and 5.3 solar radii.

The telescope optical configuration is an off-axis Gregorian. The EUV L $\alpha$  lines are separated with multi-layer mirror coatings and EUV transmission filters. These mirrors with coating optimised for 30.4 nm still have a good reflectivity at 1216 nm and in the visible. The visible light channel includes an achromatic polarimeter, based on electro-optically modulated liquid crystals.

#### Optical design

##### -Telescope

The external occulter ensures both thermal protection for the optics and better stray-light rejection. A Gregorian telescope design has been chosen because it gives real images of the external occulter and the edges of the telescope primary mirror. Field and Lyot stops will be used to reduce stray light and diffracted radiation from the telescope primary mirror. In addition, use of an annular secondary mirror and light trap captures and removes diffracted light from the external occulting disc and its supports. A light trap behind the primary mirror ensures that only the light reflected by the mirror enters the filters and detector assembly structure. The direct light from the solar disc is mostly dumped into space, though a portion of it may be used for radiometry and / or coarse imaging of the solar disc in the three wavelength bandpasses.

##### -UV and Visible-Light Channels

The instrument structure is made of carbon fibre, with Zerodur optical components. Zerodur is used for the mirrors' substrate because of its extremely small thermal expansion coefficient. Optics made with this material is also easy to polish into non-spherical figures with sub-angstrom rms surface roughness.

The basic specifications and drivers of the instrument are summarised in Table 3.24.

#### Structure

The instrument structure is of carbon fibre/cyanate or carbon-carbon composite, designed for zero coefficient of thermal expansion in the axial direction. It is in the form of a rigid rectangular baseplate to which are bonded appropriately placed brackets (also of composite) for the support of the optical and detector elements. The focus and orientation of each element is set and maintained by a precision spacer

located between the element and its support bracket. The optical system is surrounded by a lightweight rectangular composite enclosure and baffle structure that attaches to and further strengthens the baseplate. Removable covers on the top of the enclosure allow for installation and servicing of the optical and detector elements. An external door mechanism shields the telescope aperture when the instrument is not observing.

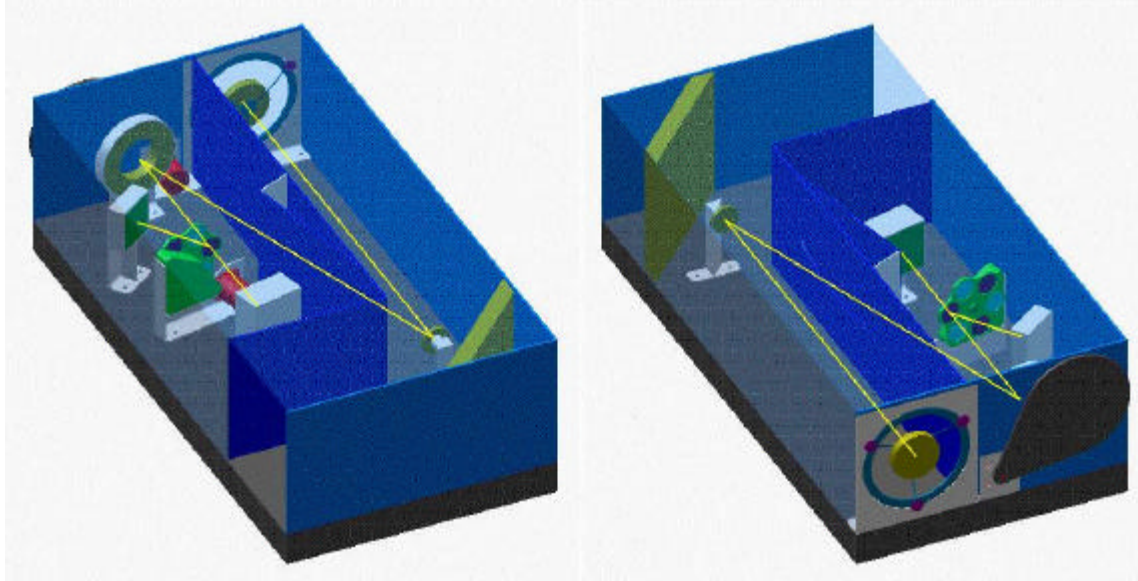


**Fig.3.14:** Two views of the optical layout of UVC.

### *Thermal*

The thermal control approach is based on shielding the instrument from most direct solar radiation, rejecting light from the solar disc that enters the annular entrance aperture, and an opto-mechanical design that is insensitive to bulk temperature changes. The use of a carbon fibre composite structural system allows the optical system to be almost completely athermalised. Moreover, the use of a low secondary magnification factor in the telescope (i.e. 3:1) makes the optical system less sensitive to dimensional changes in comparison with more traditional space instruments such as TRACE. Preliminary estimates suggest that the allowable temperature range of the opto-mechanical system may be as much as  $\pm 50^\circ\text{C}$ . Local temperature control will be needed for the liquid crystal polarisation module, which has a smaller allowable temperature range. Thus we consider it prudent to include a small power allocation for thermal control heaters (e.g. 1 W) pending further analysis.

The occulter is the element of the coronagraph, which reaches the highest temperature since it is directly exposed to the Sun, particularly when the Solar Orbiter is near perihelion. The occulter has an exiguous conductive link (represented by the thin rods of the support) with the rest of the structure. The occulter and supporting links are made of titanium and are arranged in a conical geometry such that thermally induced strain is absorbed without de-centring the occulter disc.

The temperature achieved by the occulter has been estimated by assuming a purely radiative heat transfer and an external coating of the same type as that utilised for the sunshield of the payload module. The thermal flux incident on the occulter is  $31\text{ kW/m}^2$  at 0.21 AU and  $5.5\text{ kW/m}^2$  at 0.5 AU. The temperature difference experienced by the occulter along the observation phase is at maximum  $266.5^\circ\text{C}$ . A small reduction of the temperature will be caused by the transport of part of the heat through the occulter supports.

### *Detectors*

There are two detectors, optimised for the Visible region (450 – 600 nm) and for the Extreme UV (304-121.6 nm). Both detectors have  $15\text{ }\mu\text{m}$  pixels and an array size of  $4096 \times 4096$ . The baseline visible detector is an Active Pixel Sensor (APS). This detector system is based on CMOS technology, which is attractive for high radiation dose environment. In addition, the APS architecture has the potential to allow on-chip differencing of the polarimetric signals, yielding substantial improvements in signal-to-noise performance in comparison with conventional CCD detectors.

The baseline EUV detector is a Charge Injection Device (CID) array. This detection system is highly resistant to space radiation. It can easily withstand more than 100 times the lethal dose of a typical CCD

and radiation-hardened versions can tolerate doses in excess of 1 MegaRad (Si total dosage). CID detectors have randomly addressable pixels, permitting the dynamically programmable read-out of individual pixels and sub-arrays. This feature will be used in UVC for limiting the readout area to the solar corona (excluding the occulted portion field) and for defining "Regions of Interest" to be observed with higher time resolution. EUV sensitivity will be provided by a Micro-Channel Plate image intensifier coupled to the CID array with fibre-optics. This approach results in a detector that is blind in the visible, substantially improving the stray light rejection performance of the EUV channel.

We note that both detector approaches are based to some extent on anticipated developments in rapidly evolving technologies (e.g. array sizes, APS noise performance). Heavily shielded CCD detectors are suitable alternatives in either case.

## RESOURCES AND REQUIREMENTS

### Data rates and volume

The primary driver of the data rate is UVC efficiency in the three channels. In the two EUV lines, the coronal signal is weaker and the instrument efficiency lower than in the visible band. Therefore, longer exposure times will be required for the EUV coronal observations. On the basis of the count-rate for H I and He II Lyman- $\alpha$  emission estimated from a coronal hole (i.e. worst case), we assume an average exposure time of 600 sec. A single image (4096 x 4096 pixel) with 16 bit per pixel takes about 270 Mb of memory. Assuming that only 50% of the image is used (the rest is occulted disc, extreme corners of the square matrix, etc.), and that a factor of 3 lossless compression can be achieved, we expect a data rate of 0.07 Mb/s per detector. Since the visible-light detector works simultaneously with the H I Lyman- $\alpha$  (therefore, about 50% of the time), the data volume accumulated per orbit is about 260 Gb. A factor 20 image compression is needed to reach a data rate of about 5 kb/s. It is expected that this level of compression can be achieved with an acceptable loss of information with schemes such as the "Adaptive Discrete Cosine Transform" (ADCT). The ADCT technique is being used in the Large-Angle Spectroscopic Coronagraph (LASCO) on SOHO.

### Mass

The UVC mass breakdown is given in Table 3.23.

<b>Component</b>	<b>Mass (kg)</b>
Structure	5
Optics	2
Mechanisms	1
Detectors (2)	2
CPU & Interface	2
DC/DC converter	1
ADC	1
Data compressor	1
Motor drive	2
<b>TOTAL instrument</b>	<b>17</b>

**Table 3.23:** Mass breakdown of the UVC.

Telescope	Off-axis Gregorian
Occultation	External occulter: 60 mm diam.
Optics	Primary mirror: 33 mm diam. Secondary mirror: 94 mm diam. (multilayer coated mirrors)
Eff. focal length	490 mm
Field of View	Annular, Sun-centred. Coverage: 1.2 – 3.5 R at 0.21 AU, (perihelion at mission start) 1.7 - 5.0 R at 0.30 AU, (perihelion at mission end)
Spatial resolution	UV (30.4 nm, 121.6 nm): 8 arcsec at 1.2 R (1200 km) 40 arcsec at 3.5 R (6000 km) Visible (500 nm): 40 arcsec entire FOV (6000 km)
Stray-light levels	$< 10^{-8}$ (visible light); $< 10^{-7}$ (30.4 nm, 121.6 nm)
Wavelength.	1) He II (30.4 $\pm$ 2) nm
bandpasses	2) H I (121.6 $\pm$ 10) nm 3) Visible (450 - 600) nm
Detectors	Visible-light: Active Pixel Sensor (APS) EUV (30.4 nm., 121.6 nm): Charge Injection Device (CID) (EUV intensified); 4096 x 4096 array, 15 $\mu$ m pixels
Data rate	5 kb/s
Dimensions	80 cm x 30 cm x 30 cm
Mass (kg)	17
Power (W)	25 (operational mode, peak); 20 (stand-by mode)

**Table 3.24:** UVC instrument summary.

### 3.3.6 Radiometer (RAD)

#### SCIENTIFIC DRIVERS

The mission profile of the Solar Orbiter is ideally suited for studies to improve our understanding of the angular distribution of the radiance from active regions of the photosphere. This can be done by observing e.g. the influence of faculae on the True Solar Irradiance (TSI) from different angles: from near the equator (from Earth-bound missions) and from higher latitudes (from the Solar Orbiter). Similar studies can also be done and have been done from one platform (e.g. SOHO) using the fact that the Sun rotates, which allows us to view the same feature from different angles at different times; the uncertainty, however, is limited by the evolution of the active regions themselves which are known to change on time scales of days at the level of up to 0.1%. From our present understanding, an uncertainty of about 1 part in 10000 is needed for such comparative studies. Thus, we have to ensure that the RAD measurements can be projected back to other radiometers at 1 AU for all operational modes and at all times with sufficient precision. This appears to be feasible, as is shown below, but has to be studied in detail and confirmed during a Phase A study.

#### Instrument concept

RAD is a new generation, room temperature radiometer with four channels, which can be operated independently or in groups of two for internal comparisons. Each channel has its shutter and an independent cover for protection. RAD has electrically calibrated cavity receivers. Two cavities are operated together with one closed and the other with cyclic shutter phases of 50s open and 50s closed duration. Phase sensitive detection at the fundamental shutter frequency is used to analyse the signal. This operational mode has many advantages over the normal “active cavity” operation in e.g. SOHO/VIRGO, which relies on reaching a steady state before measurements can be taken.

The operation will be controlled by software in the instrument's computer. There are essentially only two analogue circuits:

- the amplifier of the thermistor bridge measuring the temperature difference along the thermal impedance and between two cavities (one measuring irradiance the other as thermal reference),
- the highly stable voltage source for the electrical power fed to the cavity.

The bridge is powered by a sine wave at about 100Hz produced by software and its output is A-D converted and synchronously demodulated by software. The demodulated signal is used to control the heater power of the shuttered cavity to compensate for the extra radiant power during the open periods. The heater power is deduced from the highly stable voltage source which is pulse-width modulated by the output of the controller. This power signal is frequency analysed and the amplitudes and phases of the shutter fundamental frequency and the first few harmonics of it (up to about the 8<sup>th</sup>) are transmitted to ground. Only the in-phase signal at the shutter fundamental is needed to calculate the irradiance, the harmonics are for the in-flight characterisation of the temporal behaviour of the detectors. Some of the correction factors, needed for the final evaluation of the irradiance can be determined and/or checked in flight.

### RESOURCES AND REQUIREMENTS

The RAD will have a mass of 4 kg. The power consumption is less than 6.5 W.

The outer dimensions of the RAD instrument will be about 110 mm x 110 mm x 220 mm. The 110 x 110mm face has to be pointed towards the sun; in front there will be some (probably 2) radiation shields which will extend the length of the box by 40 mm and the area of the front to 140x140mm.

For normal operation, i.e. when measuring with one radiometer, a telemetry rate of 500 b/s is required. For backup operations (about once a week) 280 b/s have to added. During check-out intervals a total of 3500 b/s will be needed.

Instrument	Mass (kg)	Power (W)	Volume (cm <sup>3</sup> )	Data rate (b/s)
RAD	4	6.5	3000	500

**Table 3.25:** RAD resource requirements.

#### 3.3.7 Other potential solar instruments

A valid option to be considered in future studies of the Solar Orbiter is the addition of two corona-related instruments:

- A heliospheric imager might extend the view of the heliosphere to almost a full hemisphere, from about 3 solar radii (at 0.2 AU) to as much as the anti-solar direction. Thus, it would have almost the full Earth-Sun line within its field of view for major parts of the observation time, depending on the spacecraft attitude. This instrument would allow us for the first time to observe the propagation of transient disturbances towards the Earth from various distances and aspect angles, in particular from outside the ecliptic plane. Preliminary design studies have demonstrated that such an instrument can probably be built for less than 2 kg. A crucial requirement would be that the hemisphere to be watched must be kept free of Sun-illuminated spacecraft appendages.
- An X-ray instrument dedicated to the high-temperature portion of the coronal emission would enhance and complement the Solar Orbiter payload. A novel configuration for an imaging spectroscopic instrument would operate in the wavelength range from 4 nm to 6 nm and detect emissions from plasma at temperatures between a few  $10^6$  K and a few  $10^7$  K. Such an instrument working in extreme-grazing incidence will obtain very high spectral and spatial resolution. It would also be able to measure densities equal to or greater than  $10^9$  cm<sup>-3</sup> (through density-sensitive lines in this high-temperature range).

### 3.3.8 Solar remote-sensing instruments summary

Name	Acronym	Measurement	Specifications	Mass (kg)	Size (cm x cm x cm)	Power (W)	Tele-metry (kb/s)
Visible-light Imager and Magneto-graph	VIM	High-res. disc imaging and polarimetry	Fe 630 line	26	30 x 40 x 120	25	20
EUV Imager and Spectrometer	EUS	Imaging and diagnostics of TR and corona	EUV emission lines	22	30 x 15 x 140	25	17
EUV Imager	EXI	Corona imaging	He and Fe Ion lines	36	40 x 40 x 250	20	20
Ultraviolet and Visible Light Corona-graph	UVC	Imaging and diagnostics of the corona	Coated mirror coronagraph	17	20 x 20 x 50	25	5
Radiometer	RAD	Solar constant	Visible light	4	11 x 11 x 22	6.5	0.5

**Table 3.26:** Remote-sensing solar instruments.

---

## 4 MISSION PROFILE

---

The Solar Orbiter scientific requirements provide the outline for a mission profile, which defines the basic outline of the required mission, in terms of orbital parameters, launch windows, payload mass etc, and this profile becomes the driver for the spacecraft design.

The energy requirements for a mission such as the Solar Orbiter can be derived by studying the simple problem of a Hohmann transfer orbit to the required final orbit (perihelion as close as possible to the Sun and high orbit inclination with respect to solar equator). To achieve such a trajectory, however, requires a high Delta V and/or a long transfer period even if electric propulsion is used. To overcome this, a strategy based on low-thrust electrical propulsion and planetary gravity assists is baselined.

The orbit is based on the use of a standard Soyouz-Fregat as launcher from Baikonur. The mission profile calls for the interleaving of Earth/Venus gravity assists and SEP (Solar Electric Propulsion) firings. Stationary Plasma Thrusters (SPT) are baselined for costing purposes. The ground operations will be provided by ESOC and will involve using the 35-m ground station near Perth, in Australia. The mission profile is composed of three phases:

The **cruise phase**, starting at spacecraft separation from the launcher, and ending at the start of scientific operations (some science may be performed during the cruise phase):

1. the **nominal mission phase**, during which the main scientific mission is performed,
2. the **extended mission phase**, when further gravity assist manoeuvres will allow higher inclination observations.

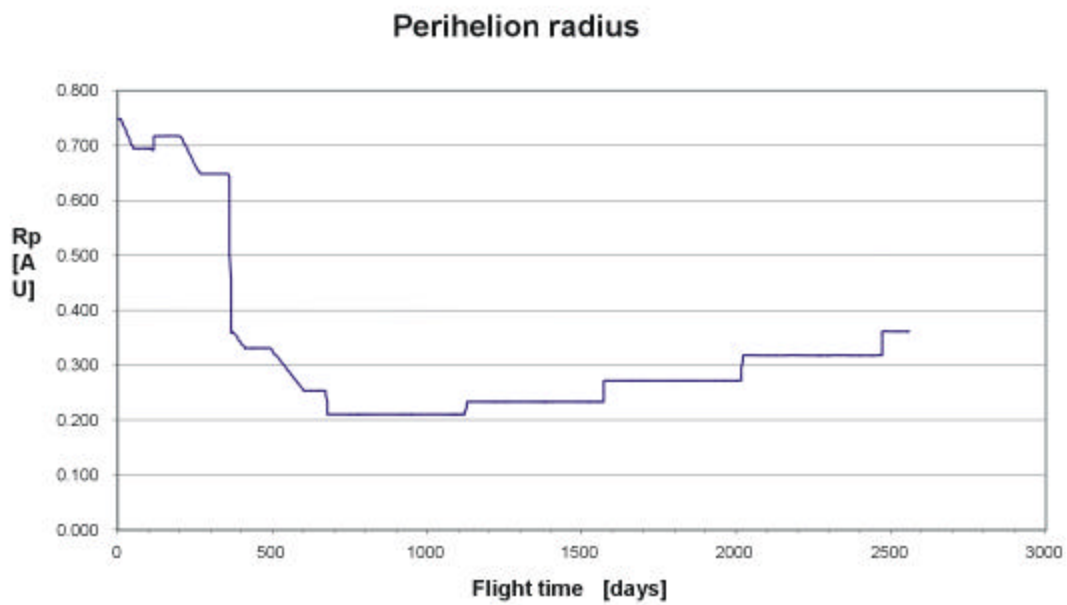
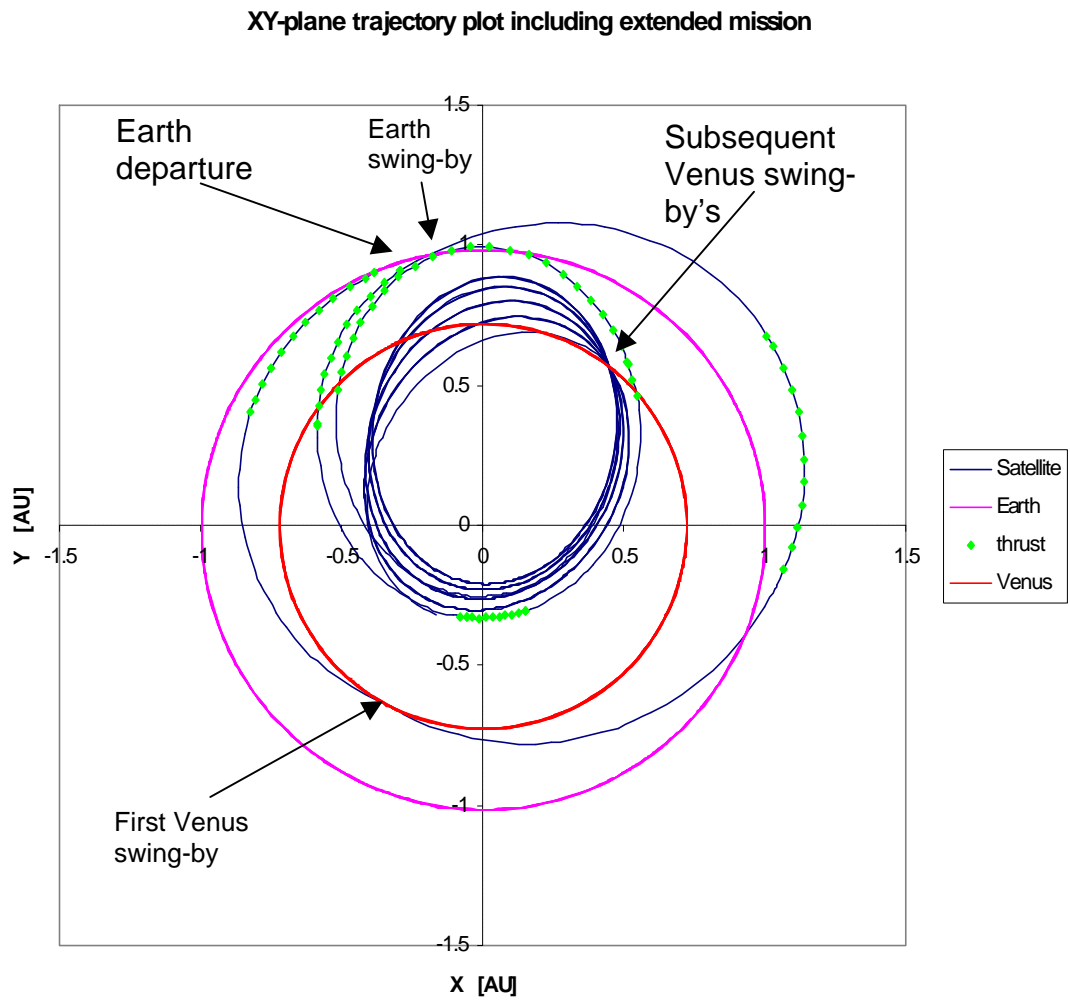
During the **cruise phase** (0 - 1.86 years) there are SEP thrust phases, with durations ranging from 6 to 105 days, and Venus swing-bys driving the semi-major axis changes and the inclination increase.

During the **nominal mission** (1.86 - 4.74 years, i.e. duration: 2.88 years), the orbit is typically of order 150 days, taking the spacecraft from about 0.2 to 0.9 AU. There are 2 Venus swing-by's in this 7-orbit phase taking the orbital inclination to over 30°.

During the **extended mission** (4.74 - 7.02 years, i.e. duration: 2.28 years), there are two further Venus swing-by's over 6 orbits for a continued increase of the orbital inclination.

The selected orbit assures the observation of the Sun with a satisfactory scientific heliographic latitude, while the design of the spacecraft is still thermally feasible. The celestial constellation of the Sun, Venus and Earth leads to a launch window of 3 weeks in every 19 months.

The ecliptic projection of the Solar Orbiter trajectory as well as the perihelion/aphelion radius and solar latitude with respect to mission time are shown in Figures 4.1 to 4.4.





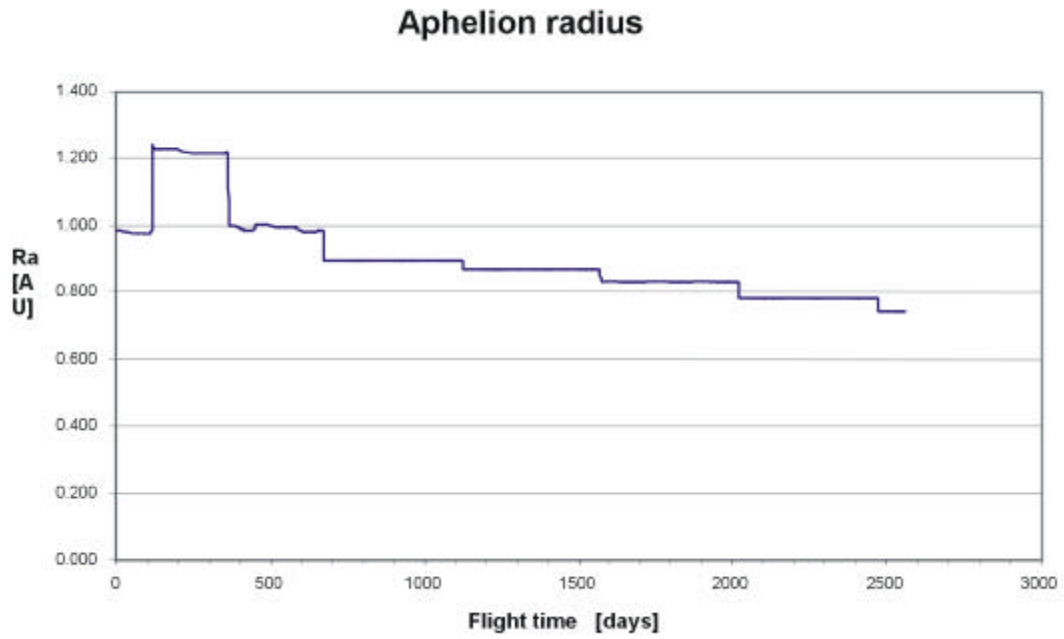


**Figure 4.3:** Aphelion distance as function of time.

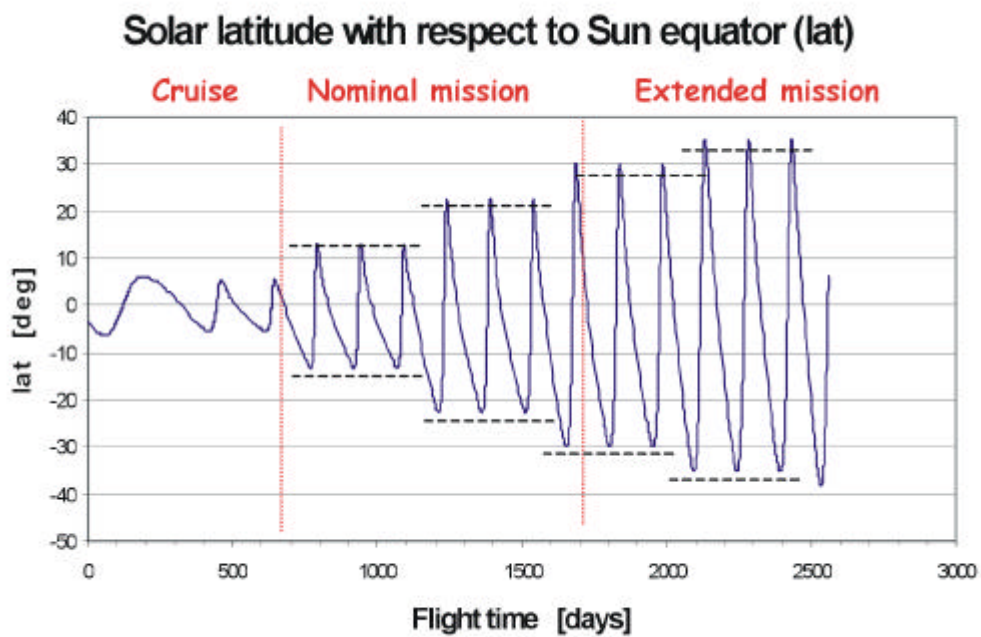


**Figure 4.4:** Spacecraft latitude with respect to the Sun's equator as function of the flight time in days.

---

## 5 SYSTEM DESIGN

---

### 5.1 DESIGN REQUIREMENTS AND DRIVERS

The system design of the Solar Orbiter is driven by the mission profile as well as by general requirements and cost objectives. The spacecraft is designed to get as close to the Sun as the materials and engineering will allow (0.21 AU). Solar radiation increases with decreasing distance from the Sun, and is, of course, the most challenging aspect of the present mission. The solar constant at a distance  $r$  (in Astronomical Units [AU]) is given by  $C_s(r) = C_{so} / r^2$ , where  $C_{so}$  is the solar constant measured at 1 AU, i.e.  $1367 \text{ W/m}^2$ . Figure 5.1 illustrates the maximum heat load, which the Solar Orbiter will encounter. Two other spacecraft, Cassini and the Mercury Orbiter, are shown for comparison.

The orbit is as highly inclined to the Sun's equator as the launcher and propulsion capability will allow. The power demand is higher during the cruise phase, the greatest demand being for the electric propulsion. The solar array sizing is set to provide adequate power at the furthest distance from the Sun. Two sets of solar arrays are used. The larger arrays are for the SEP system and these will be jettisoned after the cruise phase, i.e. when the firings are completed. The remaining array, for spacecraft/instrument power is a thermal “burden” to the system. It is protected by angling the array away from the Sun during the perihelion passages. The basic spacecraft size and shape is directly linked to those of the instruments and the service module performance.

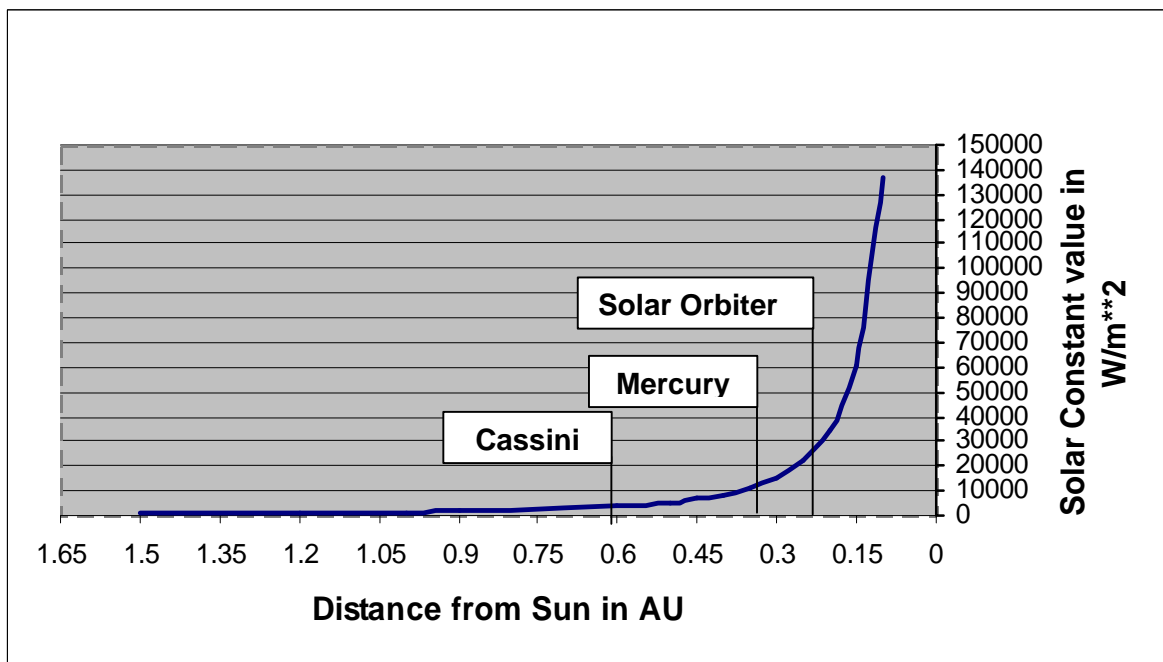


**Figure 5.1:** Solar Constant versus distance from Sun.

The major design driving features for the spacecraft were:

- instruments requirements, mainly field of view, mass, pointing requirements, stability, operations and size;
- launcher mass envelope and interfaces;
- Earth communication, mainly accommodation of the high gain antenna (HGA), and HGA pointing for data transmission; and
- use of existing hardware to minimise risk and cost.

### 5.2 MAIN SYSTEM DESIGN FEATURES

The basic spacecraft configuration is box-like - about 3.0 m long, 1.6 m wide and 1.2 m deep. It has internally mounted instruments, a 2-axis steerable HGA, two sets of one degree of freedom steerable solar arrays and the electrical propulsion system.

The spacecraft must provide accommodation for all of the subsystems and ensure compatibility between them throughout the mission. This demands a detailed consideration for all phases of the mission on each subsystem. The technical difficulties of this mission encountered during the study were many and arose in many areas: the major ones are identified below.

### 5.2.1 Requirements and constraints

The major drivers for the overall configuration of the Solar Orbiter can be summarised as follows:

- **Payload:** Instrument sensors Sun-pointing (except for the magnetometer and dust detector) with no obstacles in the fields of view. Detector radiators, assumed to be mounted on the sensor body, open to cold space. Instruments provided with stable mounting but accessible.
- **Thermal:** Cater for solar radiation input with shielding, radiating surfaces and active orientation of components.
- **Propulsion:** SEP thruster line of force through the spacecraft centre of gravity during the whole cruise phase.
- **Launcher:** Accommodation of the spacecraft in a stowed position under the SOYUZ type S fairing and mechanical interface with FREGAT.
- **Power:** Accommodation of solar array area in two sets, i.e. the cruise phase solar array (for the SEP) and the “standard” solar array.
- **Communications:** Accommodation of the large HGA.
- **Others:** Equipment mounting area and particular equipment accommodations.

### 5.2.2 Spacecraft baseline design

Figures 5.2 to 5.4 show the Solar Orbiter spacecraft overall configuration. The spacecraft body has a cross-section of 1600 mm (Y) x 1200 mm (Z) and its length is 3000 mm (X). The +X side, which faces the sun ( $\pm 30^\circ$ ), is covered by a thermal shield shadowing the spacecraft body. In order to minimise the energy input from the Sun the cross-section of the spacecraft has been minimised (in the Y, Z plane), i.e. the +X panel area is minimised.

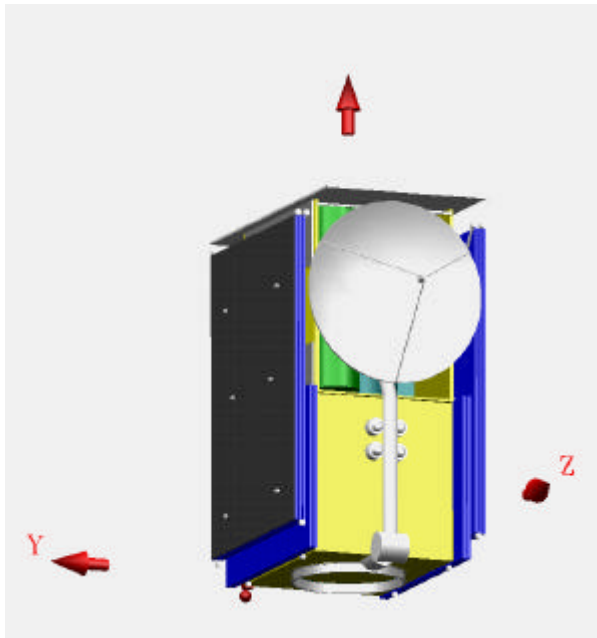


Figure 5.2a: Launch.

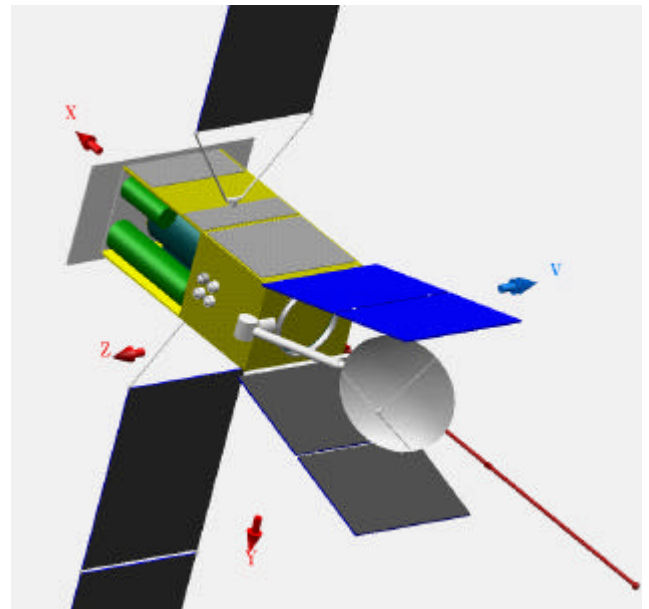
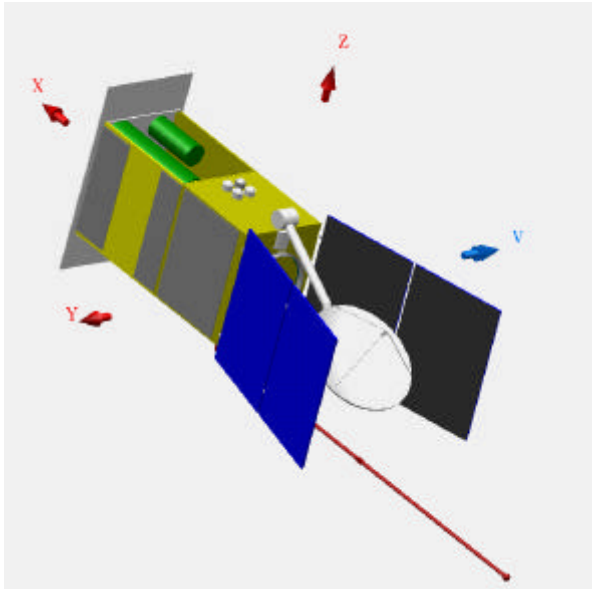
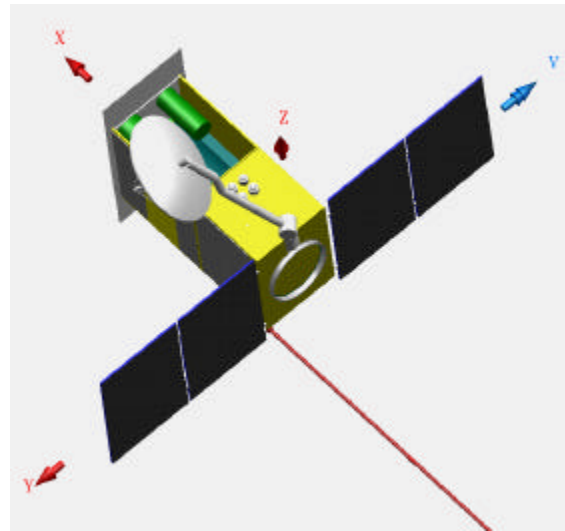


Figure 5.2b: Cruise.



**Figure 5.2c:** Observation.



**Figure 5.2d:** Downlink.

**Figure 5.2a-d:** Solar Orbiter configurations during the mission phases.

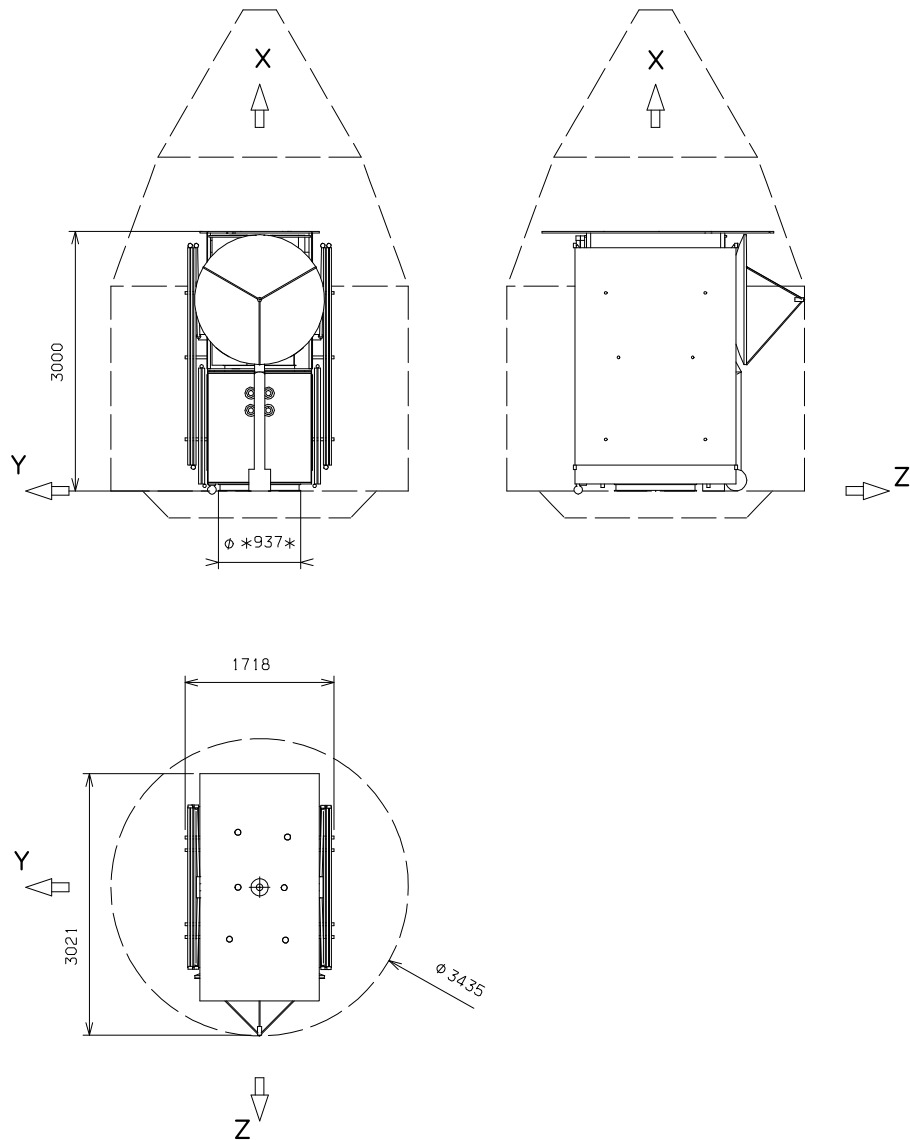


**Figure 5.3:** Solar Orbiter main dimensions. Launch configuration.

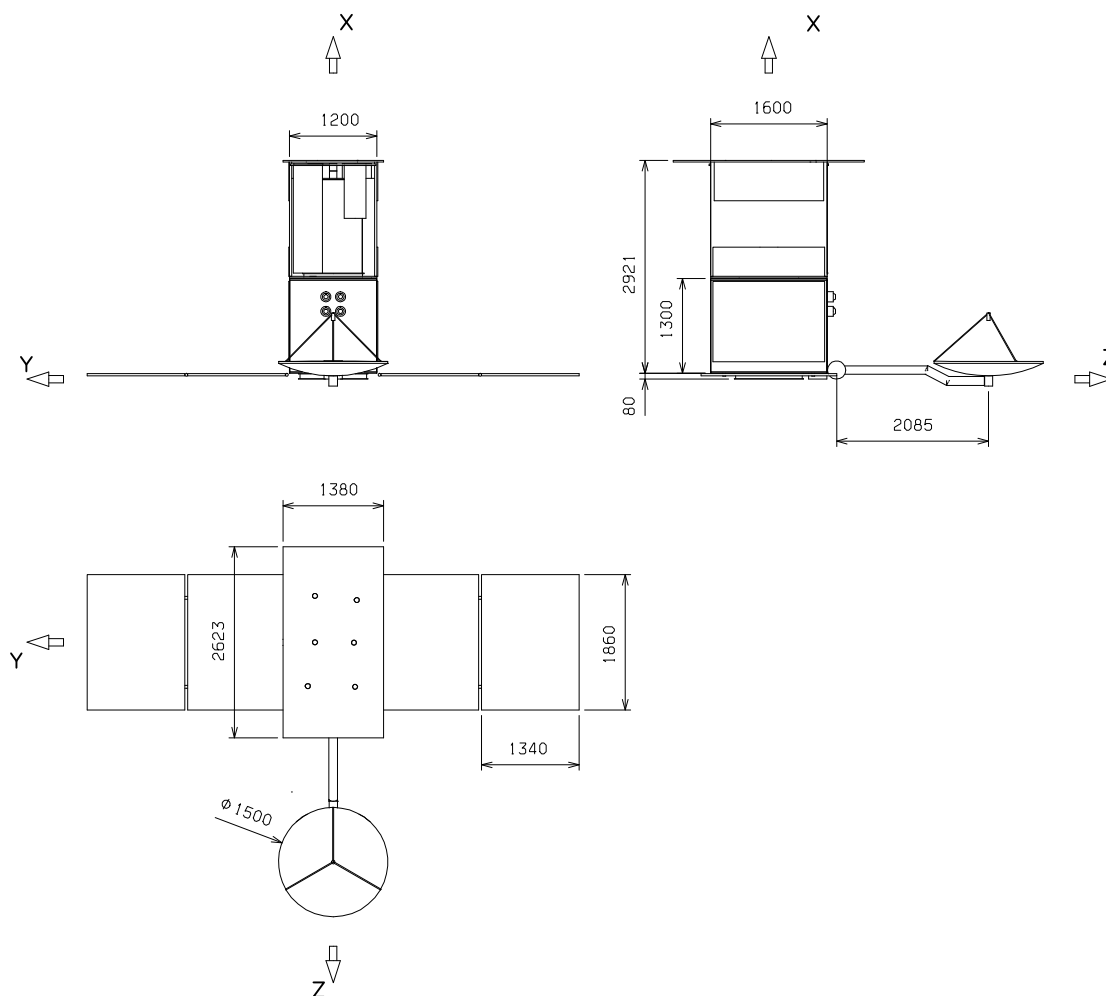


**Figure 5.4:** Solar Orbiter main dimensions. In-orbit configuration.

The spacecraft is of modular design, with a Service Module (SVM) and Payload Module (PLM). The +/-Y sides of the PLM accommodate the cruise solar array (2 wings, 3 panels per wing) and the top shield radiators. The optical instruments are right beneath the top shield, pointed in the +X direction. They are isostatically attached to the central cylinder and may be cooled by radiators to cold space in the +/- Z sides. The instrument electronic boxes are mainly mounted on the bottom panel of the PLM.

The SVM accommodates the orbit solar panels and the SEP/equipment radiators on the +/-Y panels. The HGA and the thrusters are attached on the +Z panel. The propellant tank is at the Centre Of Gravity (COG) of the S/C, inside the central SVM cylinder mounted on a dedicated ring. This design can account for possible changes on the COG height as the spacecraft design matures. The spacecraft equipment boxes are mounted internally on the SVM panels.

In order to cope with different attitudes and distances from the Sun, both solar arrays incorporate a 1 Degree of Freedom (DOF) driving mechanism. The cruise solar array can be jettisoned. The HGA mast (2 m long) is mounted on a 2 DOF mechanism and ensures coverage throughout the mission. Four configurations are considered for the 'active' externally mounted components of the Solar Orbiter (see Figs. 5.2):

- **Launch:** The solar arrays, HGA and magnetometer are stowed.
- **Cruise Phase:** The cruise solar array is deployed (19 m tip to tip). The orbit solar array is deployed (at 75° with respect to the Y-axis). The HGA is protected from the Sun behind the orbit solar array. When required, the SEP thrusters fire in the +Z direction.
- **Nominal/Extended Missions - Observation:** The cruise solar array will be jettisoned at the start of the nominal mission. The HGA will be protected behind the orbit solar array and the -X face of the spacecraft (i.e. in spacecraft shadow).
- **Nominal/Extended Missions - Downlink:** The orbit solar array angle will be varied between 0 and 75° with respect to the Y-axis, depending on the spacecraft-Sun distance. The HGA will be in the operational position.

### 5.2.3 Thermal Design

The proximity to the Sun is particularly demanding for the spacecraft appendages (e.g. the arrays, booms, HGA), which cannot be protected by thermal shielding. Figure 5.5 shows the temperature profile (perpendicular surface to the Sun is considered) with distance from the Sun using different technologies for external coatings. Special attention has been given to the selection of suitable coatings, with absorption/emissivity ( $\alpha/\epsilon$ ) values below 0.25 even after ageing effects. In addition, the requirements for ElectroStatic Discharge (ESD) and spall-resistant external coatings have to be satisfied. This is a technological challenge.

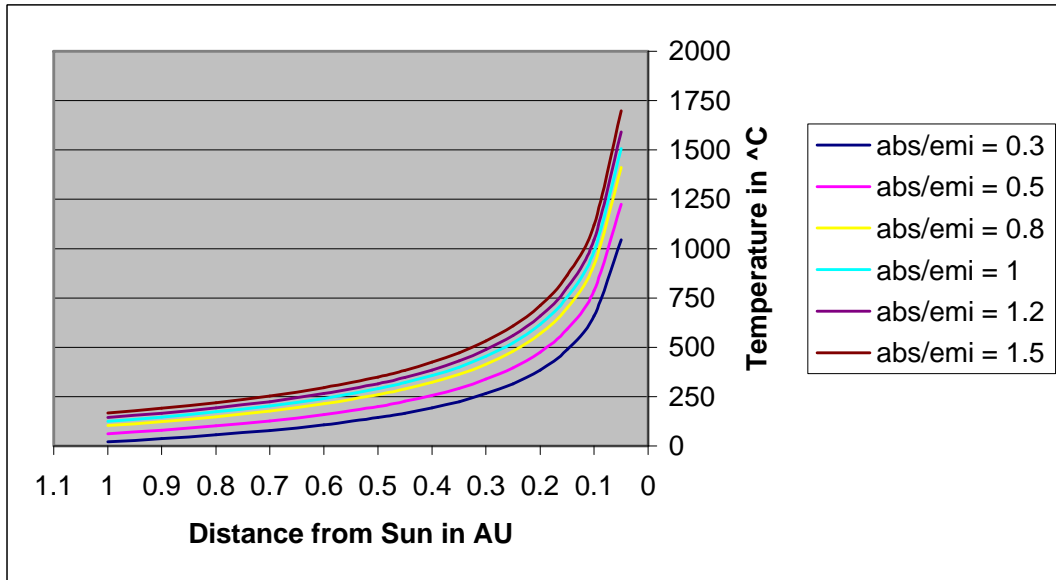


**Figure 5.5:** Temperature of a generic spacecraft surface vs the  $\alpha/\epsilon$ -ratio (abs/emi) and as a function of solar constant ( $\Theta = 0^\circ$ ).

The spacecraft is 3-axis stabilised and always Sun pointed (X-axis), except during SEP firing. The Sun pointing face of the Solar Orbiter is as small as is possible in order to minimise the thermal input from the Sun. The remaining spacecraft surfaces will carry radiators. With this approach, only one thermal shield, made of 3 titanium foils plus 15 layers Kapton/Mylar/Dracon (MLI) shall be used to protect the spacecraft bus and spacecraft +/-Z faces during the most demanding mission phases. The external surface will be painted to maintain a very low  $\alpha/\epsilon$  (see above). Furthermore, behind the structure another 15 layers of MLI will be used for further insulation of the spacecraft from the residual flux leaking through the MLI, as well as to avoid heat leak during the coldest phases of the mission.

The thermal shield has been tailored to extend beyond the +X face of the spacecraft. It will shadow the spacecraft walls during thruster firing (Sun de-pointing) at the minimum Sun-spacecraft distance. Furthermore, it is also been designed to keep the HGA and solar array mechanisms in shadow so that their expected temperatures always remain within standard limits (i.e. temperatures experienced at 1 AU) to increase reliability. In order to cool the sunshield and to avoid heat leaks inside the spacecraft, dedicated radiators are accommodated on the spacecraft +/-Y walls. Heat pipes are used to increase thermal conductance between the sunshield structure and its radiators.

The thermal shield design was driven by the following:

**Cruise Phase:** SEP firing at 0.33 AU with  $\pm 10^\circ$  off X-axis pointing (cf. Figure 6.2)

**Nominal Mission - Observation:** Minimum Sun/spacecraft distance 0.21 AU.

Particular attention had to be paid to the spacecraft appendages, such as the solar arrays and HGA.

### 5.2.4 Power Supply

Photovoltaic materials convert light to electricity but are more efficient when kept to lower temperatures. Since the spacecraft working environment is not readily compatible with this, the following strategy has been conceived.

In order to be compliant with mission requirements and spacecraft needs it is necessary to carry two sets of solar arrays on the Solar Orbiter. The first one will be used during the cruise phase for electrical propulsion. The maximal allowed temperature of this array is  $130^{\circ}\text{C}$  and a complex operation or design would be required to prevent extreme temperatures on the solar cells. Thus, since it is not possible or desirable to keep the array during the nominal mission it will be jettisoned after the last firing. One other reason why the array cannot be used during the nominal mission, over and above the thermal concerns, is the complexity imposed on the attitude and orbit control system (AOCS) design in keeping the required instrument pointing stability.

The cruise solar array will take advantage of a standard design (for GEO Missions) to power the electrical propulsion system and other functions during the cruise phase. It is made up of 2 symmetrical wings of 3 panels each, able to provide 6.2 kW at 1 AU.

The second solar array will be used during the nominal and extended mission phases. It has a maximal allowed temperature of  $150^{\circ}\text{C}$ . Its design is different from the cruise array in order to increase the upper temperature limit. Thus, panels with OSR's mounted on them, are to be made of a honeycomb core with aluminium face sheets. This reduces the thermal gradient within the panels when illuminated. The solar array size (and power output) is kept to a minimum.

Extensive work has been done to define the strategy for the variation, over the orbits of solar radiation on the solar cells, to prevent the maximum temperature being exceeded during both the cruise and nominal/extended mission phases. Figure 5.6 shows how the solar incidence angle can reduce the temperature of the solar arrays.

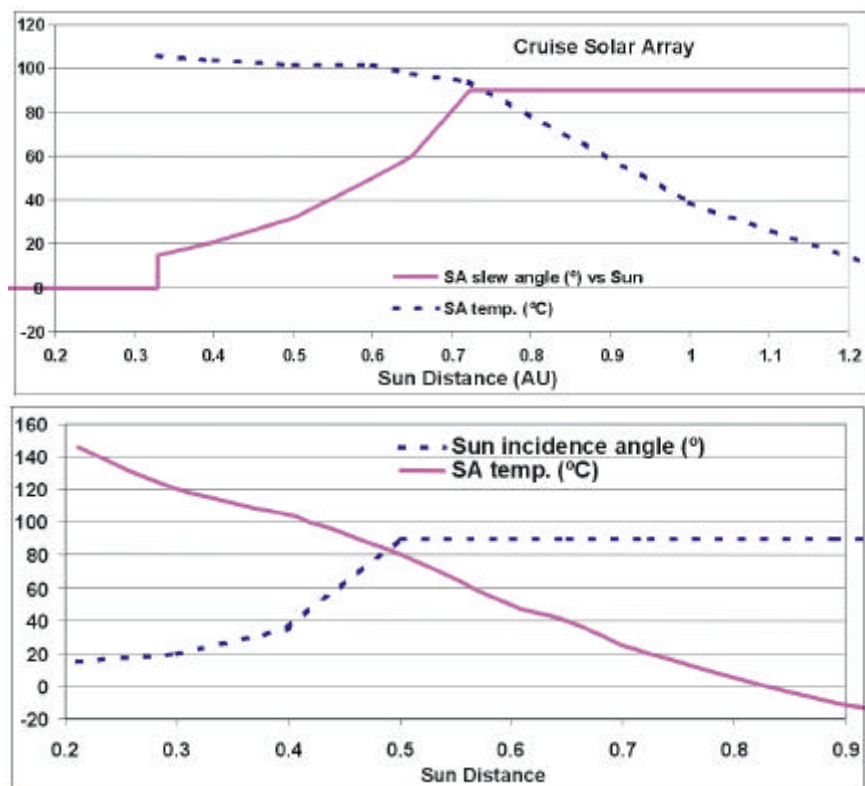


**Figure 5.6:** Cruise/orbit (top/bottom) solar array temperature versus distance from the Sun and solar angle incidence.



### 5.3 DATA COLLECTION AND TRANSMISSION

The Solar Orbiter mission will have variable transmission durations and distances from Earth within each orbit, so a clever strategy for data transmission to Earth has to be considered and some trade-offs made.

During the cruise phase the downlink data consist of housekeeping information (up to 1 kb/s). Communication via wide beam-width Low Gain Antennae (LGA) in X-Band is baselined for both uplink and downlink. If required, the High Gain Antenna (HGA) could be pointed toward the Earth and in this case a careful co-ordination with the propulsion activities and attitude manoeuvres is required.

During the nominal/extended mission phases most orbits have perihelion and aphelion figures of about 0.2 AU and 0.9 AU. The spacecraft-Earth distance will change with every orbit, from 0.3 to 1.8 AU, and consequently the downlink data rate that can be supported will vary considerably. Each orbit takes about 150 days.

The severe thermal environment close to the Sun does not allow the use of the HGA to downlink data to Earth during the perihelion passages in real-time. The data are therefore stored in a large on-board mass memory (baseline 240 Gb) and downlinked later when the Sun-spacecraft distance is larger than 0.5 AU.

Three sets of scientific observation periods (ten days each) per orbit are considered as baseline, with the observation strategy for each orbit tailored such that these periods are centred on the passages through (see Figure 5.7):

- maximum southern latitude,
- maximum northern latitude,
- perihelion.

We anticipate a high-data-rate acquisition of 75 kb/s in the nominal observation mode.

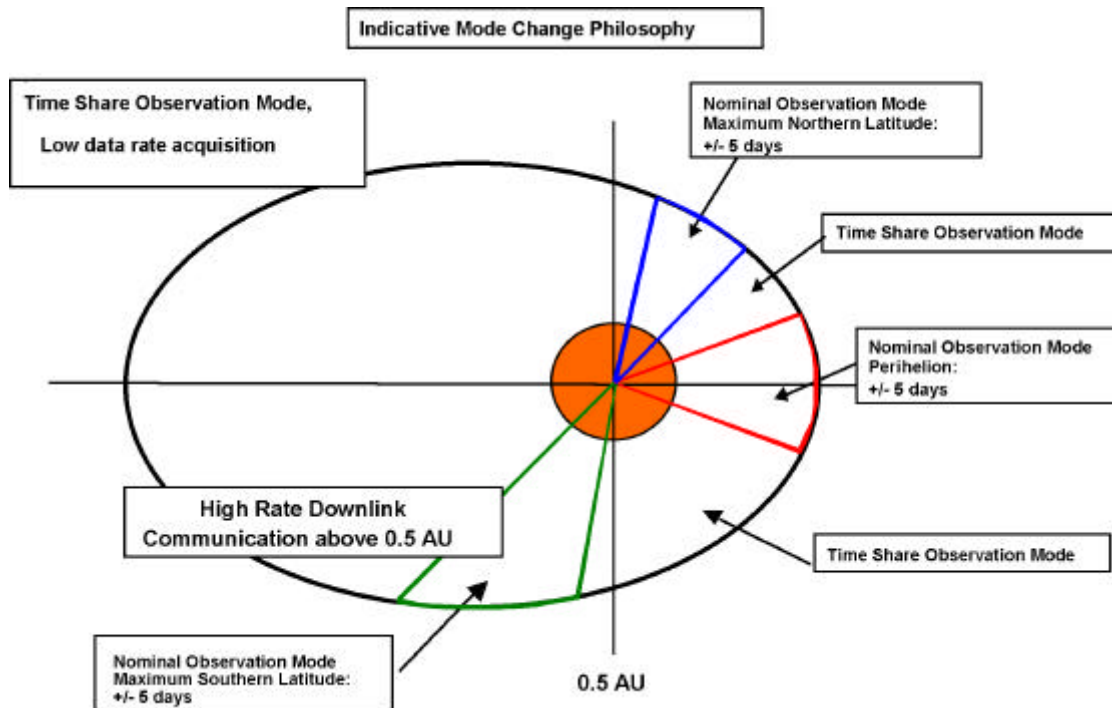


**Figure 5.7:** Modes of operation during the nominal and extended mission.

In order to avoid antenna pattern distortion as well as technological problems, a minimum Sun-spacecraft distance of 0.5 AU for downloading has been fixed. Only for larger distances the high-rate link via the HGA is feasible (approximately 110 days/orbit). Out of the 30 days of observations at 75 kb/s, scientific observations at a lower rate (11.5 kb/s) will take place. When possible these low rate data will be downlinked in real time, otherwise stored on board and dumped later as all the other stored data, according to a data dump strategy that takes into account the slant range spacecraft/Earth and the radio link capability (750 kb/s maximum at 0.6 AU spacecraft/Earth slant range).



Figure 5.8 shows the data downlink capabilities for the various orbits. It should be noted that for orbits 2, 3, 5, 7, 8, 10, and 12 much higher data rates than the baselined 75 kb/s can be supported. For these orbits, the limiting factor is the size of the on-board mass memory. Using 4 Gb chips (which should be readily available in a few years time, considering the fast pace of progress in memory technology) instead of the baselined 1 Gb chips, the data acquisition rate can be doubled for orbits 3 and 8, tripled for orbit 2, and even quadrupled for orbits 5, 7, 10, and 12. The instruments will allow for a flexible data acquisition rate. A second ground-station provided e.g. by an international partner would allow even higher data rates.

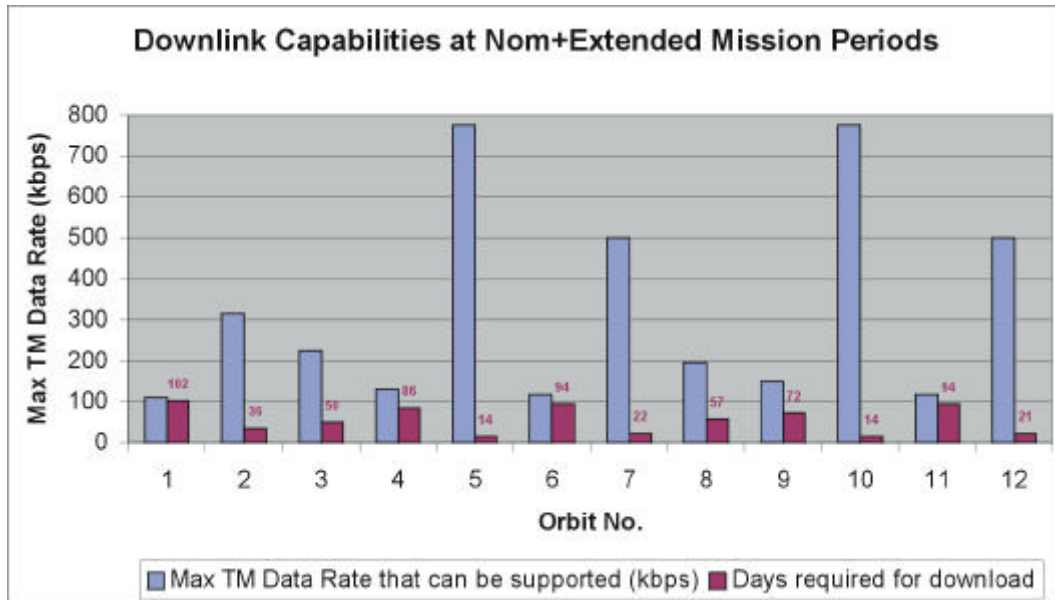


**Figure 5.8:** Downlink capabilities during the nominal and extended mission phases.

The communication link calculations show that the required telemetry and telecommand links are feasible. Figure 5.9 shows the HGA maximum telecommand data rate against the spacecraft-Earth distance and Figure 5.10 the LGA maximum telemetry data rate against the spacecraft-Earth distance, respectively.

Cruise Phase	Uplink	X - Band	34m Perth ⇒ LGA
	Downlink	X - Band	34m Perth ⇒ LGA
Nominal + Extended phases	Uplink	X - Band	34m Perth ⇒ LGA
	Downlink	X/KA - Band	34m Perth ⇒ LGA/HGA

**Table 5.1:** Communication link summary.

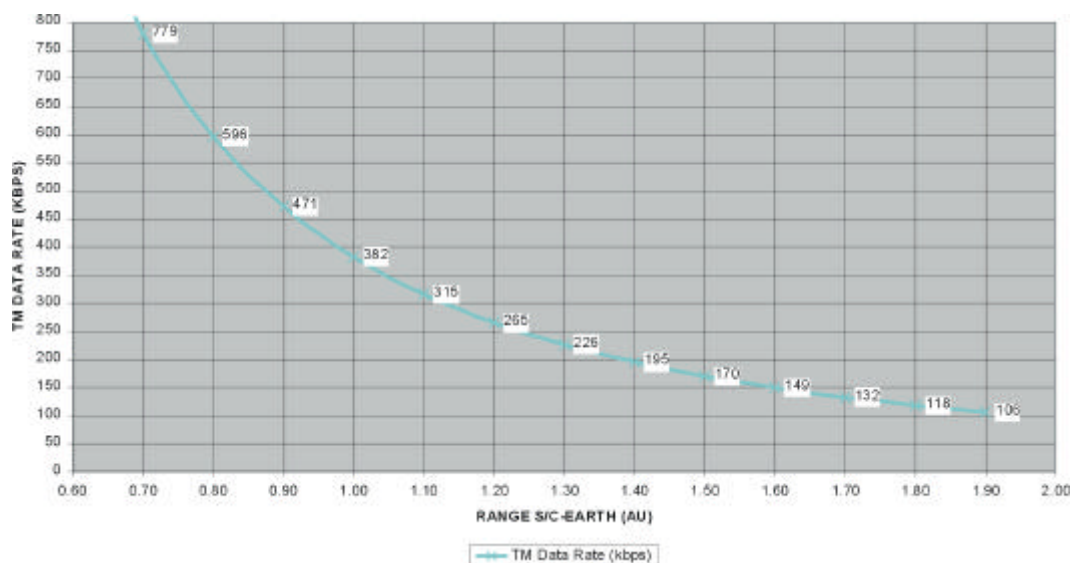


**Figure 5.9:** TM (Ka-Band) data rate against S/C-Earth distance via HGA.

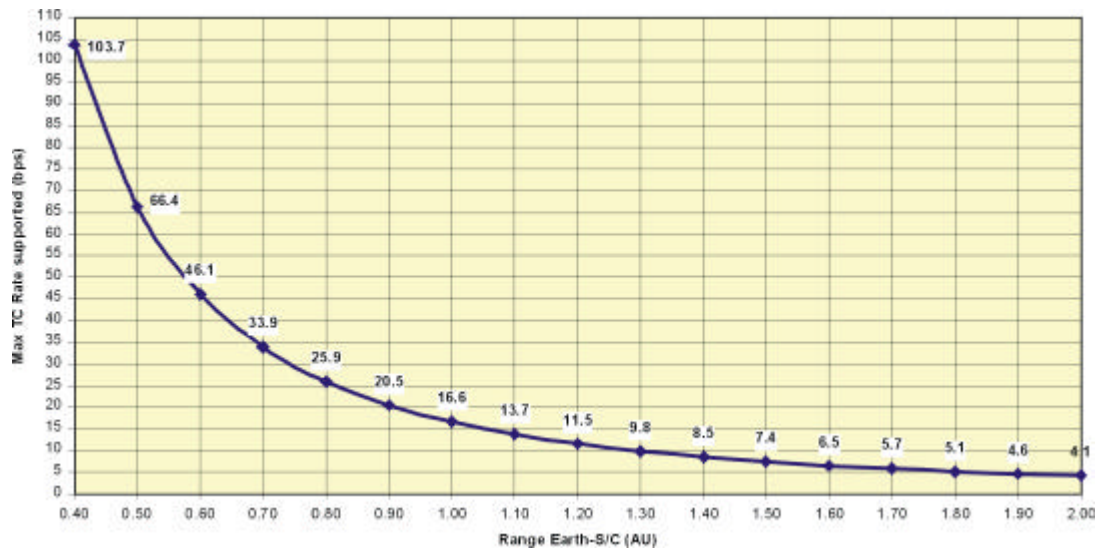


**Figure 5.10:** TM (X-Band) data rate against S/C-Earth distance via LGA (under clear sky conditions).

## 5.4 RADIATION

An evaluation of the environment radiation dose over the three mission phases has been made. Results indicated that a nominally shielded (4mm Al) silicon component is expected to receive a dose of 48 krad over the entire mission. The total ionising dose is within current engineering standards.

## 5.5 MASS BUDGETS

The mass identified in the system budget is based on the specified values of the individual units and subsystems. Depending on the maturity status of the items, contingency is applied on unit/item level. For each piece of equipment a mass margin was applied in relation to its level of development, specifically:

- 5% for off-the-shelf items,
- 10% for items to be modified,
- 20% for items to be developed.

A system level margin of 10% was placed on the spacecraft dry mass (dry mass including sub-system margins).

The Soyuz-ST Fregat launcher from Baikonur allows for a 1310 kg spacecraft (including adapter mass). The design mass of the Solar Orbiter with margin is 1308 kg, i.e. within the launch capabilities of a Soyuz-Fregat launch from Baikonur.

Structure	152 kg
Thermal control	41 kg
Mechanisms	74 kg
Pyrotechnics & pyro. harness	10 kg
Communications	30 kg
Data handling	46 kg
AOCS (including RCS)	37 kg
Propulsion (SEP)	95 kg
Power (including solar arrays)	241 kg
Harness	41 kg
Payload	130 kg
[Spacecraft dry mass	897 kg]
System margin	90 kg
<b>Total dry mass (incl. system margin &amp; excl. adapter)</b>	<b>987 kg</b>
Propellant mass (incl. margins)	271 kg
Adapter	50 kg
Total launch mass without system margin	1218 kg
<b>TOTAL LAUNCH MASS</b>	<b>1308 kg</b>

**Table 5.1:** Solar Orbiter mass budget.

---

## 6 SUBSYSTEM DESIGN

---

### 6.1 ATTITUDE AND ORBIT CONTROL

The basic functions of the attitude and orbit control subsystem (AOCS) are to support the pre-operational transfer phase, the acquisition and control of attitude to meet scientific requirements for target observation, the acquisition and control of safe attitude in case of failures, the maintenance of the operational orbit and to maintain the spacecraft in a safe Sun-pointing attitude using a minimum of on-board resources while ensuring power generation and ground communication.

The spacecraft attitude is three-axis controlled from release in orbit and throughout the mission. After initial rate reduction and Sun acquisition using gyroscopes, coarse sun sensors, and thrusters for actuation, an initial attitude (nominally Sun-pointed) is acquired using the autonomous star pattern recognition of the star tracker. The routine operations of the Solar Orbiter mission will all be performed in the Normal Mode. This mode includes all the functionality necessary to perform the communications and the nominal science observations (Sun pointing), and the slew manoeuvres necessary between all these operations. The attitude measurement is performed with the autonomous star tracker, while a set of four 4 Nms reaction wheels in a pyramid configuration is used as primary actuator. This wheel selection has been made after considering the mass constraints, and frequent wheel off-loading is required during nominal science observations. The  $\Delta V$  and insertion manoeuvres are covered by the SPT-firing mode.

The AOCS hardware architecture, Figure 6.1, is inherited from on-going ESA scientific missions. The Control and Data Management System (CDMS) includes a dedicated processor for the AOCS software and the high level monitoring functions required during the  $\Delta V$  and insertion manoeuvres for the autonomy and fail-operational capabilities. Considering the programmatic design constraints, the AOCS uses many units already developed and validated for other programmes. In the baseline, the Inertial Measurement Unit (IMU), the Sun Acquisition Sensors (SAS), the Star Tracker (STR), and the Reaction Wheels Assembly (RWA) are copies of units used for Mars Express and Smart-1, providing a good level of reuse of the AOCS interface unit (AIU). The total mass and maximum power of the AOCS baseline are 25.8 kg (without margin, which is applied at system level) and 68.4 W respectively.

A single-axis linear covariance analysis has been performed to assess the minimum AOCS error contribution, mainly star tracker noise and wheel quantisation, to the instrument pointing stability budget. For a star tracker noise of 4 arcsec ( $1\sigma$ ), resp. 1 arcsec ( $1\sigma$ ), the contribution of the AOCS errors amounts to 1.26 (resp. 0.42) arcsec which is above the pointing stability requirement (Table 6.1). Therefore, either a better noise performance star tracker or a relaxation of the system pointing stability requirement is needed.

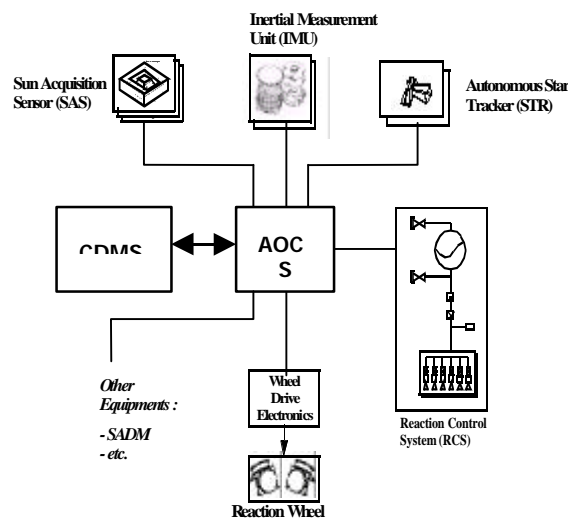


**Figure 6.1:** AOCS hardware architecture.

	Cruise Mode	Observation Mode	Comments
Attitude Control			Covariance analysis
• STR noise + RW quantisation	0.83/0.3	1.17/0.42	STR: 4 arcsec/ 1 arcsec
• Delay	0.10	0.10	Allocation
• Environmental disturbances	0.10	0.10	Allocation
Dynamic interaction			
• High-frequency disturbance (RW)	0.10	0.10	Allocation
• Thermo-elastic	0.40	0.40	Allocation
• Others	0.20	0.20	Allocation
Pointing Stability (15 min)	0.96/0.56	1.26/0.67	RSS - single axis, $1\sigma$
Requirement (single axis)	0.29	0.29	Assumptions: 1 arcsec over 15 min specified half-cone angle at $3\sigma$

**Table 6.1:** Pointing stability error budget with STR noise of 4 arcsec / 1 arcsec ( $1\sigma$ ) in the S/C body reference frame.

## 6.2 REACTION CONTROL SYSTEM

A monopropellant (hydrazine) system has been selected as the Reaction Control System (RCS) for spacecraft attitude control after separation and safe mode, and reaction wheel off-loading. It consists of 2x6 5 N thrusters, one hydrazine tank, valves, piping, heaters, and insulation. The thruster configuration has been finalised on the basis of minimised cosine losses, minimised plume impingement, and best moment arm around the spacecraft Y-axis.

## 6.3 PROPULSION

The main requirement for the propulsion subsystem is to enable the completion of Earth to solar orbit manoeuvres, as designed in the mission analysis. This translates into the total delta-V figure of 4770 m/s, with an additional 140 m/s for the gravity assist auxiliary manoeuvres. Such a high delta-V drives the selection of the thrusters towards a high specific impulse system, in order not to exceed the launch mass limit of 1310 kg imposed by the selected launcher.

A second set of requirements is originated by the attitude control subsystem. The total angular momentum needed for the off-loading of the reaction wheels is 15932 Nms, and a minimum thrust level of a few N is desired for the rate reduction and safe modes.

### THRUSTER POSITIONING

To maintain thermal control of the spacecraft, a Sun-pointing attitude is required throughout the mission. The thruster placement on one side of the spacecraft (the +Z panel) is a consequence of this requirement. In order to be able to reach the nominal mission orbits, it is necessary to have the right momentum variation. Therefore, a firing strategy needs to be defined. For the conceived mission during firing the spacecraft is positioned up to a maximum of  $30^\circ$  off Sun pointing at 1 AU. The maximum Sun-spacecraft pointing angle is a direct consequence of the fact that momentum variation, through the use of electrical propulsion, is achieved by firing for a time longer than typical times used for chemical propulsion since the thrust provided by that propulsion device is low.

In accordance with the SEP firing strategy illustrated in Figure 6.2, the thrusters would be canted by the maximum offset angle mentioned above, and thrust modulation would be used in order to rotate the thrust vector and keep it tangential to the orbit while the spacecraft would remain Sun-pointed. The thrusters would have to be placed in a line, at the intersection of the orbit plane with the +Z panel; only two thrusters would fire at the same time (one „left“ and one „right“), while the other two would be the

redundant pair. Each thruster must be capable of providing the maximum (0.3 N) thrust when aligned with the thrust direction.

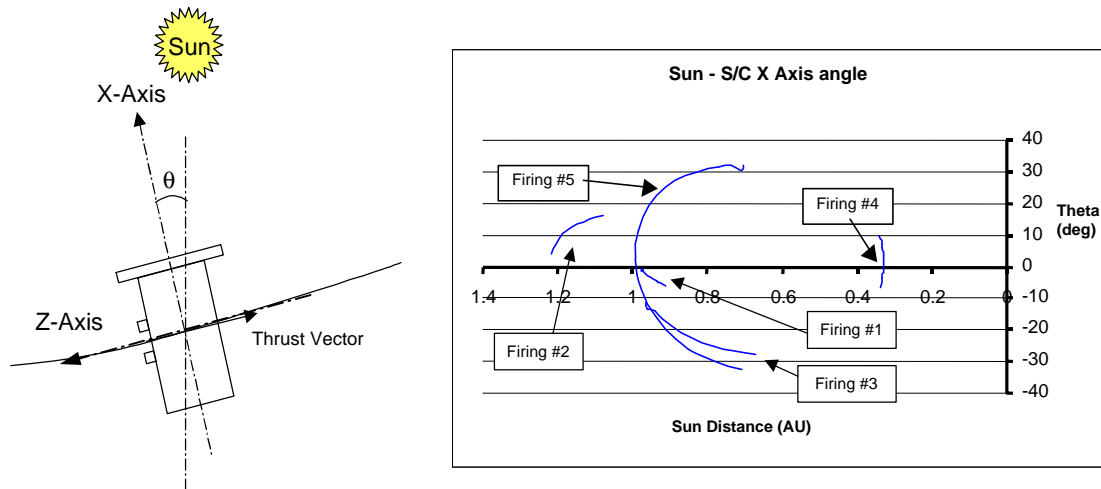


Figure 6.2: SEP firing philosophy.

## 6.4 STRUCTURE

The structure is split into two modules. This provides several benefits, including flexibility in the AIV programme, the possibility to integrate and verify concurrently the two modules, and it allows easy access to the propulsion system. A high thermo-elastic stability is provided by use of a high stability Carbon Fibre Reinforced Plastic (CFRP) structure.

The payload module includes a central cylinder that provides the required stiffness. Two shear walls link the central cylinder to the +Y and -Y panels. This results in a lightweight H-shaped beam that provides a very good combination of stiffness and accessibility to the instruments and equipment. The central cylinder is also connected to the service module with an aluminium interface ring that supports also the -X platform. At its other end is attached a heat-screen made of a CFRP panel.

The service module does not have the same stringent thermo-elastic stability requirements as the payload module and is made of a honeycomb sandwich with aluminium face-sheets. This is a cost-effective lightweight design.

The cruise solar generator is made of two wings with three panels each. The wings are attached to two opposite walls of the satellite body when stowed. In addition, another solar generator is required for the orbital phase.

## 6.5 THERMAL CONTROL

The extreme environments encountered by the spacecraft throughout the whole mission drive the thermal design of the Solar Orbiter. At one extreme, the spacecraft is orbiting the Sun at distances as close as 0.21 AU. At the other extreme, the spacecraft is as far as 1.21 AU from the Sun. Another important factor is the electrical propulsion that generates intermittently, i.e. during firing, a considerable amount of heat inside the spacecraft. Therefore the thermal design has to accommodate a wide range of heat load levels and locations.

The thermal design is of conventional type (selected surface finishes, MLI, non-operational heaters) and uses proven hardware supplemented by the use of heat pipes on the sunshield to cope with the extreme environmental conditions. The thermal design of critical items such as the cruise and the orbiter solar arrays, the HGA, the payload detector (low temperature) radiators, the sunshield and the spacecraft (ambient temperature) radiators have been investigated. As a result, the associated heater power and mass budgets have been established.

The spacecraft configuration is represented in the sub-figures of Figure 5.2. One of the major design challenges has been to cope with the extremely high solar fluxes especially during the spacecraft

depoining required when firing the SPT thrusters. Several combinations of SPT thrusters location/firing strategy were studied. The SPT thrusters have been located on the +Z spacecraft panel and the firing strategy has been tailored to the spacecraft thermal control needs.

The basic design concept consists of shading as much as possible any part of the spacecraft from the Sun at the closest approach to the Sun and during the SPT firings in the cruise phase. To this aim, a sunshield has been accommodated at the +X side of the spacecraft. It extends on the +/-Z sides to make sure that the spacecraft is shadowed even when the +X axis is depointing as much as  $10^\circ$  from the Sun. The +/-Z depointing of  $10^\circ$  occurs during the SPT firing at the closest distance to the Sun (0.33 AU) during the cruise phase. However, other SPT firings occur at higher angles: as high as  $28^\circ$  at the closest Sun-spacecraft distance of 0.67 AU. For that particular case, it has been verified that the solar intensity is harmless to the spacecraft protruding parts (detector radiators, SPT thrusters, HGA, mechanisms...) provided they are insulated with typical MLI blankets.

## 7 GROUND SYSTEMS AND OPERATIONS

### 7.1 GROUND SEGMENT FACILITIES AND SERVICES

All facilities established for the Solar Orbiter ground operations will be based on an extension of existing ground segment infrastructure, tailored to meet the requirements of the Solar Orbiter mission.

The ground operations facilities consist of:

- The ground stations and the communications network;
- The mission control centre (infrastructure, computer hardware);
- The flight control system (data processing and flight dynamics software).

An overview of the ground system is shown in Figure 7.1 below.

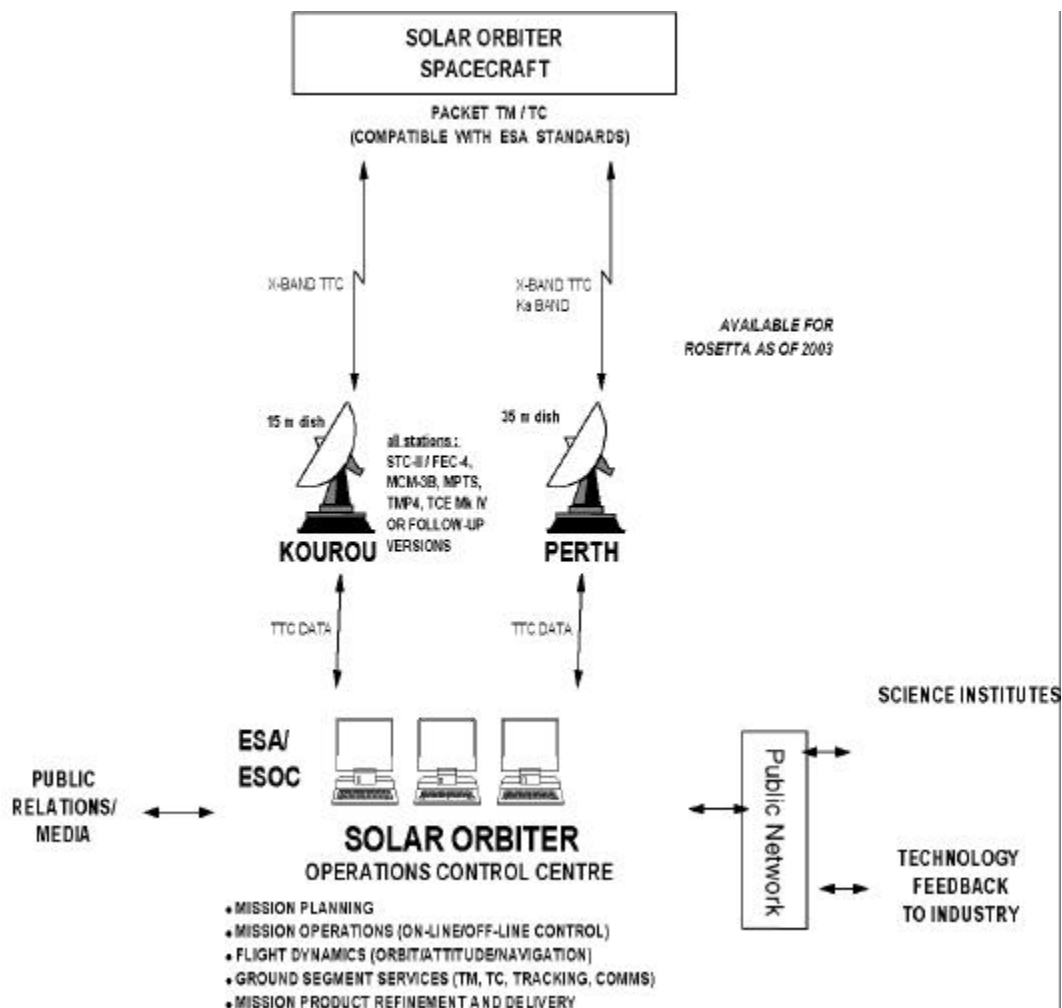


Figure 7.1: Ground systems overview.

### 7.2 GROUND STATIONS AND COMMUNICATIONS NETWORK

It is assumed that the 35 m ESA ground station at Perth will be used for contact with the spacecraft during all mission phases. Despite heavy demands for support from Perth for other ESA missions, for the cruise phase, the Perth station can be assumed to be sufficiently available for operations. For the nominal/extended mission phase, we assume that the Perth station is available for at least 8 hours per day, for costing purposes, and recognise that the actual stations used have to be clarified at a later time. A

possibility to be investigated is the use of the 70 m station in Sardinia for those times when Perth is not free.

During the first 10 days of the mission and during critical mission phases, the ESA 15 m station at Kourou will also be used. The 15 m station at Villafranca will be available as back up.

All ESA stations will interface with the control centre in ESOC (Darmstadt) via the OPSNET communications network. OPSNET is a closed Wide Area Network for data (telecommand, telemetry, tracking data, station monitoring and control data) and voice.

### **7.3 MISSION CONTROL CENTRE**

The Solar Orbiter will be operated by ESOC, and it will be controlled from the Mission Control Centre (MCC) which basically consists of the Main Control Room (MCR) augmented by the Flight Dynamics Room (FDR) and dedicated control rooms and project support rooms. During periods around major mission events mainly during launch and critical periods of the transfer phase the MCR will be used for Solar Orbiter mission control. During the science operations phase (nominal and extended mission) and also during low activity periods, the mission control will be conducted from a dedicated control room.

The control centre is equipped with workstations giving access to the computer systems used for different tasks of operational data processing. It will be staffed by dedicated Solar Orbiter spacecraft operations staff, and experts in spacecraft control, flight dynamics and network control, who will be shared between ESA programmes but will be available for the full mission duration.

### **7.4 COMPUTER FACILITIES AND NETWORK**

The computer configuration used in the Mission Control Centre for the Solar Orbiter mission will be derived from the existing infrastructure. The computer system consists of

- a mission dedicated computer system (workstation hosting SCOS 2000) used for real time telemetry processing and for command preparation and execution, telemetry and command log archiving, and also for non real-time mission planning and mission evaluation;
- a workstation hosting the flight dynamics system (ORATOS);
- a workstation hosting the science telemetry data distribution and instrument command reception system (data servers);
- the simulation computer, providing an image of the spacecraft system during ground segment verification, for staff training and during operations.

All computer systems in the control centre will be redundant with common access to data storage facilities and peripherals. All computing systems will be connected by a Local Area Network (LAN) to allow for rapid transfer of, and for joint access to, data.

The external connections to the science operations team, science data processing centres and PI's will use commercial/public networks (Wide Area Network).

### **7.5 FLIGHT CONTROL SOFTWARE SYSTEM**

A flight control system based on planned infrastructure development (SCOS 2000), using a distributed hardware and software architecture for all spacecraft monitoring and control activities will be established including

- telemetry reception facilities for acquisition, quality checking, filing and distribution;
- telemetry analysis facilities for status/limit checking, trend evaluation;
- telecommand processing facilities for the generation of command for control, master schedule updates, and on-board software maintenance, including their uplink and verification;
- monitoring of instrument housekeeping telemetry for certain parameters which affect spacecraft safety and command acceptance and execution verification;
- separation and forwarding of payload telemetry to science data processing centres;
- checking, reformatting, scheduling command request for payload.

Within the SCOS 2000 system, mission specific software will be developed wherever necessary.



## **7.6 MISSION OPERATIONS CONCEPT**

The Solar Orbiter mission operation will comprise

- spacecraft operations, consisting of mission planning, spacecraft monitoring and control, and all orbit and attitude determination and control;
- science instrument operations, consisting of the implementation of the observation schedules and collection and data quality control of the science telemetry.

Mission operations proper will commence at separation of the Solar Orbiter spacecraft from the launcher and will continue until the end of the mission, when ground contact to the spacecraft will be aborted. Mission operations will comprise the following tasks:

- mission planning, long term planning and short term planning (24 hours to one week time frame);
- spacecraft status monitoring;
- spacecraft control, based on monitoring and following the flight operations plan and the short-term plan;
- orbit determination and control using tracking data and implementing orbit manoeuvres;
- attitude determination and control based on the processed attitude sensors data in the spacecraft telemetry and by commanded updates of control parameters in the on-board attitude control system;
- on-board software maintenance;
- operations support for the experimenters in terms of telemetry packet routing and command checking with respects to spacecraft safety, and telecommand uplink;
- maintenance of ESA ground facilities and network.

## **7.7 SCIENCE INSTRUMENT OPERATIONS AND TEAM STRUCTURE**

The Solar Orbiter is a Principal Investigator (PI) mission. The instruments will be provided and run by PI teams who will take on responsibility for the health and scientific operation of their instruments.

Each team will interface with the MCC to monitor all instrument health and operational aspects. This may be done through dedicated workstation facilities at the home institutes, which are linked to ESOC for the monitoring of instrument parameters and the receipt of data.

The Solar Orbiter is not run by day to day real-time operation, as is SOHO. We will have a 150 day orbit with approximately 30 days of observation for the remote sensing instruments centred on the perihelion and maximum latitude passages. The observation period around perihelion is called the Nominal Observing period and the rest of the orbit is the Time-Share Observation period. During the latter, the high-resolution remote sensing instruments will usually be off. The full disc imagers and the particle and field instruments will be in a synoptic mode and stored data from the last solar passage will be relayed to Earth.

The scientific planning for the solar passes (Nominal Observation periods) will be determined through regular PI-team workshops held once per orbit, i.e. once in every 150 days (5 months), about 2 months prior to the onset of the start of the Nominal Observation period. These workshops may be held at any PI institute, ESA institute or a convenient meeting location. The 30 days of the next pass will be mapped out and instrument teams will return home to prepare the observation sequences ready to install prior to the onset of the pass. Observations for the pass must be loaded into deferred command stores (time-tagged) due to the lack of contact during the pass, i.e. commands for the 30 days must be well defined prior to the onset of the pass. Some features of the plan may be deferred to the last few days before the 30 day period, in order to make target selection at the last minute, but the basic sequences should be arranged well ahead of time.

It is expected that most operations will involve a co-ordination of the instruments, i.e. the bulk of the observations will be through Joint Observing Programmes (JOPs) which may be defined in detail and posted on the Web for inspection.

Further details will be arranged through a suite of Web pages with a planning and scheduling tool facility. The Web pages will also include public understanding facilities, publication and background information.

The PI teams will be responsible for the calibration of data and the archiving of their instrument data. Full archives will be available, possibly located at the sites of current solar archives such as the SOHO archives at IAS and RAL, with Web interfaces to the world community.

The Solar Orbiter mission exploitation must not be restricted to the instrument PI teams. The data should be made public and accessible to the general scientific community, a procedure which has been shown by the SOHO community to be very successful and allowing the best possible use of the data.

---

## 8 COMMUNICATION AND OUTREACH

---

Previous solar missions have received great public and media interest. This is partly due to a raised public awareness of the Sun and its influence on Earth, and due to the highly appealing and startling imagery – in particular from the SOHO and TRACE missions. The public can relate to the Sun and is in awe of its complexity and power.

SOHO results have been the subject of hundreds of media interviews over the last 4.5 years, and countless talks have been given by the SOHO community to public audiences. There have been 14 SOHO-related stories on CNN interactive and 8 on BBC interactive since January 1, 2000 and over 5,000,000 requests per month to the SOHO Web servers. The SOHO real-time image screensaver has been requested by over 150,000 distinct hosts since its launch in November 1999. SOHO is a major feature of the IMAX movie “SolarMax” which was released internationally in July 2000. People see the Sun as an exciting astronomical body which has a direct influence on them.

There is no doubt that the ambitious mission profile of the Solar Orbiter, passing close to the Sun and climbing out of the ecliptic using flybys at Venus will also be of great interest to the public. High resolution images taken close to the Sun and pictures from over the polar regions will capture the attention of the media. Exploring the inner regions of our solar system is something that the person in the street can understand and be excited by. Exploring the sources of “space weather” is seen by the public as a topic which agencies such as ESA should address. The Solar Orbiter is a mission which has enormous potential for public interest.

The mission will provide excellent material to fuel the public interest with close-up images of the Sun. A Web site will be maintained with the most recent images displayed and with good background information on the mission and its objectives, including a picture gallery. The mission Project Scientist and the instrument PIs are responsible for this. The Web site includes contact information for all of the groups; the media are always looking out for contacts in their own countries. Major new results will be highlighted as “hotshots” with good images and captions for public use and press releases should be written whenever appropriate and certainly at the time of major mission milestones.

Basic, colourful brochure information will be made available, as well as CD-ROMs, which can be distributed widely (see e.g. the SOHO CD-ROM).

A close liaison will be maintained between the Solar Orbiter project and the ESA public relations offices to ensure the best possible utilisation of Orbiter results.

Special attention will be paid to the provision of information and materials for schools and students. Astronomy is a popular topic and the Solar Orbiter is able to provide excellent material for use by educational establishments.

---

## 9 MANAGEMENT

---

### 9.1 F2/F3 PROCUREMENT APPROACH

Here, we describe a possible management approach for the Solar Orbiter mission implementation. The exact approach to be taken may differ from this and will be known when the mission is approved. Furthermore, the procurement schedule and model philosophy as shown in the following sections is provided for illustrative purposes only, as this was the basis for the assessment study. The approach is based on the Mars Express Project approach. This approach gives more responsibility to industry than in previous ESA scientific projects, with a fixed price contract instead of a cost reimbursement type of contract.

### 9.2 PROCUREMENT PHILOSOPHY

The proposed procurement scheme for the Solar Orbiter is based on the concept that the payload, consisting of a number of instruments and the associated control and data handling/processing electronics, will be provided by Principal Investigators (PI's) with funding from ESA member states. For the purpose of the study, it has been assumed that all booms relevant to instruments will be provided by the PI's.

ESA would be responsible for

- the overall spacecraft and mission design,
- provision of the spacecraft bus and payload module (PLM)
- integration of the PLM onto the spacecraft bus,
- system testing,
- spacecraft launch and operations,
- acquisition and distribution of data to Science Data Centre(s) (SDC).

### 9.3 SCIENTIFIC MANAGEMENT AND PAYLOAD SELECTION

After the approval of the mission, the agency will issue an open call for tender (ITT) for the selection of two (TBC) competitive industrial contractors for a definition phase. This is equivalent to a Phase A study, as performed in the past, but includes studies of the payload design and requirements. The payload will be selected by means of an Announcement of Opportunity (AO) which is released in parallel with the definition phase ITT. In this way, a large part of the definition phase will be performed taking into account the design of the selected instruments and not on the basis of the model payload.

The AO will outline the spacecraft mission and resources, technical interfaces, schedule, deliverable items, the responsibilities of all parties, etc. The AO contains a description of the model payload and requests proposals for the complete instrumentation (and their integration) and for the Solar Orbiter scientific operations concept (see Section 7.). These proposals must describe in detail the scientific objectives and the design and development of the envisaged instrumentation and associated software. The proposals must also describe the management structure for each instrument and show how the responsibilities for the scientific, technical, operational and analysis aspects are discharged.

Selection of the Solar Orbiter experiments will take place through normal procedures which include a technical evaluation by the ESA executive, supported by the selected industrial contractor for the definition phase, and a scientific evaluation by ESA's scientific advisory bodies and approval by the Science Programme Committee (SPC).

The selected PI's will be responsible for obtaining the necessary funding from the appropriate national authorities. Following selection, refined resource allocations and instrument interfaces will be negotiated with the PI's prior to the start of the Phase B study. These resources and interfaces will be frozen at the end of Phase B. Special items of mechanical ground support equipment and electrical/optical check-out equipment will also have to be supplied by the Solar Orbiter collaboration. This applies in particular for payload tests required at satellite level.

The payload module (PLM) and associated electronics are considered to be qualified and accepted at payload level, with a very well defined set of interfaces at satellite level. The satellite prime contractor

will integrate the instruments with the service module (SVM), forming the protoflight model (PFM) satellite, to be tested for acceptance.

During the instrument development phase, the project team conducts, with the Solar Orbiter collaboration, a preliminary design review, a critical design review and a flight model review. A Solar Orbiter science team comprising the scientists from the collaboration, discipline scientists and the ESA project scientist will be established to support the project.

## **9.4 INDUSTRIAL MANAGEMENT**

It is proposed that an industrial prime contractor, having responsibility for the integration and testing of the Solar Orbiter payload assembly and the spacecraft, should carry out the Solar Orbiter spacecraft procurement. Furthermore, the prime contractor will assist ESA in the procurement of the launcher, and related services, and for the acquisition of the PLM. The industrial contracts will be funded and placed by ESA. The responsibility for control and monitoring the contracts and provision for liaison between partners, contractors and PI groups are with the ESA project team.

## **9.5 DEVELOPMENT PHILOSOPHY AND SCHEDULE**

### **9.5.1 General**

The proposed Solar Orbiter development scheme has the aim of minimising the spacecraft development cost at reasonable risk. It is based on a minimum number of modules and spacecraft models and the maximum utilisation of each model. It is assumed that all parts, units and assemblies would be available off-the-shelf or taken from the BepiColombo project. No technology developments have been considered, only adaptation of design when necessary, like for the orbit solar array.

The first system level test at spacecraft level will be conducted on the Structural Model (SM), to establish the structural characteristics and compatibility at the system level. Other tests, like mass properties and alignment, will be also performed on the spacecraft SM module. Then, the PFM models of the PLM and of the SVM will be assembled at spacecraft level, and the final testing is performed to finally accept the PFM spacecraft. The facilities to test the extreme thermal aspects of the mission are assumed to be available also from BepiColombo, and only the adaptation to the Solar Orbiter requirements have been considered.

### **9.5.2 Payload model philosophy**

The model philosophy chosen is based on the requirement for a single flight instrument supported by adequate spares, e.g. a set of kits of parts to cope with random failure and allowing a unit repair within 3-4 weeks, when spare units do not exist.

To meet the early system level test a Structural Thermal Model (STM) will be built, fitted with at least one active unit of the instrument detectors, the rest being representative dummies. This would allow a full verification of the thermo-mechanical design of the payload. For electrical and functional testing an Engineering Model (EM) is required. All payload elements will undergo qualification testing, if necessary, prior to delivery for AIV (Assembly, Integration, and Verification) and test activities.

### **9.5.3 Service module model philosophy**

A protoflight approach is proposed where only one model, the PFM, is built to flight standard level. However, to perform the early system level tests with the payload, a SM model of the bus would be utilised, using mechanically representative dummies instead of flight parts. The SM spacecraft structure will be at flight standard. The SM will be subjected to a reduced test programme (sinus vibration, modal survey, mass properties, alignment) which allows verification of the design concept and interfaces. It is expected that most of the units will have been qualified on previous programmes. However, when deemed necessary to qualify a unit for the project, this unit, duly refurbished, will become a flight spare. It is assumed that spare units/components kits will be available to cope with random failures and to allow repair of any unit within 3 to 4 weeks.

9.5.4 Schedule

The schedule of the Solar Orbiter programme is shown in Figure 9.1. While the assumed programmatic launch date for the Solar Orbiter is the year 2008, the schedule shows that the earliest possible launch date is less than 6 years after the start of the programme. It should be noted that the schedule doesn't account for funding availability problems. It is only a technical assessment of the time required to implement the Solar Orbiter Project. There are other constraints such as the need to have satellite parts designs available from the BepiColombo cornerstone, for cost and availability purposes, or that the cruise module of BepiColombo be launched six months ahead of the Solar Orbiter, for operations resources availability and cost. There are launch windows in May 2007, January 2009, August 2010, and in principle every 18 months.

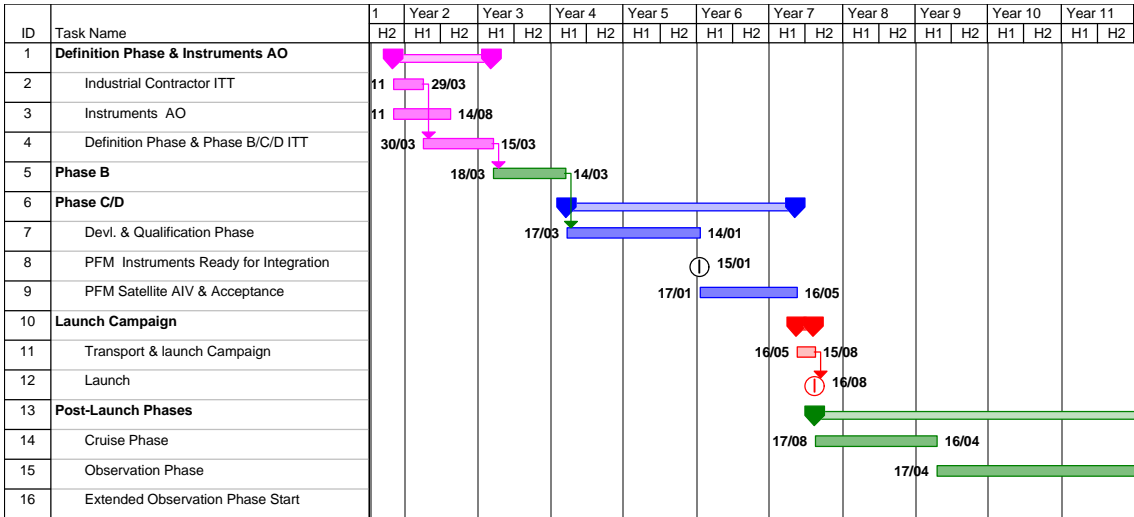


Figure 9.1: Solar Orbiter programme schedule.

---

## 10 LIST OF ACRONYMS

---

ACE	Advanced Composition Explorer
ADCT	Adaptive Discrete Cosine Transform
AIU	AOCS Interface Unit
AIV	Assembly, Integration, and Verification
AO	Announcement of Opportunity
AOCS	Attitude and Orbit Control Subsystem
APS	Active Pixel Sensor
ASP	Advanced Stokes Polarimeter
AU	Astronomical Unit, 150 Mio km
BOL	Beginning of Life
CCD	Charge Coupled Device
CDMS	Control and Data Management System
CDS	Coronal Diagnostic Spectrometer (on SOHO)
CELIAS	Charge and Element and Isotope Analysis System (on SOHO)
CFRP	Carbon Fibre Reinforced Plastic
CID	Charge Injection Device
CME	Coronal Mass Ejection
COG	Center of Gravity
CRS	Coronal Radio Sounding
CTOF	Charge determining Time-of-Flight sensor (of CELIAS on SOHO)
DOF	Degree of Freedom
DPU	Data Processing Unit
DUD	Dust Detector
EAS	Electron Analyser System (of SWA)
EIT	EUV Imaging Telescope (on SOHO)
ELF	Extreme Low Frequency Waves
EM	Engineering Model
EMC	Electro-Magnetic Cleanliness
ENA	Energetic Neutral Atoms
EOL	End of Life
EPD	Energetic Particle Detector
ESA	European Space Agency
ESD	ElectroStatic Discharge
ESOC	European Space Operations Centre
EUI	EUV Imager
EUS	EUV Spectrometer
EUV	Extreme UltraViolet
FDR	Flight Dynamics Room
FDT	Full Disc Telescope (of VIM)
FIP	First Ionisation Potential
FO	Filtergraph Optics (of VIM)
FOV	Field-of-View
FSI	Full Sun Imager (of EUI)
HGA	High Gain Antenna
HRI	High Resolution Imager (of EUI)
HRT	High Resolution Telescope (of VIM)
IDP	Interplanetary Dust Particles
IMPACT	In-situ Measurements of PArticles and CME Transients (STEREO)
IMU	Inertial Measurement Unit
ISS	Image Stabilisation System
ITT	Invitation To Tender
JOP	Joint Observing Programme
KIS	Kiepenheuer-Institut für Sonnenphysik (in Freiburg, Germany)

LAN	Local Area Network
LASCO	Large Angle and Spectrometric Coronagraph (on SOHO)
LGA	Low Gain Antenna
LOS	Line-of-Sight
MAG	Magnetometer
MCP	Micro Channel Plate
MCR	Mission Control Room
MHD	Magneto-Hydrodynamics
MIS	Minor Ion Sensor (of SWA)
MLI	Multi Layer Insulation
NASA	National Aeronautics and Space Administration
NEAR	Near Earth Asteroid Rendezvous
NED	Neutron Detector
NPD	Neutral Particle Detector
OSR	Optical Surface Reflector
PAS	Proton and $\alpha$ -particle Sensor (of SWA)
PFM	ProtoFlight Model
PLM	Payload Module
PMP	Polarisation Modulation Package (of VIM)
PWA	Plasma Wave Analyser of RPW
RAD	Radiometer
RAS	Radio Spectrometer (of RPW)
RCS	Reaction Control System
RPW	Radio and Plasma Wave Analyser
RW	Reaction Wheel
RWA	Reaction Wheel Assembly
SAS	Sun Acquisition Sensor
SEP	Solar Electric Propulsion
SM	Structural Model
SPC	Science Programme Committee
SPT	Stationary Plasma Thruster
STM	Structural Thermal Model
S/C	Spacecraft
SiC	Silicon Carbide
SOHO	Solar and Heliospheric Observatory
STEREO	Solar-TERrestrial Relations Observatory
STR	Star Tracker
SUMER	Solar Ultraviolet Measurement of Emitted Radiation (on SOHO)
SVM	Service Module
SWA	Solar Wind Analyser
SWICS	Solar Wind Ion Composition Sensor (on Ulysses)
TBC	To Be Confirmed
TDS	Time Domain Sampler
TM	TeleMetry
TOF	Time-of-Flight system
TRACE	Transition Region And Coronal Explorer
TSI	Total Solar Irradiance
UVC	Ultraviolet an Visible-Light Coronagraph
UVCS	UltraViolet Coronagraph Spectrometer (on SOHO)
VIM	Visible-light Imager and Magnetograph
VIRGO	Variability of solar Irradiance and Gravity Oscillations (on SOHO)
VLf	Very Low Frequency waves